

STRAIN-INDUCED REMODELING OF URINARY BLADDER SMOOTH MUSCLE

by

Rebecca Ann Long

BS in Chemical Engineering, Carnegie Mellon University, 2003

Submitted to the Graduate Faculty of
The Swanson School of Engineering in partial fulfillment
of the requirements for the degree of
Doctor of Philosophy

University of Pittsburgh

2008

UNIVERSITY OF PITTSBURGH
SWANSON SCHOOL OF ENGINEERING

This dissertation was presented

by

Rebecca Ann Long

It was defended on

June 6, 2008

and approved by

Lance Davidson, Ph.D., Assistant Professor, Department of Bioengineering

Changfeng Tai, Ph.D., Assistant Professor, Department of Urology

David A. Vorp, Ph.D., Associate Professor, Departments of Surgery and Bioengineering

Dissertation Director: Michael S. Sacks, Ph.D., Professor, Department of Bioengineering

Copyright © by Rebecca Ann Long

2008

STRAIN INDUCED REMODELING OF URINARY BLADDER SMOOTH MUSCLE

Rebecca Ann Long, PhD

University of Pittsburgh, 2008

Numerous pathologies that affect the urinary bladder, such as spinal cord injury (SCI), bladder outlet obstruction, or diabetes, cause bladder wall remodeling. Bladder remodeling is marked by changes in the extracellular matrix (ECM) proteins collagen and elastin as well as alterations in bladder smooth muscle cell (BSMC) hypertrophy and phenotype. Previous work has examined the bladder following SCI and found an early increase in elastin and hypertrophy followed by longer term fibrosis. These studies indicated that the mediating factor in bladder remodeling in response to early stage SCI and other pathologies such as obstruction and diabetes is strain. In the SCI bladder, the strain history is changed from normal filling and voiding to over distension and intermittent smooth muscle cell contraction. The goals of this study were to utilize an *ex vivo* organ culture model to examine the effects of strain on bladder smooth muscle remodeling, examine the effects of TGF- β 1, found to be up regulated in the SCI bladder, and to utilize a tissue engineering methodology to examine the effects of strain in cell-seeded biologic scaffolds. The first aim from this study showed that abnormal strain frequency profoundly induces elastogenesis in the *ex vivo* bladder. Further examination with the addition of TGF- β 1 with and without mechanical stimulation showed that mechanical stretch of the *ex vivo* bladder mimics the early stage SCI bladder in remodeling and cell phenotype, and the addition of TGF- β 1 alters this phenotype. Additionally, it was found that TGF- β 1 added to culture of BSMC on collagen gels decreases gel contraction but increases collagen organization of the gels. Finally, in

a tissue engineered construct it was found that the growth factors VEGF and FGF-2 promote penetration of BSMC into small intestinal submucosa and that strain frequency alters the ECM proteins that the BSMC produce with a frequency of 0.1 Hz promoting elastogenesis and a frequency of 0.5 Hz promoting collagen production. The information gained in this study gives further insight into the role of strain in pathological remodeling of the bladder, and it provides a basis for tissue engineering constructs with controlled BSMC penetration and ECM composition.

TABLE OF CONTENTS

PREFACE.....	XXI
1.0 INTRODUCTION.....	1
1.1 THE URINARY BLADDER	1
1.1.1 Bladder layers and cell types.....	1
1.1.2 ECM components.....	8
1.2 PHYSIOLOGY AND DISEASE STATES OF THE URINARY BLADDER ..	15
1.2.1 Normal filling and voiding	15
1.2.2 Neurogenic disorders	17
1.2.3 Obstructive and congenital disorders	20
1.3 EXPERIMENTAL PLATFORMS TO STUDY BLADDER WALL SMOOTH MUSCLE IN NATIVE AND REMODELED STATES.....	21
1.3.1 Organ baths and biomechanical testing.....	21
1.3.2 Ex vivo bladder culture	24
1.3.3 Mechanical stimulation of BSMC.....	26
1.4 TISSUE ENGINEERING THE BLADDER WALL.....	28
1.4.1 Need for bladder wall replacement	28
1.4.2 Bladder development	29
1.4.3 Tissue engineering methodology	30
1.5 MOTIVATION AND AIMS OF PRESENT STUDY	36

2.0	THE EFFECTS OF TISSUE LEVEL STRETCH ON URINARY BLADDER WALL EXTRACELLULAR MATRIX REMODELING	40
2.1	INTRODUCTION	40
2.2	PROTOCOLS	43
2.2.1	Ex vivo organ culture.....	43
2.2.2	Tissue strains experienced in the tension bioreactor system.....	45
2.2.3	Collagen and elastin assessment	45
2.2.4	Matrix metalloproteinase (MMP) activity	46
2.2.5	Histological assessment.....	47
2.2.6	Statistical analysis	48
2.3	RESULTS.....	48
2.3.1	Realized tissue deformations.....	48
2.3.2	Collagen remodeling in the tissue	49
2.3.3	Collagen turnover	51
2.3.4	Elastogenesis	51
2.4	DISCUSSION.....	55
2.4.1	Bladder wall tissue remodeling.....	55
2.4.2	Strain induced alterations in collagen biosynthesis	56
2.4.3	Strain induced elastogenesis in the UBW	57
2.4.4	Stretch frequencies.....	60
2.4.5	Influence of strain history	61
2.4.6	Examining the limits of ex vivo organ culture.....	62
2.4.7	Implications for engineered smooth muscle tissues	63
2.4.8	Summary.....	65

3.0	THE EFFECT OF EXOGENOUS TGF-β1 ON EX VIVO BLADDER EXTRACELLULAR MATRIX COMPOSITION AND SMOOTH MUSCLE CELL PHENOTYPE.....	66
3.1	INTRODUCTION	66
	3.1.1 Role of TGF-β1 in disease state and fibrosis	67
	3.1.2 Cellular phenotype shift	68
3.2	PROTOCOL	70
	3.2.1 Dynamic ex vivo organ culture	70
	3.2.2 ECM assays.....	71
	3.2.3 RT-PCR.....	71
	3.2.4 Mechanical testing.....	72
	3.2.5 Bladder decellularization	73
	3.2.6 Immunohistochemistry	74
	3.2.7 Statistics	75
3.3	THE EFFECT OF TGF-β1 IN EX VIVO ORGAN CULTURE	76
	3.3.1 TGF-β1 antibody staining of normal, SCI-10 day, and cultured bladder strips	76
	3.3.2 Collagen and elastin in the cultured bladders	77
	3.3.3 Mechanical properties of cultured bladder tissue.....	81
	3.3.4 BSMC phenotype	85
3.4	DISCUSSION.....	87
	3.4.1 Alterations in ECM composition and mechanical properties.....	87
	3.4.2 Phenotype.....	90
	3.4.3 Relation to SCI affected bladders.....	91
	3.4.4 Limitations.....	92
	3.4.5 Summary.....	93

4.0	THE EFFECT OF TGF- β1 ON BSMC MEDIATED COLLAGEN GEL REMODELING	94
4.1	INTRODUCTION	94
4.2	PROTOCOL	96
4.2.1	Cell culture.....	96
4.2.2	TGF-β1	97
4.2.3	Anchored collagen gels	97
4.2.4	Immunohistochemistry	99
4.2.5	Small angle light scattering (SALS)	100
4.2.6	Cell morphology	101
4.2.7	Statistics	101
4.3	THE EFFECT OF TGF-β1 ON COLLAGEN GEL CONTRACTION AND ORGANIZATION.....	102
4.3.1	TGF-β1 expression in SCI bladders	102
4.3.2	TGF-β1 decreases contraction of collagen gels at early time points	104
4.3.3	TGF-β1 alters collagen reorganization	108
4.3.4	TGF-β1 causes BSMC bundling	108
4.4	DISCUSSION.....	112
4.4.1	Influence of TGF-β1 on gel contraction and cellular phenotype.....	112
4.4.2	Influence of TGF-β1 on collagen gel organization	113
4.4.3	Implications	114
5.0	IN VITRO MECHANICAL CONDITIONING OF BSMC SEEDED ON SIS	115
5.1	INTRODUCTION	115
5.1.1	Previous SIS studies	116
5.1.2	Growth factors VEGF and FGF-2.....	121
5.2	PROTOCOL	122

5.2.1	Cell culture.....	122
5.2.2	Mechanical stimulation.....	123
5.2.3	DNA quantification	123
5.2.4	Collagen and elastin assessment	124
5.2.5	Matrix metalloproteinase (MMP) activity	124
5.2.6	Cell migration assays	125
5.2.7	Histological staining.....	126
5.2.8	Statistical analysis	126
5.3	RESULTS.....	127
5.3.1	Cellular proliferation.....	127
5.3.2	Cellular migration.....	129
5.3.3	Collagen and elastin.....	133
5.3.4	MMP activity and collagen in the media.....	137
5.4	DISCUSSION.....	140
5.4.1	VEGF and FGF-2.....	140
5.4.2	Stretch protocols	141
5.4.3	Limitations.....	142
5.4.4	Summary.....	143
6.0	SUMMARY, IMPLICATIONS, AND FUTURE DIRECTIONS.....	144
6.1	SUMMARY OF MAIN FINDINGS.....	144
6.1.1	Specific Aim 1: Determine the effect of strain history on ECM remodeling of the ex vivo organ cultured bladder	144
6.1.2	Specific Aim 2: Examine the role of TGF-β1 with and without cyclic stretch on bladder smooth muscle remodeling.....	145
6.1.3	Specific Aim 3: Engineer a cell-ECM construct to further examine the effect of strain on BSMC remodeling with future applicability in tissue engineering the bladder wall.....	146

6.2	IMPLICATIONS OF MAIN FINDINGS.....	146
6.2.1	Implication for treatment of pathological bladders.....	146
6.2.2	Implication for mathematical modeling the remodeling of the urinary bladder wall	147
6.2.3	Impact on tissue engineering urinary bladder wall replacements	148
6.3	FUTURE STUDIES.....	149
6.3.1	Examining remodeling in augmented smooth muscle tissues	149
6.3.2	Examining regulation of elastogenesis and phenotypic shift in the BSMC 151	
6.3.3	BSMC response to contact guidance and cyclic mechanical stretch	152
6.3.4	Summary of future directions	156
APPENDIX A		157
BIBLIOGRAPHY		162

LIST OF TABLES

Table 2-1. Stretch protocols.....	44
Table 3-1. PCR primers.....	71
Table 3-2. Mechanical testing conditions for bladder strips following culture.....	73

LIST OF FIGURES

Figure 1-1. The urinary bladder. (academic.kellogg.cc.mi.us/herbrandsonc/bio201).....	2
Figure 1-2. Urothelial organization [1].....	3
Figure 1-3. Layers of the urinary bladder wall [5].....	4
Figure 1-4. Depiction of BSMC contraction through shortening [1].....	6
Figure 1-5. Collagen coils during filling [26].....	11
Figure 1-6. Assembly of mature elastic fibers [37].....	13
Figure 1-7. Mechanism of storage and voiding reflexes. A , Storage reflexes. During the storage of urine, distention of the bladder produces low-level bladder afferent firing. Afferent firing in turn stimulates the sympathetic outflow to the bladder outlet (base and urethra) and pudendal outflow to the external urethral sphincter. These responses occur by spinal reflex pathways and represent “guarding reflexes,” which promote continence. Sympathetic firing also inhibits detrusor muscle and transmission in bladder ganglia. B , Voiding reflexes. At the initiation of micturition, intense vesical afferent activity activates the brainstem micturition center, which inhibits the spinal guarding reflexes (sympathetic and pudendal outflow to the urethra). The pontine micturition center also stimulates the parasympathetic outflow to the bladder and internal sphincter smooth muscle. Maintenance of the voiding reflex is through ascending afferent input from the spinal cord, which may pass through the periaqueductal gray matter (PAG) before reaching the pontine micturition center [1].....	16

Figure 1-8. Histological sections from normal and SCI rat bladders stained using the Movat’s pentachrome. Compared to normal (Frame A), the SCI rat bladder (Frame B) was much thicker and contained more smooth muscle (stained in red). Although comparable amounts of collagen (stained in yellow) were present in the sections of both normal (Frame C) and SCI (Frame D) bladders, there were significantly more elastic fibers (stained in black; indicated by arrows) in the SCI bladder. Mags.= 10X (Frames A, B); 40X (Frames C, D). From Nagatomi et al. [54].....	19
Figure 1-9. Biaxial testing set up and device.....	23
Figure 1-10. Representative stress strain curves from biaxial testing of a normal bladder [64]...23	
Figure 1-11. A. Example images of a bladder with markers from both cameras before and after filling. Axes were defined for the longitudinal, L, and circumferential, C, directions. B. Higher pressures during filling indicated less compliance of the rat bladders in the passive state. Average peak pressure values were 16.7 and 6.4 mm Hg in the passive and inactive states, respectively, and were significantly different ($p<0.05$). Data are presented as the mean \pm standard error ($n=5$). The greater variability in the passive data was a result of spontaneous bladder contractions throughout the experiment.....	23
Figure 1-12. Rhodamine-phalloidin of staining of BSMC under uniaxial stretch for 48 hours (A), in static culture (B), and under equibiaxial stretch for 48 hours (C). The white arrows in (A and C) show the direction of strain. BSMC appear to line up perpendicularly to the direction of strain in A. In static culture, the BSMC have no apparent preferred orientation (B). BSMC show a slight preferred direction under equi-biaxial stretch (C).....	27
Figure 1-13. Bladder augmentation schematic.[96].....	33
Figure 1-14. Engineered neo-bladder. [99].....	34
Figure 1-15. Small intestinal submucosa.....	35
Figure 1-16. Flowchart of specific aims.....	39
Figure 2-1. Sample waveforms for (A) two cycles of “1 hour cycle”, (B) two cycles of “8 hour cycle” and (C) several cycles of “0.5 Hz cycle” in the ex vivo rat bladder strips. (D) A photograph of the tension bioreactor.....	44

Figure 2-2. Total collagen concentration (pepsin insoluble and soluble) of cultured bladder strips following 7 and 14 days in culture. (A) Pepsin soluble collagen at 7 and 14 days. The 0.5 Hz and 1 hr groups are significantly different $p < 0.01$ than all other groups. The Native group is significantly higher than the 0.5 Hz and 1 hr groups at 7 days and the 1 hr and 8 hr groups at 14 days * $p < 0.05$. (B) Pepsin insoluble collagen at 7 and 14 days. There were no statistically significant differences in insoluble collagen between the groups except for between the 7 and 14 day time points in the 1 hr group ($p = 0.033$). All data are presented as mean \pm sem with $n = 5$ or 6 per group.....50

Figure 2-3. Soluble collagen and MMP activity found in the culture media (A) 7 and 14 day soluble collagen found in the media. Significantly more soluble collagen was found in the 0.5 Hz group media than in all other groups, $p < 0.05$. The soluble collagen in the media from 8 hour group at 14 days was significantly greater than the soluble collagen from the 8 hour group at 7 days, $p = 0.050$. (B) 7 and 14 day MMP activity found in the media. Significantly more MMP activity was found in the 0.5 Hz group media at 14 days than in all other groups, $p < 0.05$. All data are presented as mean \pm sem with $n = 4$ for 7 day groups and $n = 5$ or 6 for 14 day groups.....52

Figure 2-4. Elastic trichrome staining of cross sections of (A) fresh tissue, (B) 7 day statically cultured tissue, (C) 7 day 1 hr cycle, (D) 7 day 8 hr cycle, (E) 7 day 0.5 Hz cycle, (F) portion of 7 day 0.5 Hz magnified to display the elastin. Images are reduced from 400x. Red arrows in (E) indicate areas of elastin formation.....53

Figure 2-5. Immunohistochemistry with antibody to elastin and DAPI nuclei staining. (A) Overlaid image of static culture specimen, note elastin (green) is only seen around blood vessels (arrows). (B) Overlaid image of 0.5 Hz group at 7 days, note the large portion of fibrillar elastin (green).....54

Figure 2-6. Elastin concentration of bladder samples following 7 and 14 days in culture. Data are presented as mean \pm sem with $n = 5$ or 6 for each group. The 0.5 Hz group at both 7 and 14 days was significantly greater, $p < 0.001$, compared to all other groups. The 1 hour group at 14 days was significantly greater, $p < 0.05$, compared to native tissue.....55

Figure 2-7. A. Soluble collagen following 7 days organ culture. Significance determined by one way ANOVA followed by Student Newman Keuls test for multiple comparisons. B. Fold increase over native elastin concentration. Data are presented as mean \pm sem, $n = 5-6$ per group. $p < 0.001$ compared to native. $p < 0.001$ compared to native.....62

Figure 3-1. Photographs of excised bladders from A. Normal and B. SCI rats. Small ruler increments are in mm.....67

Figure 3-2. Gene array expression of key genes involved in ECM remodeling of the SCI bladder. Nagatomi et al [35].	68
Figure 3-3. Mechanical testing set up [127].	73
Figure 3-4. TGF- β 1 antibody staining on en face bladder sections. A. Normal native bladder, B. Static culture 7 days, C. 0.5 Hz culture 7 days, D. 10-day SCI bladder, E. Static culture + TGF- β 1 7 days, F. 0.5 Hz culture + TGF- β 1 7 days. Blue represent cell nuclei. Images are reduced from 200x.	76
Figure 3-5. Fold increase in elastin compared to the native bladder. Data are presented as mean \pm s.e.m. n=6 per group. *p<0.001 compared to native, + p<0.01 compared to native.	77
Figure 3-6. Soluble collagen protein found in A. bladder tissue of native and cultured bladders and B. media assay of soluble collagen. Data are presented as mean \pm sem with n=5-6 per group.	79
Figure 3-7. RQ values of RT-PCR gene expression for Type I collagen, Type III collagen, and elastin from native (black) and 0.5 Hz cultured bladders (gray). Data are presented as mean \pm st.dev. n=3 per group.	80
Figure 3-8. Elastic trichrome staining of A. native bladder, B. statically cultured bladder, C, statically cultured bladder + TGF- β 1, D. 0.5 Hz cultured bladder, E. 0.5 Hz cultured bladder + TGF- β 1. Images are reduced from 200x. Red/purple are smooth muscle cells, blue staining is collagen, black staining is elastin.	81
Figure 3-9. Representative tension vs. stretch curves of passive testing and inactive testing.	82
Figure 3-10. Representative tension vs. stretch curves of decellularized bladder tissue.	83
Figure 3-11. Tension values at 1.2 stretch from strip biaxial biomechanical testing. A. Tension values from passive testing and inactive testing. B. Tension values following decellularization of the bladder strips. All data are presented as mean \pm se.m. with n=4 per group. In graph A, * indicates that the TGF- β 1 groups are significantly statistically lower (p<0.05) than all other groups within each testing mode. In graph B, * indicates significantly greater (p<0.05) than all other test groups, and # indicates significantly lower than native and static groups but not from each other.	84
Figure 3-12. Representative images from alpha smooth muscle actin staining of en face sections of A. Normal native bladder, B. Static culture 7 days, C. 0.5 Hz culture 7 days, D. 10-day SCI bladder, E. Static culture + TGF- β 1 7 days, F. 0.5 Hz culture + TGF- β 1 7 days. Images are reduced from 400x.	86

Figure 3-13. General caldesmon staining of en face sections of A. Normal native bladder, B. Static culture 7 days, C. 0.5 Hz culture 7 days, D. 10-day SCI bladder, E. Static culture + TGF-B1 7 days, F. 0.5 Hz culture + TGF-B1 7 days. Images are reduced from 200x.....	86
Figure 3-14. h-caldesmon (smooth) staining of en face sections of A. Normal native bladder, B. Static culture 7 days, C. 0.5 Hz culture 7 days, D. 10-day SCI bladder, E. Static culture + TGF-B1 7 days, F. 0.5 Hz culture + TGF-B1 7 days. Images are reduced from 200x.....	87
Figure 4-1. Polar plots of directionality of smooth muscle bundles in normal A. and SCI B. bladders.[54].....	95
Figure 4-2. Schematic of anchored collagen gels and calculation of % contraction of the gels...	98
Figure 4-3. Fluorescent antibody labeling of TGF- β 1 in normal and 10 day post-surgical SCI bladders in both cross- and lateral-sections indicates greater TGF- β 1 expression in the SCI smooth muscle tissue.....	102
Figure 4-4. TGF- β 1 expression is quantitatively greater in the SCI tissue in both the cross- and lateral-sections. Expression was calculated as the ratio of total fluorescent area to total smooth muscle area. n=48 for all cases but the lateral control case which was n=44. Values represent mean +/- SEM and * indicates p<0.005.....	103
Figure 4-5. Basal BSMC contraction of anchored collagen gels is greater for the highest population of cells at 2 and 4 hours. All anchored collagen gel assays were performed using the three cell populations in control conditions (RPMI 1640 and 2% FBS). n=13-18, 16-21, and 9-17 for 5×10^4 , 1×10^5 , and 2.5×10^5 BSMCs, respectively. Values represent mean +/- SEM and * indicates p<0.05.....	104
Figure 4-6. TGF- β 1 inhibits contraction of anchored collagen gels by (A) 5×10^4 , (B) 1×10^5 , and (C) 2.5×10^5 BSMCs. Anchored collagen gel contraction was assessed in control conditions with and without 1 ng/ml TGF- β 1. n=8-18, 10-21, and 7-17 for 5×10^4 , 1×10^5 , and 2.5×10^5 BSMCs, respectively, for the control and TGF- β 1 cases. Values represent mean +/- SEM and * indicates p<0.05.....	105
Figure 4-7. Fluorescent antibody labeling of caldesmon (both isoforms) and h-CaD in BSMCs after 4 hours on glass coverslips for control and TGF- β 1 cases. Caldesmon labels intensely in the actin cytoskeleton and cytoplasm for both cases, whereas h-CaD staining is less intense, cytosolic, and further diminished in the TGF- β 1 case.....	106

Figure 4-8. (A) An example of a contracted anchored collagen gel between the steel mesh anchors 5×10^4 BSMCs after 24 hours. (B) SALS image of the same collagen gel. Dotted box depicts area of analysis containing the 704 OI values averaged to represent the physical remodeling or reorganization of each collagen gel. Areas of red depict highly oriented fibril networks (corresponding to small OI values), whereas areas of blue indicate randomly oriented fibril networks (corresponding to large OI values).....106

Figure 4-9. TGF- β 1 increases collagen gel alignment and orientation (smaller OI values) for 2.5×10^5 BSMCs. 2.5×10^5 BSMCs physically remodel and organize the collagen gels (smaller OI values) more than the other two BSMC populations (not shown statistically on graph). OI values were assessed after 24 hours of contraction for the 5×10^4 and 1×10^5 BSMCs and 18 hours for the 2.5×10^5 BSMCs. n=4-7, 5, and 8-9 for 5×10^4 , 1×10^5 , and 2.5×10^5 BSMCs, respectively, for the control and TGF- β 1 cases. Values represent mean +/- SEM and * indicates $p < 0.005$107

Figure 4-10. Contracted anchored collagen gels and accompanying SALS images for control and TGF- β 1 cases for (A) 5×10^4 BSMCs at 24 hours, (B) 1×10^5 BSMCs at 24 hours, and (C) 2.5×10^5 BSMCs at 18 hours. Highly aligned areas of collagen fibrils (red) increase with increasing cell populations and are more prominent at higher cell populations. TGF- β 1 induces the formation of white patches on the collagen gels (B, C).....109

Figure 4-11. Cell morphology on anchored collagen gels for (A) 5×10^4 , (B) 1×10^5 , and (C) 2.5×10^5 BSMCs at 4 and 24 hours for control and TGF- β 1 cases. Spreading depends on cell population with a higher number of cells spreading faster on the collagen gel surfaces at 4 hours and maintaining this morphology at 24 hours in the control cases. By 24 hours, the majority of BSMCs are spread and elongated in the control conditions. However, TGF- β 1 induces cell bundles or aggregates (B, C) which correspond to white patches on the collagen gels and regions of high collagen fibril alignment.....110

Figure 4-12. An anchored collagen with 2.5×10^5 BSMCs after (A) 18 hours of contraction and followed by (B) 4 days of trypsinization shows that the changes in collagen gel architecture caused by the BSMC aggregates are conserved.....111

Figure 5-1. Scanning electron microscopy images of control SIS (a), SIS digested with collagenase-I for 5 hours (b), MDSC on SIS for 24 hours (c), and MDSC on SIS for 7 days in culture (d) [171].....116

Figure 5-2. Normalized MMP-1 activity of supernates of (a) MDSC on SIS and MDSC on tissue culture polystyrene and (b) SIS alone. In b, SIS releases residual MMP-1, which decreases linearly over time. Data are mean +/- s.e.m. n=3 per group in triplicate [171].....118

Figure 5-3. Representative plot of equi-biaxial testing experiments in the longitudinal direction (a) and circumferential direction (b) on SIS digested with 0.16 U/mL collagenase-I for 5 hours, MDSC seeded SIS for 10 days, and control	119
Figure 5-4. DNA quantification at 7 days growth factor treatment. n=6 per group. *,+ p<0.05 compared to all other groups except each other.....	127
Figure 5-5. DNA quantification following 14 days culture with 7 days static growth factor treatment, 7 days no treatment static or stretched. Data are presented as mean +/- s.e.m, n=6 per group. All VEGF groups and FGF-2 groups are statistically significantly greater than the no growth factor treated group, p<0.01.....	127
Figure 5-6. Top panel, DAPI stained nuclei following 7 days with growth factor treatment on SIS. Bottom panel, light microscopy image of SIS cross section.....	128
Figure 5-7. DAPI stained cell nuclei at days 2, 4, and 7. Images are reduced from 100x.....	129
Figure 5-8. Normalized cell nuclei counts on the unseeded side of transwell inserts at A. 2 days, B. 4 days, C. 7 days. N=3 transwells per group with 5 images from each transwell analyzed. *p<0.01 compared to regular media controls.....	130
Figure 5-9. Elastic trichrome staining of A. NG 14 day static B. VEGF 7 day NG 7 day static C. FGF-2 7 day NG 7 day static D. Unseeded SIS E. VEGF 7 day Stretch 7 day 0.1 Hz F FGF-2 7 day Stretch 7 day 0.1 Hz G. VEGF 7 day 0.5 Hz 7 day, H. FGF-2 7 day 0.5 Hz 7 day. Images are reduced from 200x. Scale bar represents 100 μ m.....	132
Figure 5-10. Elastin protein concentration per gram wet weight of BSMC seeded SIS. Data are presented as mean +/- s.e.m. with n=6 per group. *indicates statistical significance with p<0.01 compared to all other groups.....	133
Figure 5-11. Soluble collagen concentration per gram wet weight of BSMC seeded SIS. Data are presented as mean +/- s.e.m. with n=6 per group. *indicates statistical significance with p<0.05 compared to all other groups.....	134
Figure 5-12. Verhoff's Van Gieson staining of A. SIS, B. Seeded SIS treated with VEGF for 7 days stretched at 0.1 Hz for 7 days, C. Seeded SIS treated with FGF-2 for 7 days then stretched at 0.1 Hz for 7 days. Black lines indicate presence of elastin. Images are representative from n=4 per group and are reduced from 400x. Scale bar represents 50 μ m.....	135
Figure 5-13. Top: MMP activity in collected media. Bottom: collagen in collected media.....	137

Figure 5-14. Summed totals of soluble collagen found in media (top) and MMP-2 and 9 activity found in media (bottom) of BSMC seeded SIS. Data are presented as mean +/- s.e.m. with n=6 per group. * indicates p<0.05 compared to all other groups. + indicates p<0.05 compared to all groups except FGF-2 at 0.5 Hz.....	138
Figure 6-1. Organ culture preparation. A. Bladder wall divided with UBM sutured in between the two halves B. Schematic of uniaxial bioreactor set up with UBM augmented bladder strip.....	149
Figure 6-2. UBM sutured in between 2 halves of a rat bladder strip. The bladder strip was prepared with stainless steel spring grips attached to the longitudinal ends (original length 10 mm), it was then cut in half and a piece of UBM (8 mm) was sutured to each edge. Arrows show interface between UBM and bladder wall.....	150
Figure 6-3. Scanning electron microscopy of BSMC on alternating 100 μm grooves (A) and 10 μm grooves with 100 μm raised in between (B), depth of all grooves was 5 μm.....	153
Figure 6-4. Bright field microscopy of overgrown BSMC on alternating 100 μm grooves (A) and 10 μm grooves with 100 μm raised in between (B), depth of all grooves was 5 μm.....	153
Figure 6-5. Elastin deposition onto silicone under static, uniaxial, and biaxial stretch. n=4 for static and uniax, n=3 for biax in 0.5Hz group n=1 for 1Hz group; * p<0.05.....	154
Figure 6-6. Collagen deposition onto silicone surface under static, uniaxial, and biaxial conditions. n=3 or 4 for each group, *p<0.05.....	155
Figure A-1. Photolithography process.....	158
Figure A-2. Biaxial stretch bioreactor. A. Bath with 4 grips and silicone sample, B. Running bioreactor with 4 linear actuator motors.....	159

PREFACE

Firstly, I would like to thank the Department of Bioengineering at the University of Pittsburgh and its chair, Dr. Harvey Borovetz for all of his support. I would also like to thank the administrative staff in the Department of Bioengineering, particularly Ms. Lynette Spataro and Mrs. Joan Williamson for all of their help along the way. I would like to thank my dissertation committee for their helpful comments and questions that led to improvements in my research. I'd also like to thank Dr. Michael Chancellor for his guidance and collaboration as well as others in the Center for Urological Research Excellence including Vickie Erikson, Dr. Naoshi Yoshimura, and Dr. Fernando de Miguel. Additionally I would like to thank Dr. Chet de Groat for his amazing knowledge base, wisdom, and input. Finally I would like to thank Dr. Michael Sacks for his mentoring and support, the opportunity to learn and work in a competitive research environment, and the many opportunities he gave me to present my work at numerous scientific conferences.

My great appreciation and thanks also goes to two postdoctoral associates who helped me during my 5-year tenure as a graduate student. Dr. Jiro Nagatomi, thank you for your help and mentoring in getting me started in my graduate career. Dr. Aron Parekh, thank you for all of your help, mentoring, and friendship in the crucial moments of my dissertation work. I really appreciate all of your input. Also, I'd like to specifically thank Dr. David Merryman whose help in brainstorming turned into the start of this dissertation project. I'd also like to thank my

undergraduate assistant, Miss Julia Ivanova, for all of her help with cell culture, assay assistance, catching some of my mistakes, and making me feel old. I'd further like to thank Jennifer DeBarr, for her great help in histological sectioning and staining, Marc Rubin and the Center for Biological Imaging for all of their help with microscopy, Dr. Sandy Hu for teaching my photolithography, The Badylak Laboratory, for their assistance in my assays, and The Russell Laboratory, for their friendships, BBQs, and allowing me to use their microscope. A big thank-you also goes to several administrative assistants for all of their help: Anna Goldman, Lynn Ekis, and Beth Markocic. I would also like to thank the members past and present of the ETM²L in no particular order: Dave Merryman, Jon Grashow, Dan Hildebrand, George Englemayr, Jiro Nagatomi, Leigh McClure, Heather (Gray) Bolton, Khash Toosi, Brett Zubiate, Todd Courtney, John Stella, Ajay Abad, Aron Parekh, Erinn Joyce, Jun Liao, Silvia Wognum, Diana Gatian, Chad Eckert, Dave Schmidt, Julia Ivanova, Mike McCall, Bahar Fata, and Chris Carruthers. Thank you all for your friendship, humor, appreciation of Belgian beer, political discussions, and general commiserating. I certainly couldn't have finished this work if it weren't for all of you. Best wishes and good luck in all your future endeavors!

Most importantly I would like to thank my family and my fiancé Matthew Heise. To my parents, siblings, and to be in-laws, I can't thank you enough for always being there for me. Matt, the absolutely positively best thing about graduate school was meeting you. You have been so incredibly supportive as we both have gone through this dissertation process. You have all my love and gratitude, and I can't wait to start our future together.

NOMENCLATURE

ECM – extracellular matrix

BSMC – bladder smooth muscle cells

GAG – glycosaminoglycan

Cx43 –connexin 43

α -SMA – alpha smooth muscle actin

nmMHC – non-muscle myosin heavy chain

CaD – caldesmon

h-CaD – heavy molecular weight form of caldesmon

l-CaD – light molecular weight form of caldesmon

SCI – spinal cord injury

UBW – urinary bladder wall

EGFP - enhanced green fluorescent protein

SIS – small intestinal submucosa

UBM – urinary bladder matrix

BAM – bladder acellular matrix

MMP – matrix metalloproteinase

FGF-2 – basic fibroblast growth factor

VEGF – vascular endothelial growth factor

TGF- β 1 – transforming growth factor beta 1

MDSC – muscle derived stem cells

ANOVA – analysis of variance

SNK – student Neuman Kiels

s.e.m. – standard error of the mean

TE – tissue engineering

1.0 INTRODUCTION

1.1 THE URINARY BLADDER

The urinary bladder is a hollow organ that sits on the pelvic floor muscles behind the pelvic bone. The urinary bladder's main function is to store large volumes of urine that flow to the bladder from the kidneys through the ureters. When the bladder is full, the bladder voids with a coordinated smooth muscle contraction with a simultaneous relaxation of the urethral sphincter. When this simultaneous contraction and relaxation occurs, urine flows from the bladder through the urethra out of the body. The urinary bladder, while seemingly a simple hollow organ, is composed of several different layers containing many cell types and extra cellular matrix (ECM) proteins that contribute to maintaining the bladder's normal function.

1.1.1 Bladder layers and cell types

The layers of the bladder wall are: the mucosa, submucosa, detrusor, and adventitia (depicted in Figure 1-1). Each of these layers provides both a biological and biomechanical function. The most interior layer of the bladder is the mucosa. The mucosa contains both the transitional epithelium and the lamina propria. The transitional epithelium or urothelium contains a superficial layer of umbrella or flat cells with a deeper layer of columnar and cuboidal cells that function together to create a barrier to urine, maintain the urine composition, and facilitate

voiding. The umbrella cells provide an initial barrier to urine and are covered with a glycoaminoglycan (GAG) layer (Figure 1-2) [1]. The umbrella cells have the ability to change surface area dramatically and are the largest epithelial cells in the body, ranging up to 200 μ m in diameter. They may also be multinucleate and possess maintain a large pH gradient from the urine to the plasma within the cell. The differentiated urothelium expresses uroplakins that may be used as cellular markers to discriminate urothelial cells from other epithelium.

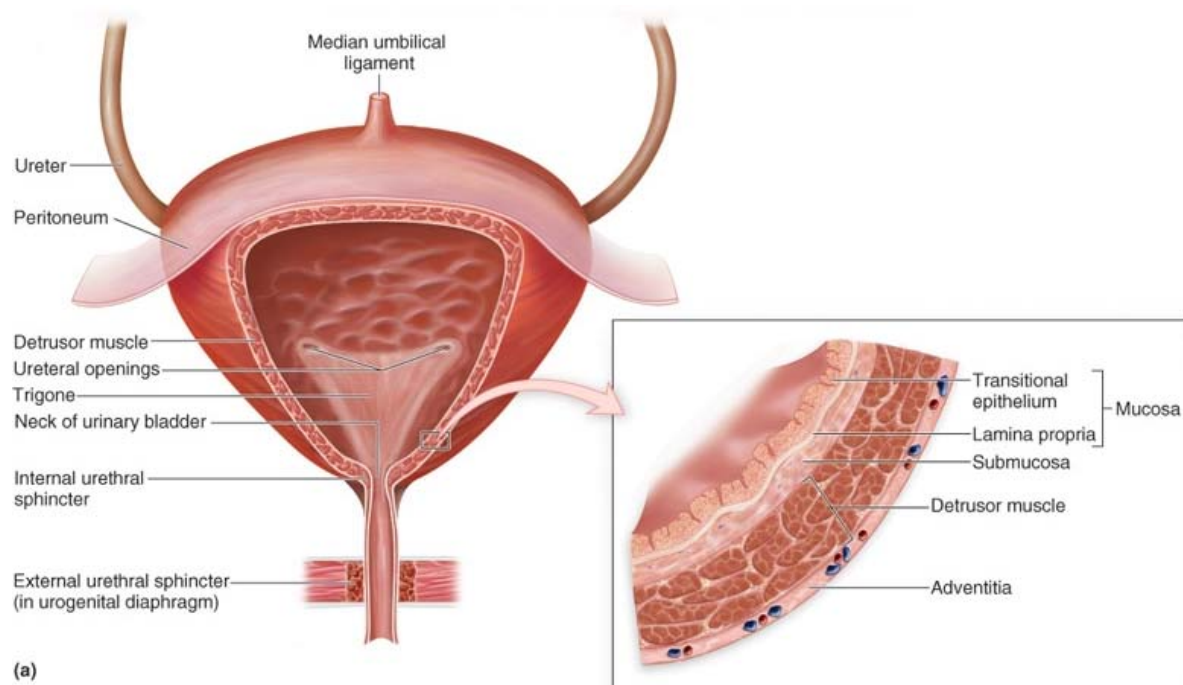


Figure 1-1. *The urinary bladder.* Reprinted from academic.kellogg.cc.mi.us/herbrandsonc/bio201 .

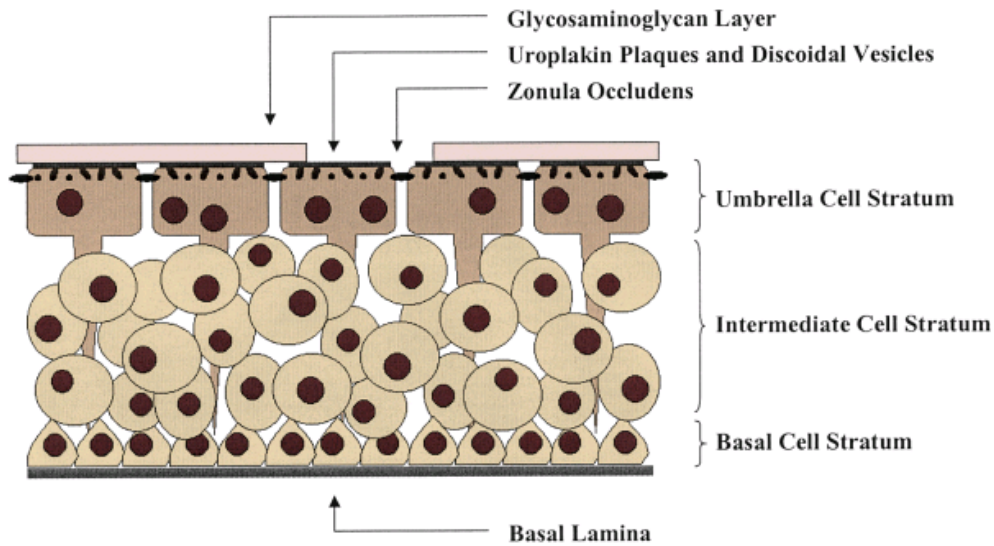


Figure 1-2. Urothelial organization. Reprinted from [1].

The lamina propria interior to the urothelial lining is a membrane consisting of a dense ECM with nerves, blood vessels, glands, and myofibroblast cells. The ECM of the lamina propria is composed mainly of collagen types I, III and IV with some elastin interspersed throughout. A previous study has suggested that the lamina propria is responsible for bladder compliance at the early and late stages of bladder filling [2]. Among the cell types associated with blood vessels (vascular smooth muscle cells and epithelium), innervation, and lymphatic glands, the prominent cell type in the lamina propria is the myofibroblast. Until recently, the suburothelial myofibroblast was poorly understood; however, there is now more concrete evidence that the myofibroblast plays a valuable role in communication between the urothelium and the detrusor smooth muscle. The myofibroblasts lie in rows under the urothelium and have alignment and projections parallel to the urothelium [3]. The myofibroblasts are the main place in the bladder where the gap junction protein connexin 43 (Cx43) is found co localized in cells with positive staining for vimentin in this region of the bladder. The general understanding of the

myofibroblasts function is that they form part of a sensory response to filling that cause the urothelium to release transmitters [3].

Exterior to the mucosal layer of the bladder is the detrusor layer. The detrusor is comprised of bundles of detrusor smooth muscle cells, referred to in the present study as bladder smooth muscle cells (BSMC). These muscular bundles are organized in 2 layers in the rat bladder and 3 layers in the human bladder. In the human bladder, the smooth muscle bundles in the outer and inner layers are arranged longitudinally and the middle layer is arranged circumferentially [4]. These layers are depicted in Gray's anatomy Figure 1-3.

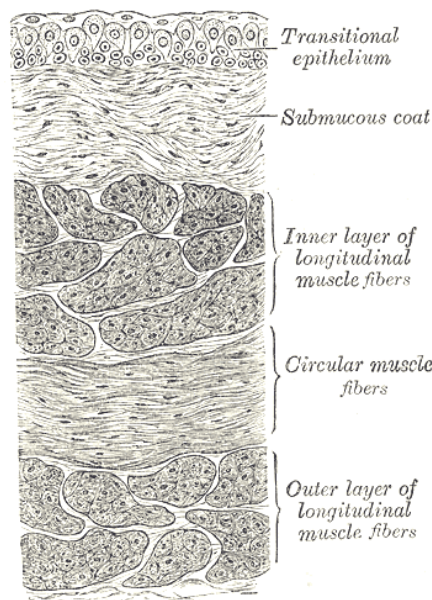


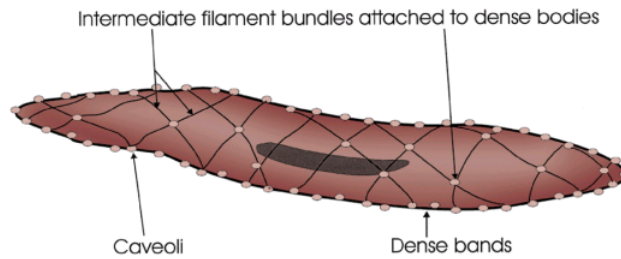
Figure 1-3 . Layers of the urinary bladder wall. Reprinted from [5].

Each muscle bundle within the detrusor is surrounded by collagen and a thin layer of elastin. The surrounding ECM is composed of mainly collagen with some elastin in a matrix of proteoglycans [1]. The ECM in the detrusor has been shown to change in composition in pathological states. In spinal cord injury, our laboratory has found previously that elastin and

collagen content is altered within the detrusor [6]. Changes in the ECM content within the detrusor ultimately affect the biomechanical properties of the bladder wall. Following SCI, the viscoelastic properties of the bladder wall change due to corresponding changes in ECM [7]. Other studies of bladder outlet obstruction have shown similar changes in the ECM within the detrusor. However, it has not been shown conclusively that changes in biomechanical properties following these pathologies is due to the changes in the ECM alone or in combination with the detrusor smooth muscle bundles.

The smooth muscle in the bladder contains actin and myosin scattered throughout the cell, not in a sarcomeric pattern as in skeletal muscle. The smooth muscle in the bladder must regularly undergo immense length changes that are not matched anywhere else in the body. It is the arrangement of the contractile machinery in the smooth muscle that allows for this immense length change [8, 9]. The smooth muscle maintains a tone that can be modulated with pharmacologic agents. The smooth muscle excitation/contraction coupling is shown in Figure 1-4. The detrusor muscle also has the ability to generate contractile force without external stimuli through the electrical coupling between BSMCs. The muscle exhibits spontaneous rhythmic activity witnessed both *in vitro* and *in vivo* [4]. Under pathological conditions such as obstruction or spinal cord injury (SCI), these cell-cell interactions may be disrupted causing changes in transmission of excitation leading to hypertrophy and dysfunction of the bladder [10].

A) Relaxed smooth muscle cell



B) Contracted smooth muscle cell

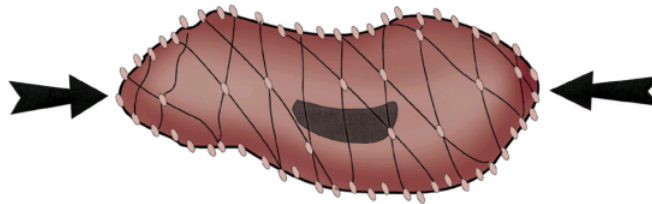


Figure 1-4. Depiction of BSMC contraction through shortening. [1].

The BSMCs themselves are characterized by expression of specialized contractile machinery found specifically in smooth muscle. The precise arrangement of thin actin filaments and thicker myosin filaments has not been fully characterized in smooth muscle [4]. There are four different isoforms of actin expressed in smooth muscle α -, β -, and two isoforms of γ - actin. The most prominent of these isoforms in rat and human are α - and γ - actin [4]. The functional roles of these actin isoforms are unclear at present and are an area of future research. Alpha-smooth muscle actin (α -SMA) is commonly used as a marker of smooth muscle cells as it is predominately found in smooth muscle, but it also may be located in fibroblasts and myofibroblasts under pathological conditions in multiple organs, such as heart valve leaflets, vascular networks, the airway, and liver among others. Probably the most important contractile protein in the BSMC crucial to proper function is myosin. There exists 3-5 times less myosin in

smooth muscle than in skeletal muscle, and the ratio of actin to myosin is approximately 15:1 [4]. Smooth muscle myosin is in the myosin II superfamily of myosin motors [11]. The myosin molecule is formed with two heavy chains and two pairs of light chains. The inserted heavy chain myosin isoform, SM-B, is expressed highly in the urinary bladder and is responsible for the bladder smooth muscle being a relatively fast smooth muscle type [12]. The myosin heavy chains are generally thought to be responsible for contractile kinetics in bladder smooth muscle, but it is thus far unknown exactly how these heavy and light chains interact with the entire cytoskeletal structure. In addition to the muscle myosin, smooth muscle can also express non-muscle myosin heavy chain (NM-MHC). These chains are not heavily expressed in the adult, and have been shown to be important in development, migration, and proliferation of the BSMC in culture [13]. Additionally in the contractile domain of the cytoskeleton, there are dense bodies that are associated with a network of the intermediate filaments. The intermediate filaments are mainly composed of desmin and vimentin. The urinary bladder in rat and humans contain predominantly desmin filaments [4]. Other contractile proteins of interest commonly used as markers for smooth muscle, are caldesmon (CaD) and calponin. CaD is bound to thin filaments and interacts with tropomyosin, myosin, and calmodulin [4]. CaD has been found to stabilize actin as well as intermediate filaments [14]. There are two isoforms of CaD: h-CaD (high molecular weight) and l-CaD (low molecular weight). H-Cad is specific to smooth muscle cells. The l-CaD is present in nonmuscle cells, although it is present in small amounts within smooth muscle [14]. In longer-term BSMC culture as well as in the hypertrophic bladder the l-CaD content increases. It is for this reason that the present study utilized BSMC prior to passage 10 in culture. It is thought that the l-CaD protein is important in regulating cell division, migration, and shape changes [14]. The protein calponin is also associated with actin filaments and is localized

in both the contractile and cytoskeletal domains of the smooth muscle cells [15]. It has been shown in assays to inhibit contractions and filament sliding [4]. The contractile sequence of the BSMC is as follows:

1. Ca^{2+} binds to calmodulin, activating it.
2. Calmodulin activates the kinase enzyme.
3. Kinase enzyme catalyzes phosphate transfer from adenosine triphosphate to myosin, allowing myosin to interact with actin of the thin filaments.
4. Smooth muscle relaxes to widen intracellular decrease in Ca^{2+} levels [1].

All of the aforementioned contractile and synthetic cytoskeletal proteins serve important roles in maintaining the function of BSMC within the detrusor.

Finally, on the exterior of the detrusor lie an adventitia on one side of the bladder and the serosa on the other. The serosa is a peritoneal layer covering the superior surface of the bladder. Where there is no serosa, the adventitia covers the rest of the bladder. The adventitia is a loose collagenous network interspersed with vasa vasorum [1]. These layers are also surrounded by peritoneal fat.

1.1.2 ECM components

The collagen within the bladder wall ECM is composed of primarily collagen type I and III with varying ratios among species [16]. Collagen type IV is found in large amounts within the lamina propria of the bladder wall [17]. Collagen types I and III surround the smooth muscle bundles and make up the majority of the ECM found within the bladder wall. Collagen types I and III are

among the five types of collagen that are capable of forming fibrils that can be visualized with electron microscopy [18]. The interstitial collagens (including types I and III) are formed through cells producing pre-procollagen chains along the rough endoplasmic reticulum that are later cleaved within the rough endoplasmic reticulum to form procollagen. Then, lysine and proline amino acids on the procollagen are hydroxylated and the glycosylated to form a triple helix structure. The procollagen is then moved outside of the cell via exocytosis following packaging from the Golgi apparatus. Within the ECM, peptides are cleaved and tropocollagen is formed by procollagen peptidase. Then, multiple tropocollagen molecules can form collagen fibrils. Multiple collagen fibrils form collagen fibers. Collagen type I is found in most connective tissues within the body. Type I and III collagens are capable of forming co-fibrils in many tissues [18]. Collagen type III can also form a separate population of thin fibrils.

In the human bladder, it has reported that the ratio of collagen type I to collagen type III is 1:11.1 [16]. However, in the rat bladder there is more collagen type I than collagen type III [19]. The concentration of collagen within the bladder becomes altered under pathological conditions. In poorly compliant bladders, it has been found that most fibrosis is due to collagen type III [20]. Macarak and Howard have performed extensive work on the collagen within the bladder [17, 21, 22]. They have suggested that in non-compliant bladders the collagen fibers can no longer alter their tortuosity, reducing bladder capacity [22]. In the SCI bladder, collagen protein concentration is up-regulated following 2 months after SCI [23]. The diverted sheep bladder undergoes smaller bladder capacity with contracted collagen, underlining the importance of mechanical stimulation on maintenance of collagen architecture. Alterations in collagen content alter the biomechanical properties of the bladder wall, leading to dysfunction.

The mechanical role of the collagen during bladder filling and voiding has been explored previously. During filling between 0-25%, the lamina propria thins more rapidly than the rest of the detrusor indicating that it plays more of a mechanical role during this portion of filling [24]. From 25%-50% the detrusor carries the mechanical load, and then from 50%-100% of filling the lamina propria again bears the mechanical load [24]. An additional study by Ewalt et al indicated that the lamina propria was responsible for normal bladder compliance while changes in collagen types I and III within the detrusor were responsible for fibrotic bladder compliance [2]. As the lamina propria is made up mostly of connective tissue, the mechanical properties depend on the structure of this tissue. Collagen type III has been found in super coils within the lamina propria of the bladder [25]. These collagen supercoils appear to uncoil while the bladder is filled providing some distensibility; however even at 100% filling the collagen fibers still remain in a coil structure (Figure 1-5, [26]). Chang et al. have theorized that the collagen in the bladder exists in a hierarchy of folding and coiling beyond simple uncrimping in which large coils of collagen fibers are able to accommodate very large strains [25]. The impact of collagen types I and III on the biomechanical properties of the bladder wall has further been demonstrated by studies in our laboratory wherein biaxial mechanical testing was performed this is described in section 1.2.3.

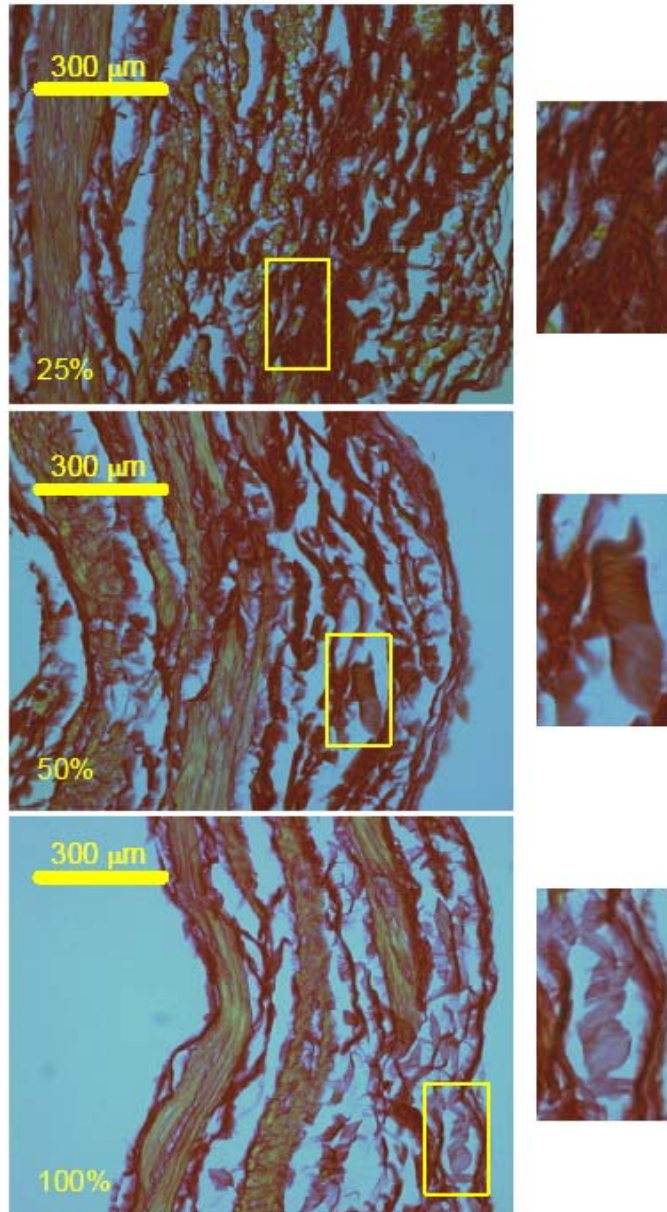


Figure 1-5. *Collagen coils during filling.* [26].

Elastic fibers in the bladder are found in all layers of the bladder wall. These elastic fibers allow the bladder to recoil to its original shape following distension. Elastic fibers are made up of a microfibrillar component and an elastin component (Figure 1-6). The microfibrillar component is composed of 5 different proteins predominantly fibrillin, found in forms fibrillin-1 and fibrillin-2 [27]. Other microfibrils of note are the microfibril associated glycoproteins 1 and

2 (MAGP-1 and -2). The elastin component is synthesized in monomer form as tropoelastin, a 70 kDa protein. Outside of the cell, the tropoelastin monomers are assembled into polymeric form within the ECM. The elastin polymers are covalently cross linked together through side chains of lysine after oxidative deamination by lysyl oxidase [27]. Figure shows the assembly of elastic fibers with an elastic core surrounded by microfibrils. Once assembled into an elastic fiber, these fibers may be ordered with the aid of cells (mainly fibroblasts) within the ECM [27]. However, the elastin proteins do have the unique ability to self-assemble and conglomerate outside of the cell [27].

It is generally assumed that elastin, once laid down and crosslinked, turns over at a rate of less than 1% [28] in any tissue other than the uterus [29]. Elastic fibers making up a large majority of ECM in skin, arterial blood vessels, lung parenchyma, and elastic ligaments are formed in gestation and in the first year of life with little to no new elastin being produced past the first decade [28]. While degradation of elastin is common to many disease states, such as vascular disease and uterine prolapse, several organs have been shown to synthesize elastin under pathological conditions. In the dermis it has become well accepted that elastin synthesis occurs following injury [30]. Elastin synthesis is also observed in the fibrotic liver [31]. In an experimental model of liver fibrosis the common bile ducts in the liver are ligated, increased tropoelastin and fibrillin synthesis is observed in a rat [30]. It has been demonstrated in the inflamed airway, the smooth muscle cells produce large amounts of ECM proteins, including elastin [32]. It has also become generally accepted that hypertensive arteries experience a thickening in the tunica media as a result of increased elastin synthesis [33]. In the urinary bladder, gene expression of tropoelastin and lysyl oxidase were shown to be up regulated in rat models of both diabetes [34] and SCI [35]. Elastin has also been observed in obstructed bladders

both intra- and inter- fascially in the detrusor [36]. Elastin synthesis following SCI will be discussed in the next section.

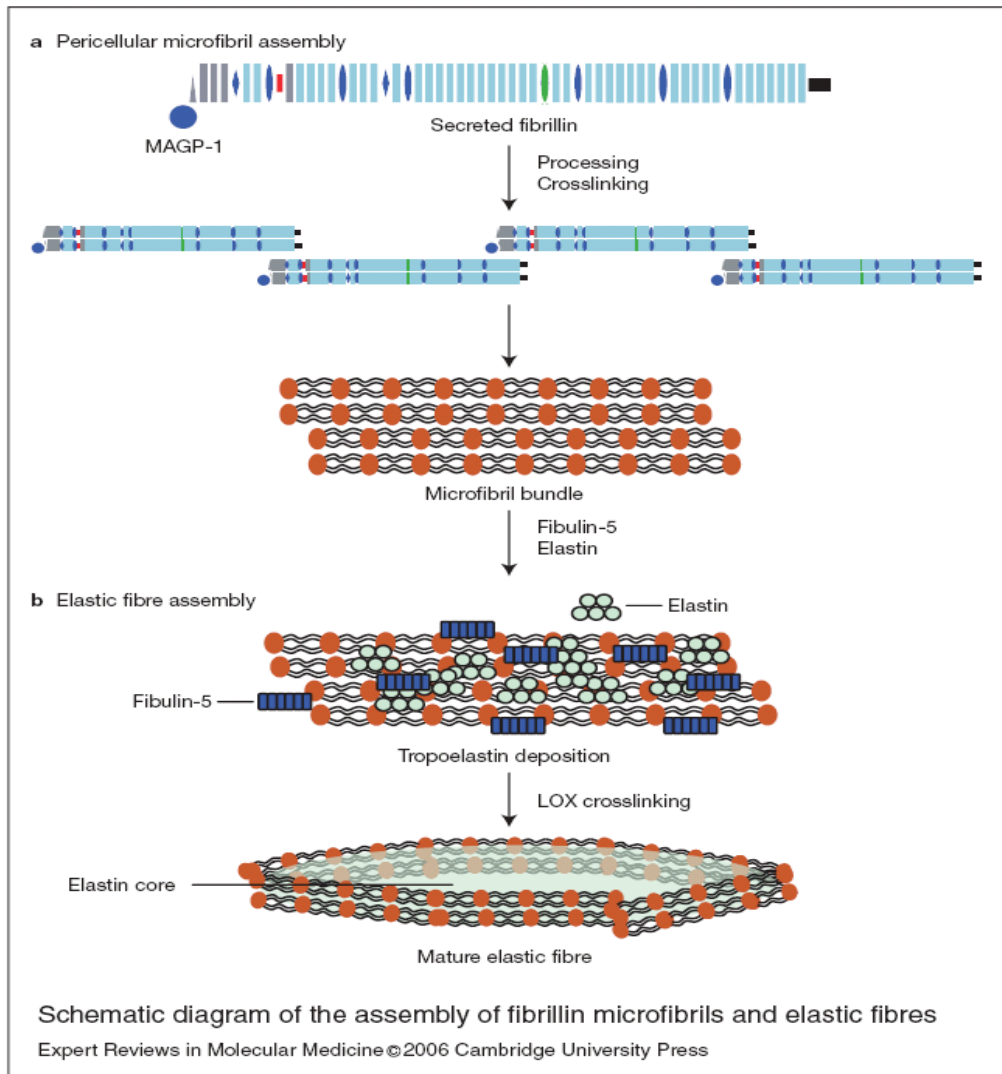


Figure 1-6 *Assembly of mature elastic fibers. Reprinted from [37]*

The majority of the elastin synthesis that occurs under these aforementioned pathologic conditions is presumably in response to mechanical forces on the tissue. The effect of mechanical force on ECM production has been examined in a wide variety of cell types and

tissues. In development, many of the ECM structures run parallel to the development of cardiac pressure, such as has been found in the lamb pulmonary artery [38]. In response to mechanical stimulation in vitro, organ culture of pulmonary arteries have produced enhanced elastin synthesis in response to sustained mechanical stretch or pressure [38]. Human gingival fibroblasts produced significantly more elastin when mechanically stretched at 1 Hz, 10% strain compared to statically cultured cells [39]. Several studies have demonstrated that vascular smooth muscle cells produce elastin when seeded on collagen gels or synthetic scaffolds and exposed to pulsatile flow and/or mechanical stretch [40]. It should be noted however, that the elastin produced by stretching isolated cells and intact tissue is of an amorphous nature, and it has been difficult, until the present study, to coax the cells into producing assembled elastin fibers in vitro.

There are several other ECM proteins in the bladder wall. Laminin and cellular adhesion molecules are found abundantly in the submucosa of the bladder [41]. In addition to assisting the urothelium in retaining a barrier against urine, the GAGs in the bladder wall are found throughout the matrix. The GAGs give the bladder the ability to create a compartment of tissue water that allows the bladder to have viscous behavior when deformed during filling [1].

1.2 PHYSIOLOGY AND DISEASE STATES OF THE URINARY BLADDER

1.2.1 Normal filling and voiding

Normal filling of the bladder results from peristaltic contractions of the urinary tract which move urine produced in the kidney through the ureters into the bladder. These peristaltic contractions occur 1-5 times/ minute. The bladder wall smooth muscle relaxes and the urothelial layers and ECM matrix stretch as the bladder is filled to accommodate the increasing volume of urine. Once the bladder has reached a certain capacity (350-400 mL in humans and 0.7-0.8 mL in rats), a signal is sent from urothelial and smooth muscle stretch receptors to the afferent nerves found in the mucosal layer of the bladder to the brain. When voiding is to occur, the signal is then sent through the efferent nerves to the detrusor which signals the bladder smooth muscle to contract (Nerve pathways shown in Figure 1-7). Simultaneously, signals are sent to the pudendal nerve causing the urethral sphincter to relax allowing urine to flow out of the body [42]4 #26].

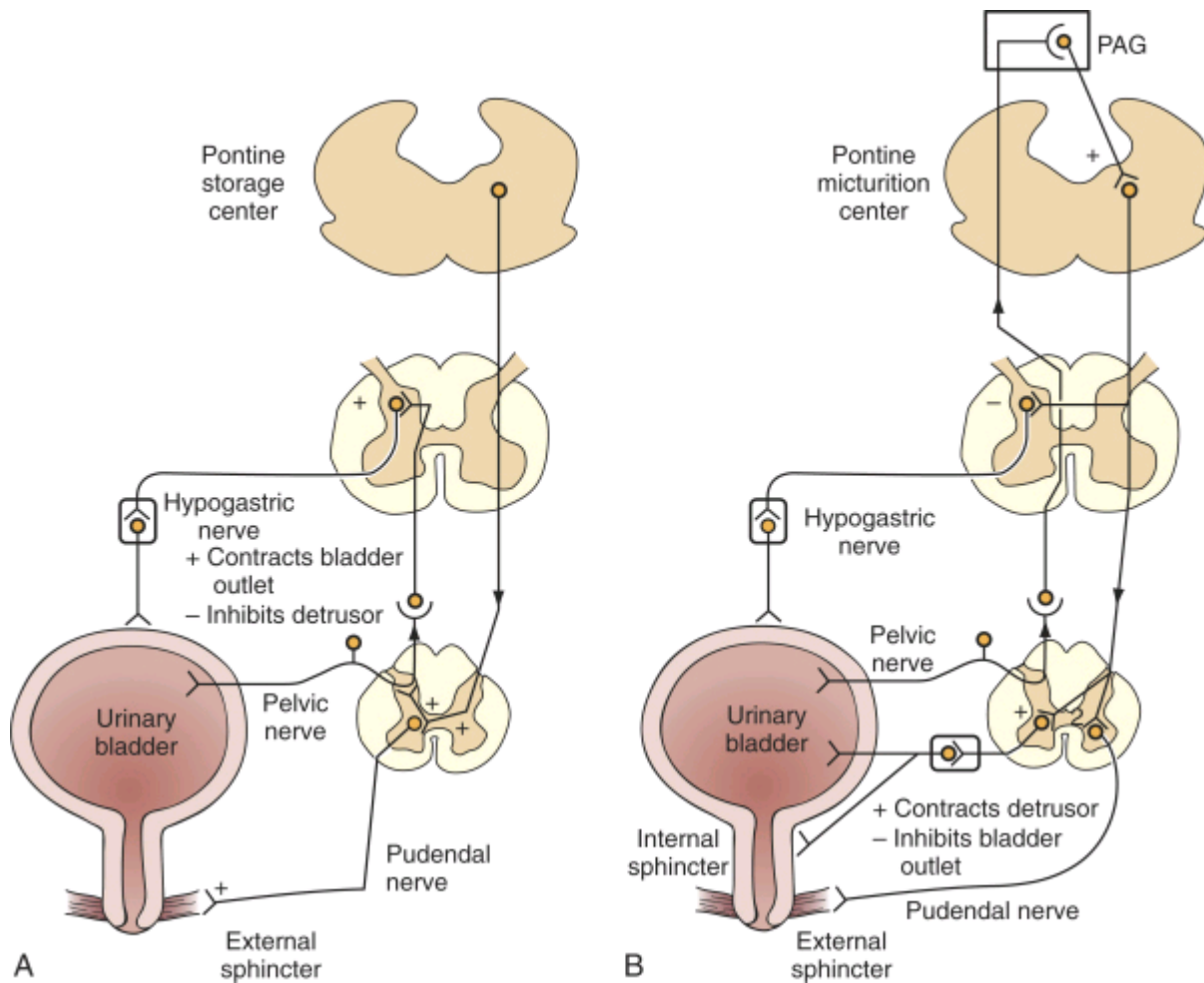


Figure 1-7. Mechanism of storage and voiding reflexes. **A**, Storage reflexes. During the storage of urine, distention of the bladder produces low-level bladder afferent firing. Afferent firing in turn stimulates the sympathetic outflow to the bladder outlet (base and urethra) and pudendal outflow to the external urethral sphincter. These responses occur by spinal reflex pathways and represent “guarding reflexes,” which promote continence. Sympathetic firing also inhibits detrusor muscle and transmission in bladder ganglia. **B**, Voiding reflexes. At the initiation of micturition, intense vesical afferent activity activates the brainstem micturition center, which inhibits the spinal guarding reflexes (sympathetic and pudendal outflow to the urethra). The pontine micturition center also stimulates the parasympathetic outflow to the bladder and internal sphincter smooth muscle. Maintenance of the voiding reflex is through ascending afferent input from the spinal cord, which may pass through the periaqueductal gray matter (PAG) before reaching the pontine micturition center. Reprinted from [1].

1.2.2 Neurogenic disorders

Neurogenic bladder pathologies can develop as a result of spinal cord injury (SCI), infarction of the frontal cortex of the brain such as seen in Parkinson's disease, or lesions of the nerves of the bladder such as seen in Multiple Sclerosis. Simply put the neurogenic bladder results in 2 classifications of dysfunction. The first is failure to store urine and the second is failure to empty urine. These two modes of dysfunction are caused by 5 different complications, which occur at in combination or at different phases depending on the severity of SCI or cause of neurogenic bladder [43]. The first complication is decreased sensitization. This results from loss of nerve sensation from the bladder causing the inability to stimulate a simultaneous contraction of the detrusor to void [43]. This causes urinary retention over time. The second complication is hyperreflexia. This occurs when the bladder loses the signal from the brain that inhibits voiding. The hyperreflexic bladder contracts frequently even at relatively small volumes. The third complication is hypocontractility of the detrusor [43]. Hypocontractility occurs when there is sensory loss and the brain cannot detect that the bladder is full. The fourth complication is poor bladder compliance [43]. When the bladder loses its ability to store urine at low pressures, it eventually loses its ability to expand due to many years of central nervous system injury or continuous infection and inflammation. The non-compliant bladder can lead to pressure build up to over 40 cm H₂O which causes severe damage to the kidneys. The fifth complication seen in neurogenic bladders is sphincteric dysfunction [43]. This dysfunction often manifests as detrusor sphincter dyssynergia wherein the urethral sphincter and bladder contracts simultaneously. Additionally, sphincter dysfunction may manifest as intrinsic sphincter dysfunction which may be the result of previous sphincter injury [43].

In the U.S. alone approximately 11,000 new people suffer from spinal cord injury (SCI) each year. As mentioned above, SCI rostral to the lumbar spine can lead to severe lower urinary tract dysfunctions including bladder outlet obstruction and detrusor instability [44]. In addition to the functional deficiency, these bladder dysfunctions are often accompanied by changes in the wall tissue morphology such as hypertrophy [45], trabeculation [46], and fibrosis [47] as well as by significant changes in the mechanical properties of the wall [48-50]. The majority of these SCI patients develop urologic complications, which include urinary retention (due to incomplete voiding) and overactive bladders (due, for example, to abnormal neurogenic inputs and/or alteration in myogenic functions) [44, 51-53]. It has also been reported in the literature that these neurogenic bladders develop hypertrophied and/or fibrotic walls and that compliance of the bladder is significantly altered in the chronic SCI patients compared to normal individuals [47, 50]. These findings suggest that there may be strong correlations between the tissue morphology, mechanical properties of the wall and the health state of the bladder.

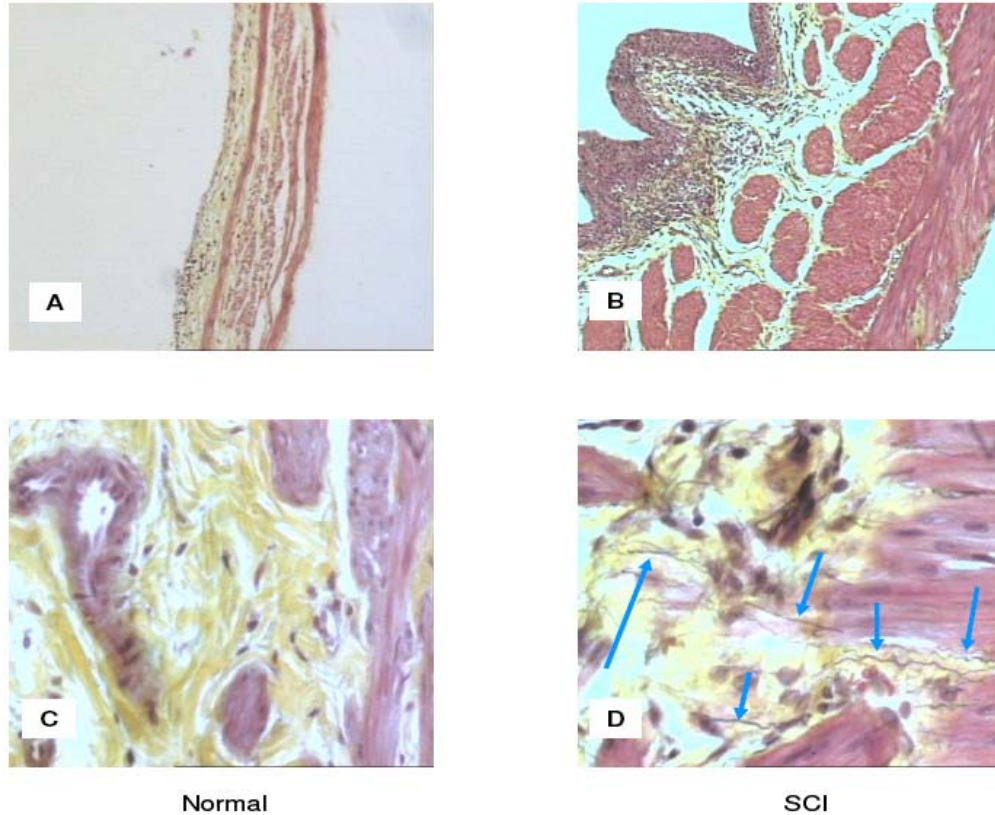


Figure 1-8. *Histological sections from normal and SCI rat bladders stained using the Movat's pentachrome. Compared to normal (Frame A), the SCI rat bladder (Frame B) was much thicker and contained more smooth muscle (stained in red). Although comparable amounts of collagen (stained in yellow) were present in the sections of both normal (Frame C) and SCI (Frame D) bladders, there were significantly more elastic fibers (stained in black; indicated by arrows) in the SCI bladder. Mags.= 10X (Frames A, B); 40X (Frames C, D). From Nagatomi et al. [54]*

Our laboratory has shown previously that biaxial mechanical testing methods can be successfully applied to the normal and SCI rat bladder wall [55]. Our mechanical studies have demonstrated that the bladder wall exhibits complex biomechanical behaviors that are profoundly altered post-SCI. In particular, we have observed that during the initial areflexic phase of SCI, the UBW undergoes profound remodeling to compensate for increased wall stretch from over-distension. This is then followed by a hyper-reflexic phase in which the UBW further alters its structure and mechanical behavior, primarily through changes in smooth muscle function and collagen content, resulting in an eventual stiffening of the UBW and reduced

bladder compliance. The stimuli for these profound functional changes are presumably due to differing mechanical stimuli; large tissue strain during areflexia and increased tissue stress during hyper-reflexia. The biomechanical changes are thus a direct result of rapid and profound bladder wall tissue remodeling, including changes in smooth muscle cell orientation, collagen and elastin concentrations [7, 55-57]. Figure 1-8 depicts the severe hypertrophy and elastin deposition what occurs in the SCI affected bladders.

1.2.3 Obstructive and congenital disorders

Bladder wall remodeling is also seen in other pathological conditions. Obstruction of the bladder neck and urethra usually results from benign prostate hyperplasia in older men, but may result from some congenital defects. In bladder outlet obstruction, there are marked changes in bladder tissue morphology caused by BSMC hypertrophy and hyperplasia [58]. These changes usually result in the inability to store and void urine [59]. Collagen ratio has also been found to be decreased in the obstructed bladder due to the large amount of detrusor hypertrophy [1]; however, in long term obstructed bladders a fibrotic response is observed with increased collagen content [60]. These changes in the bladder structure following obstruction may often be resolved when the obstruction is removed, depending on the severity and length of bladder obstruction.

Bladder exstrophy is the most common congenital abnormality of the bladder. Exstrophy occurs when the bladder grows on the exterior of the body which results from a complete ventral defect of the urogenital sinus and the overlying inferior abdominal wall musculature and integument [61]. This defect results in urine draining into the abdominal wall and inflammation of the exposed bladder mucosa. Treatment of exstrophy usually involves extensive surgery on the newborn with penile reconstruction and eventual continence in approximately 50% of

patients. Prune belly syndrome is a structural abnormality for which the cause is not known. Prune belly syndrome results in urine reflux from the bladder which severely damages the kidneys [61]. Current management involves repairing the abdominal wall defect and prescribing prophylactic antibiotics to prevent renal infection. Functional tissue engineering may provide a better reconstructive therapy for the treatment of these abnormalities and will be further discussed in section 1.4.

1.3 EXPERIMENTAL PLATFORMS TO STUDY BLADDER WALL SMOOTH MUSCLE IN NATIVE AND REMODELED STATES

1.3.1 Organ baths and biomechanical testing

The pathologies discussed in the previous section point out the many areas in which bladder dysfunction remain poorly understood. Several studies to date have focused on understanding the many aspects of bladder wall function with in vitro techniques. At the organ level, whole bladders may be isolated and pressure measurements may be recorded to determine intravesical pressure and wall stress estimated via the Law of Laplace. Although, often interpreted as a contractility measure, the intravesical pressure does not provide accurate information about the contractility of the smooth muscle [62].

Alternatively, there exist a number of studies on bladder smooth muscle contractility performed at the tissue level using organ baths, wherein a strip of tissue is suspended in a physiological solution with one end fixed and the other attached to a load in order to measure isotonic contraction under a variety of conditions. Problems arise in the tissue strip studies

mostly due to the set up of the experiments, such as sample size issues, diffusion of chemical agents, and the mode of attachment of sample to transducer [63]. While these studies continue to provide valuable information regarding the molecular mechanisms of SMC contraction, they do not take into account the effects of force generation in more than one direction or the structural considerations involved in the surrounding ECM.

In order to obtain specific material properties of the bladder wall, planar biaxial mechanical testing may be utilized in the passive and active states that allow for quantification of force production biaxially by the SMC (Figure 1-9). Biaxial testing of the bladder wall allows us to obtain specific mechanical data describing the stress strain response of the bladder wall under more physiological conditions (Fig 1-10). Recently, our laboratory has examined the whole organ strain of the passive and inactively filling of bladders (Figure 1-11). We found that bladder stretching while filling was anisotropic and stiffer in the circumferential direction. Although the bladders in the passive state exhibited less overall compliance, bladders stretched to the same degree in both directions yielded similar areal stretches in both states (Parekh submitted). However, there were some qualitative differences between the two states were seen early in the filling process that were a result of smooth muscle tone. The results of this study emphasize the importance of considering the whole bladder in contributing to its mechanical behavior. However with all of the mechanical testing methods, actual contributions of BSMC, passive connective tissues, effects of innervation and transport are difficult to separate in these approaches.

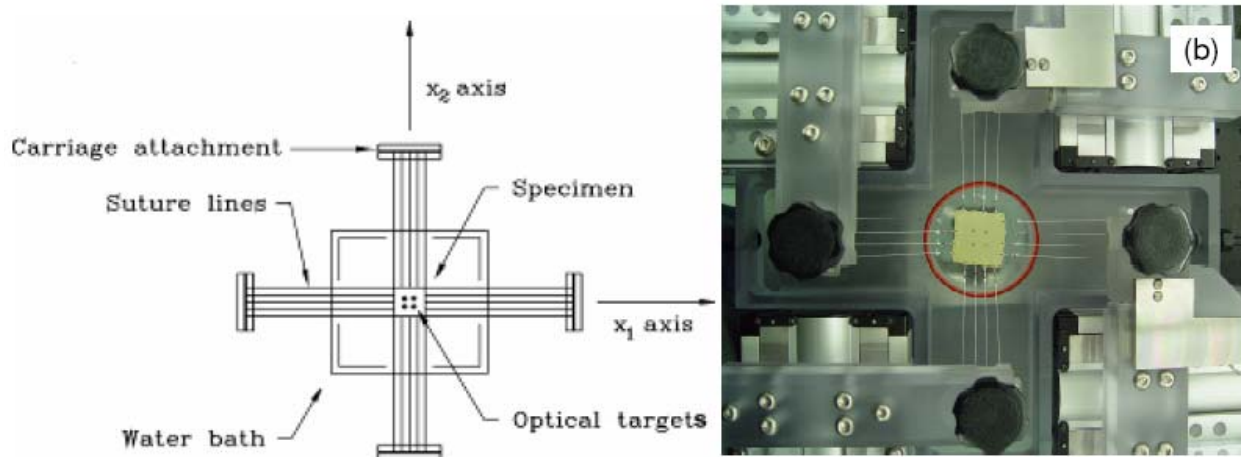


Figure 1-9 . Biaxial testing set up and device

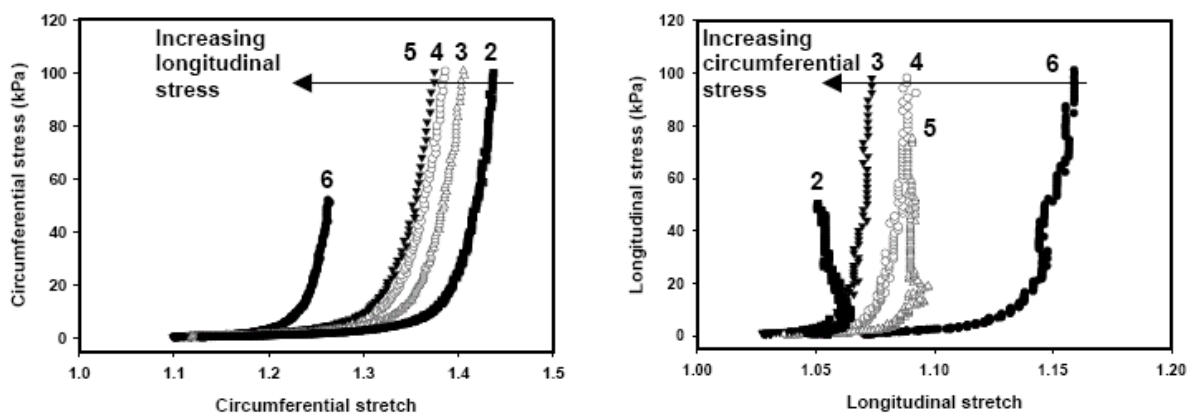


Figure 1-10. Representative stress strain curves from biaxial testing of a normal rat bladder [64].

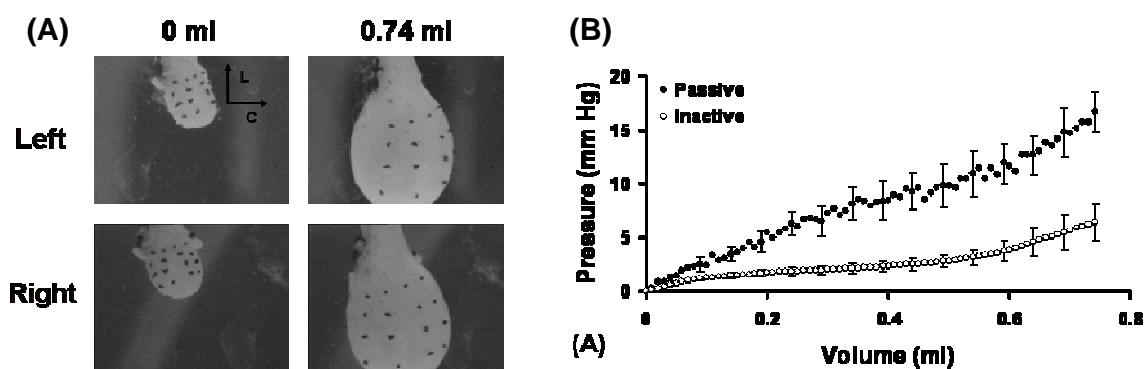


Figure 1-11. A. Example images of a bladder with markers from both cameras before and after filling. Axes were defined for the longitudinal, L, and circumferential, C, directions. B. Higher pressures during filling indicated less compliance of the rat bladders in the passive state. Average peak pressure values were 16.7 and 6.4 mm Hg in the passive and inactive states, respectively, and were significantly different ($p < 0.05$). Data are presented as the mean \pm standard error ($n=5$). The greater variability in the passive data was a result of spontaneous bladder contractions throughout the experiment.

1.3.2 Ex vivo bladder culture

Ex vivo organ culture of the bladder provides a means to separate the effects of innervation and the tension associated with bladder filling from contractile forces. It also maintains the native tissue cell-ECM interaction of the intact organ and allows isolation of the intact organ from systemic humoral and neurological influences [65]. Furthermore, organ culture provides an alternative to using SCI models where the spinal cord is transected, which are difficult and have high morbidity rates for the animals.

Organ culture of the urinary bladder has been utilized to examine bladder cell metabolism, bladder outlet obstruction, and most frequently, bladder cancer. Hardin et al studied mitochondrial oxidative substrate selection in porcine bladder smooth muscle strips cultured in physiological saline solution up to 4 days [66]. The authors concluded that BSMC have the ability to induce lipotoxicity causing dysfunctional detrusor smooth muscle [66]. The mouse bladder has also been used ex vivo to study bladder development. Beauboeuf et al examined bladder development in fetal mice with ex vivo organ culture of the bladder [67]. Ligation of ureters and urethra prompted more orderly packing of the collagen along luminal edge of the developing bladder after 4 days ex vivo culture [67]. Ex vivo culture has also been used as an experimental model for the obstructed bladder. Capolicchio et al examined ECM gene response in an ex vivo model of rat bladder outlet obstruction [68]. They found that collagen I, III, and XII as well as RHAMM gene expression is up regulated under stretch injury. Collagen I and III gene up regulation depends on time of distention, not on extent of distention. The effect of a peptide that binds in place of the hyaluronic acid receptor, RHAMM, attenuates collagen I, III, and XII gene up regulation in a stretched ex vivo rat bladder for 24 hours [68]. Mechanical stretch has been shown to alter ECM gene expression as well as alter the release of growth factors and other

cytokines. Adam et al showed that mechanical stretch of bladder smooth muscle cells on a flex-cell device up regulated expression of many genes related to HB-EGF and COX-2 [69]. The study also examined PDGF-BB along with mechanical stretch as a stimulator for SMC hypertrophy in the isolated cells as well as in an organ culture of a rat bladder at 24 hours [69]. These studies proved that ex vivo organ culture may be utilized to examine a pathological bladder condition.

The most frequent use of organ culture of the bladder has been to examine invasive bladder carcinoma. Fujiyama et al found that the urokinase system is important for bladder cancer invasion through the use of explanted, de-epithelialized bladder sections underneath a collagen gel seeded with human bladder cancer cell lines up to 28 days [70]. This system and others like it may be used to study the dose effects of therapeutic cancer drugs. Furthermore, Estrada et al utilized an ex vivo model of the rat bladder to study the behavior of human transitional cell carcinoma (TCC) [65]. The model was a filled rat bladder with the urothelium layer removed by digestion in acid. Following digestion, the TCC cells, previously labeled with quantum dots, were injected into the bladders. The bladder was grown in cell culture media which was changed every other day for up to 20 days [71]. This assay system, termed EViTAS, can mimic tumor growth in the host bladder. All of these previous studies exemplify the utility of an ex vivo organ culture model of the bladder. While the studies by Capoliccio and Adam examined the role of distension of the bladder wall, there currently are not any published reports of utilizing a dynamic ex vivo organ culture system of the bladder.

1.3.3 Mechanical stimulation of BSMC

On the whole, BSMCs are poorly understood in their development, contractile properties, ECM production, and remodeling within the bladder wall. Previous studies have focused on the organ, tissue, or isolated BSMC levels [62]. While organ and tissue studies can provide valuable information, they are also limited in that the contributions of BSMC, passive connective tissues, innervation, and transport are difficult to separate [62]. In attempts to further understand bladder smooth muscle, many have turned to stretching BSMC in culture. It has become well known that BSMC exhibit various cellular/molecular-level changes in response to mechanical stimuli such as cyclic stretch [72, 73]. These previous studies exposed smooth muscle cells and urothelial cells (cultured on flexible membrane) to repetitive mechanical stretch/relax stimuli at various frequencies (in the order of 5 – 60 cycles / minute) and magnitudes (in the order of 1% – 25%) for hours using commercial or custom devices and examined changes in mRNA and/or protein expressions for growth factors, cytoskeletal proteins, extracellular matrix proteins, and integrins [69, 72, 74]. In a pilot experiment, it has been shown that mechanical stimulation can also affect cellular alignment of BSMC (Figure 1-12). Under uniaxial stretch the BSMC aligned perpendicular to the direction of stretch while under equi-biaxial mechanical stretch the BSMC showed little to no preferred alignment. These results are further discussed in Appendix A.

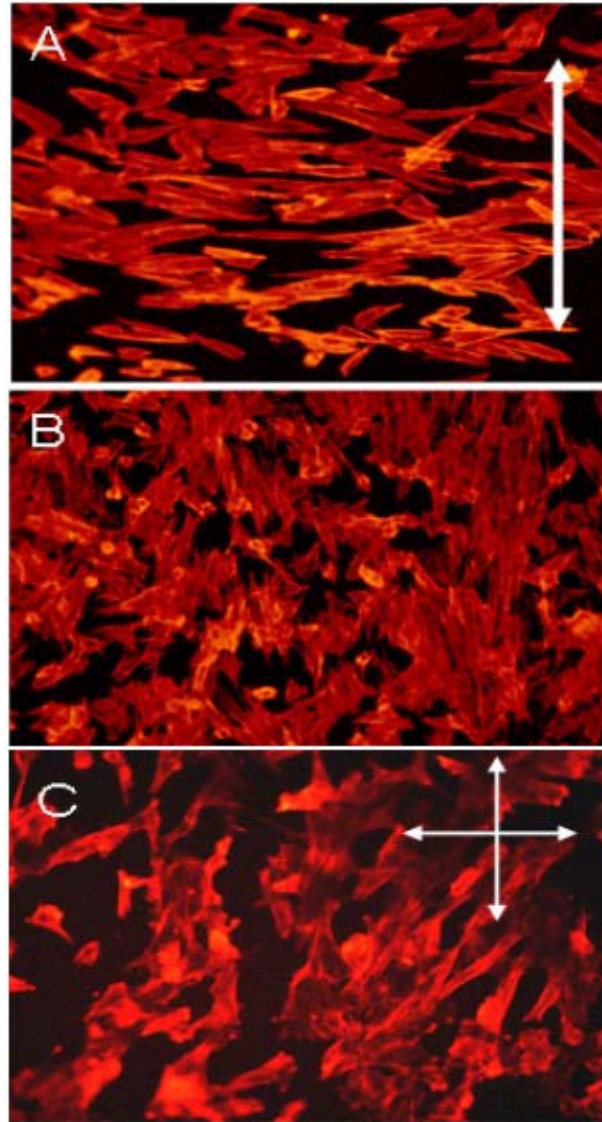


Figure 1-12. Rhodamine-phalloidin of staining of BSMC under uniaxial stretch for 48 hours (A), in static culture (B), and under equibiaxial stretch for 48 hours (C). The white arrows in (A and C) show the direction of strain. BSMC appear to line up perpendicularly to the direction of strain in A. In static culture, the BSMC have no apparent preferred orientation (B). BSMC show a slight preferred direction diagonally under equi-biaxial stretch (C)

While information gained from cell stretch experiments is highly valuable at the cellular level, it does not provide an environment wherein the BSMC proliferate and organize their ECM under the mechanical stimulation. Furthermore, existing devices such as the Flexercell® for mechanical stimulation of cells in a 2-D environment produce stretch that is heterogeneous,

which cannot be reliably controlled in the biaxial strain state [62, 75]. BSMC studies are thus limited in that critical functional connections to the surrounding ECM and BSMCs are severed, and moreover are not subjected to a sufficiently controlled mechanical environment. An in vitro model, such as those in the present study, may provide such a platform to perform novel studies that examine intrinsic bladder smooth muscle cell physiology and cell-cell and cell-matrix interactions.

1.4 TISSUE ENGINEERING THE BLADDER WALL

1.4.1 Need for bladder wall replacement

Bladder wall tissue replacement could be a useful treatment of pathologies present in cancer, chronic inflammation, diabetes, or neurogenic disorders [76]. Many neurologically impaired patients develop refractory neurogenic detrusor overactivity that are resistant to anticholinergic drugs or medication. Although sacral nerve neuromodulation and bladder botulinum toxin injection are being investigated for the treatment of refractory detrusor overactivity [77], the “gold standard” therapy for neuropathic bladders as well as those affected by bladder cancer and chronic inflammation is enterocystoplasty. Addition of a segment of intestine to the bladder is a major operation with long term risks including not only bladder rupture and bowel obstruction but also new cancer formation [78, 79]. Tissue engineering of the bladder wall is a promising method to significantly improve upon on enterocystoplasty.

1.4.2 Bladder development

In order to tissue engineer the bladder wall, it is helpful to understand bladder wall development. In the case of the urinary bladder, epithelial-mesenchymal interactions are crucial to development. Embryologically, the urinary bladder is derived from undifferentiated mesenchyme and endoderm of the urogenital sinus and allantois as a tubular organ following subdivision of the cloaca by the urorectal spectrum. During development, the undifferentiated mesenchyme differentiates into bladder smooth muscle [80]. Similarly, bladder epithelial cells begin as undifferentiated, which in time, form urothelium characterized by expression of cytokeratins and uroplakins [81]. It has been shown previously that urothelial and smooth muscle cells undergo differentiation in an orderly fashion defined by smooth muscle and cytokeratin markers [81]. Given the orderly differentiation of the bladder layers, the mesenchymal-epithelial interactions likely play a role in development of the epithelium, lamina propria, and smooth muscle development. In order to assess these cell-cell interactions in bladder development, a study was performed by Baskin et al in 1996 where undifferentiated bladder mesenchyme was isolated and grown alone or in combination with bladder epithelium [81]. Baskin and his colleagues found that in vitro as well as in vivo, tissue recombinants showed evidence of smooth muscle differentiation. Without the urothelium, bladder smooth muscle does not develop normally if at all [82]. These studies confirm that signaling from the epithelium appears to be required for smooth muscle development [83].

The mechanism(s) by which the epithelium signals the mesenchyme in bladder development are not fully understood. It has been determined that peptide growth factors such as keratinocyte growth factor (KGF), TGF alpha and TGF beta are regulated during bladder development [84]. Additionally, in a tissue recombination experiment wherein 14-day bladder

mesenchyme was combined with rat epithelium from several different tissues, it was found that epithelium induces bladder mesenchyme to differentiate into smooth muscle regardless of the source of epithelium [85]. More recent studies shed light on new experimental techniques to determine the molecular mechanisms behind mesenchymal-epithelial interactions in the bladder. In the bladder, as in many other developing organs, mechanical cues such as cell stretch and pressure influence the epithelium to release growth factors such as FGF-7 and VEGF that can act as potential mitogens [86]. Transgenic mouse models have also been used to examine urinary bladder development. The use of transgenic mice allows manipulation of the genetic make-up, which simplifies the task of determining the specific effect of a variable in the complex system of mesenchymal-epithelial interactions [87]. Going one step further, green fluorescent protein may be used in transgenic mice in order to better sort and characterize smooth muscle cells as they differentiate from the mesenchyme. In 2004, Szusik et al generated six lines of transgenic mice to express the enhanced green fluorescent protein (EGFP) reporter gene under the control of a smooth muscle gamma actin protein fragment. The EGFP tagged bladder smooth muscle cells were easily isolated, making it more feasible to examine the genetic programs controlling development and differentiation of bladder SMC [88]. These techniques may also be used on the adult bladder to determine the importance of mesenchymal-epithelial interactions in tissue regeneration.

1.4.3 Tissue engineering methodology

As stated in section 1.4.1, there is a substantial clinical need for new bladder wall replacement tissues. While it is apparent that mesenchymal- epithelial interactions are important in bladder wall development, they are also important in maintenance of functional bladder wall in the adult.

Mesenchymal-epithelial interactions are important in maintaining bladder homeostasis in response to injury [84]. The bladder may be severely affected by disease entities including the following: neurogenic bladder dysfunction related to spinal cord injury, bladder dysfunction related to urethral obstruction, bladder exstrophy, interstitial cystitis, or bladder cancer. In terms of bladder remodeling, it has been known for some time that the urothelium of the bladder turns over at a slow rate, about once a year [89]. However, the regenerative capacity of urothelium is known to occur at an incredible rate, during the first 48 hours after injury such as bladder outlet obstruction [87]. Great knowledge can be obtained through understanding mesenchymal-epithelial interactions in the regenerating bladder. This knowledge will aid in the understanding of organogenesis of the bladder and vice versa.

Experimental models for studying bladder regeneration arise from the diseased state of the bladder. These models specifically come from bladder cancer and bladder augmentation. Mesenchymal-epithelial interactions have been examined in many types of cancer due to the fact that epithelial morphology and function are under stromal control in the embryo and adult. In 1977, some of the first evidence supporting the theory that carcinogenic agents elicit non-neoplastic effects in the stroma, which in turn mediate neoplastic development in the epithelium, was found in bladder epithelia co-cultured with carcinogenic bladder stroma; the epithelia developed cancerous cells [90]. Further evidence was provided by Pritchett et al in 1989, where epithelial cells from a highly invasive cancerous bladder invaded fibroblast layers in the presence of stromal cells [91]. More recent studies have moved away from bladder carcinoma and focus on the changes in mesenchymal-epithelial interactions between prostate epithelium and stroma [92]. However, a lot can be learned about the mechanisms behind cancer resulting from disrupted mesenchymal-epithelial interactions that may be applied to a variety of tissues.

As stated before, reciprocal cellular signaling between the urothelial and stromal components are required for development and presumably used to maintain the adult tissue. The interactions between the urothelium and the stroma are disrupted when there is a need for bladder augmentation [83].

Current strategies for bladder augmentation are based on the use of sheets of tissue derived from the intestinal tract. Implanting a piece of such tissue into the bladder disrupts the interaction between the urothelium and smooth muscle cells and may cause adenocarcinoma in some patients [83]. In the majority of patients, however, bladder augmentation provides the bladder with increased capacity and aids in voluntary voiding. Replacing the bladder with gastrointestinal segments demonstrates the plasticity of the urothelial phenotype. Li et al performed tissue recombination experiments by combining a 14-day embryonic rat and mouse rectal mesenchyme with urothelium from embryonic and adult rats or mice [93]. They found that the phenotype of both mouse and rat urothelium transdifferentiated into glandular epithelium demonstrating that plasticity of urothelium is a result of mesenchymal/stromal stimulation. Another study demonstrated in vitro the importance of urothelial-smooth muscle interactions in a tissue engineering setting. Bladder acellular matrix was seeded with urothelial and smooth muscle cells alone and in combination, but smooth muscle cell penetration was found only in the co-culture condition [94]. This study further emphasizes the reciprocal need for mesenchymal-interactions in tissue growth, yet the mechanisms behind the cellular signaling are still not fully understood.

In general, an ideal bladder wall replacement should consist of [95]:

- 1) A normal urothelium lining to prevent abnormal urine resorption

- 2) A substantial, well organized contractile smooth muscle layer(s) to facilitate bladder emptying.

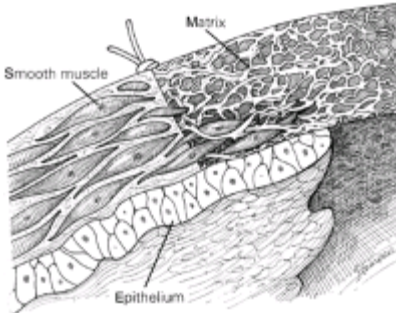


Figure 1-13 . *Bladder augmentation schematic.* [96]

The field of tissue engineering (TE) has made significant advances toward improving treatments for bladder wall augmentation. TE of bladder smooth muscle includes a variety of approaches. Synthetic materials are strong, can be fabricated to degrade following implantation at predetermined rates, and can be designed to mimic the material properties of the native tissue they are designed to replace [97]. However, these materials have a higher occurrence of infection, erosion, and urethral fistula formation [98]. There has been significant initial success in engineering a neo-bladder utilizing a polymeric scaffold seeded with autologous urothelial and smooth muscle cells (Shown in Figure 1-14) for replacement in children with myelomeningocele (a congenital abnormality causing little to no bladder capacity) [99]. This pioneering study achieved its primary goal, to increase bladder capacity and thus decrease pressure build up in the bladder that would eventually lead to kidney damage. However, these neo-bladders were grossly disorganized and did not have the ability for a coordinated contraction of the bladder smooth muscle bundles.

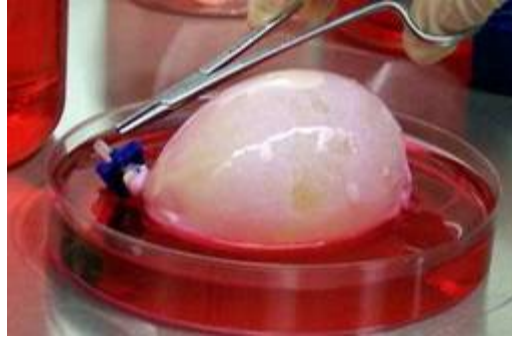


Figure 1-14. *Engineered neo-bladder. [99]*

Xenographic ECM grafts have also been shown to be useful in reconstructing parts of the lower urinary tract [100], though their use as a bladder wall substitute has led to bladder wall stiffness, and incomplete, disorganized muscle regeneration [101]. Porcine small intestinal submucosa (SIS) is one such scaffold composed mainly of collagen type-I. SIS has shown to be resorbable [102] and support vascularization *in vivo* [103]. Many preliminary studies have shown that SIS is useful for several types of urologic surgery applications where reinforcement of native structure or new tissue is needed [104, 105]. It has been pointed out, however, that SIS initially exhibits higher mechanical stiffness than the native bladder and leads to incomplete, disorganized muscle regeneration in the urinary bladder [106]. Prior studies have suggested that seeding SIS with autologous cells may be advantageous in regenerating functional and mechanically sound tissue replacements. Autologous skeletal muscle cells suspended in a collagen gel seeded onto SIS showed higher mechanical tensile strength than unseeded SIS when implanted into the abdominal muscles of Lewis rats [107]. In addition, using a de-cellularized bladder matrix seeded with canine autologous urothelial and bladder smooth muscle cells for bladder augmentation resulted in an increase in bladder capacity [108] and a more complete retention of implanted diameter [109] compared to unseeded matrix. These studies provide evidence that a tissue engineering approach, utilizing autologous cells and a 3-D, biological

scaffold, toward urologic tract repair and replacement may provide better long-term successes. Figure 1-15 depicts a piece of SIS.



Figure 1-15. *Small intestinal submucosa.* www.medscape.com

Cell seeded scaffold approaches have focused on BSMC, since urothelium have a great regenerative capacity [110], have had better results in decreasing the contracture of the graft and increasing host cell integration [111]. However, there still exists the risk for inflammation and disorganized muscle regeneration as well as issues with cell survival post implantation. One possible cause behind the shortcomings of current techniques is that most existing TE approaches to bladder wall repair are not conditioned in vitro due to the difficulty in mimicking the in vivo environment with a scaffold.

1.5 MOTIVATION AND AIMS OF PRESENT STUDY

Multiple bladder wall pathologies, such as overactive bladder, bladder outlet obstruction, SCI and related neurogenic disorders, and diabetes result in tissue remodeling marked by hypertrophic BSMC and altered extra-cellular matrix components. This remodeling results in changes in bladder wall biomechanical properties leading to altered bladder function. Our previous studies have revealed that during the initial areflexic phase of SCI the bladder wall undergoes profound remodeling that appears to be a compensatory mechanism for the increased wall stretch resulting from over-distension [112, 113]. Remodeling in the bladder wall results in changes in biomechanics and ultimately the ability of the organ to normally fill and void [55]. The stimuli and precise mechanisms that are responsible for bladder remodeling in SCI remain unknown. In order to improve our understanding of post-SCI remodeling events that will lead to improved treatment bladder disorders, one must first have an understanding of the primary stimulus that triggers remodeling events in the bladder. Specifically, it is **hypothesized that BSMC respond to altered strain histories with tissue remodeling marked by changes in ECM composition resulting from a shift in BSMC phenotype**. As a first step, the proposed study assessed remodeling events specific to the areflexic phase following SCI. Our rationale is that this is the first phase of bladder remodeling and is likely caused by an abnormal strain history differing from the normal filling and voiding patterns of the healthy bladder wall. Based upon the aforementioned research areas, the aims of the present study were as follows with a depiction of the aims in a flowchart in Figure 1-16:

Specific Aim 1: Determine the effect of strain history on ECM remodeling of the ex vivo organ cultured bladder. We hypothesized that abnormal strain frequency would promote ECM

synthesis. In order to test this hypothesis we utilized female Sprague Dawley rat bladders stretched in a strip-biaxial bioreactor at varying strain frequencies. Remodeling was assessed via quantification and visualization of collagen and elastin content. The scientific endpoints were to establish organ culture as an experimental model to examine strain induced remodeling of the bladder wall and to determine the strain history protocol to promote BSMC remodeling of ECM.

Specific Aim 2: Examine the role of TGF- β 1 with and without cyclic stretch on bladder smooth muscle remodeling.

Aim 2.1: Utilize ex vivo culture model to examine role of TGF- β 1. We hypothesized that TGF- β 1 will increase BSMC mediated ECM remodeling in the ex vivo organ culture by altering BSMC phenotype. This hypothesis was tested using the same organ culture system as described in Aim 1. Phenotype of the BSMC within the cultured bladders was assessed by utilizing immunohistochemistry to stain the sections for contractile and synthetic smooth muscle cell markers. The scientific endpoint of this sub-aim was to assess the role of TGF- β 1 with and without strip biaxial stretch on BSMC phenotype, ECM synthesis, and mechanical properties and compare these outcome measures to established data on the SCI rat bladder.

Aim 2.2: Further examine role of TGF- β 1 in cell remodeling with collagen gels. We hypothesized that TGF- β 1 will increase BSMC mediated ECM remodeling of collagen gels. This hypothesis was testing using an anchored collagen gel model. We measured contractility of the gels as well as organization of the collagen within the gels. The scientific endpoint of this aim was to quantitatively and qualitatively assess the impact of exogenously added TGF- β 1 on BSMC remodeling ability.

Specific Aim 3: Engineer a cell-ECM construct to further examine the effect of strain on BSMC remodeling with future applicability in tissue engineering the bladder wall. We

hypothesized that:

1. Cytokines VEGF and FGF-2 will promote cellular penetration into SIS.
2. Non-physiologic strain histories will promote a similar response in the cell-ECM construct as demonstrated in organ culture.

These hypotheses were tested utilizing BSMC, the cytokines VEGF and FGF-2, and the tension bioreactor described in Aim 1. Two stretch frequencies were examined, 0.5 Hz and 0.1 Hz with strain up to 15%. The scientific endpoints of this aim were to ascertain a method to rapidly promote penetration of the BSMC into SIS and to promote ECM remodeling within the SIS construct with the use of cyclic mechanical stimulation.

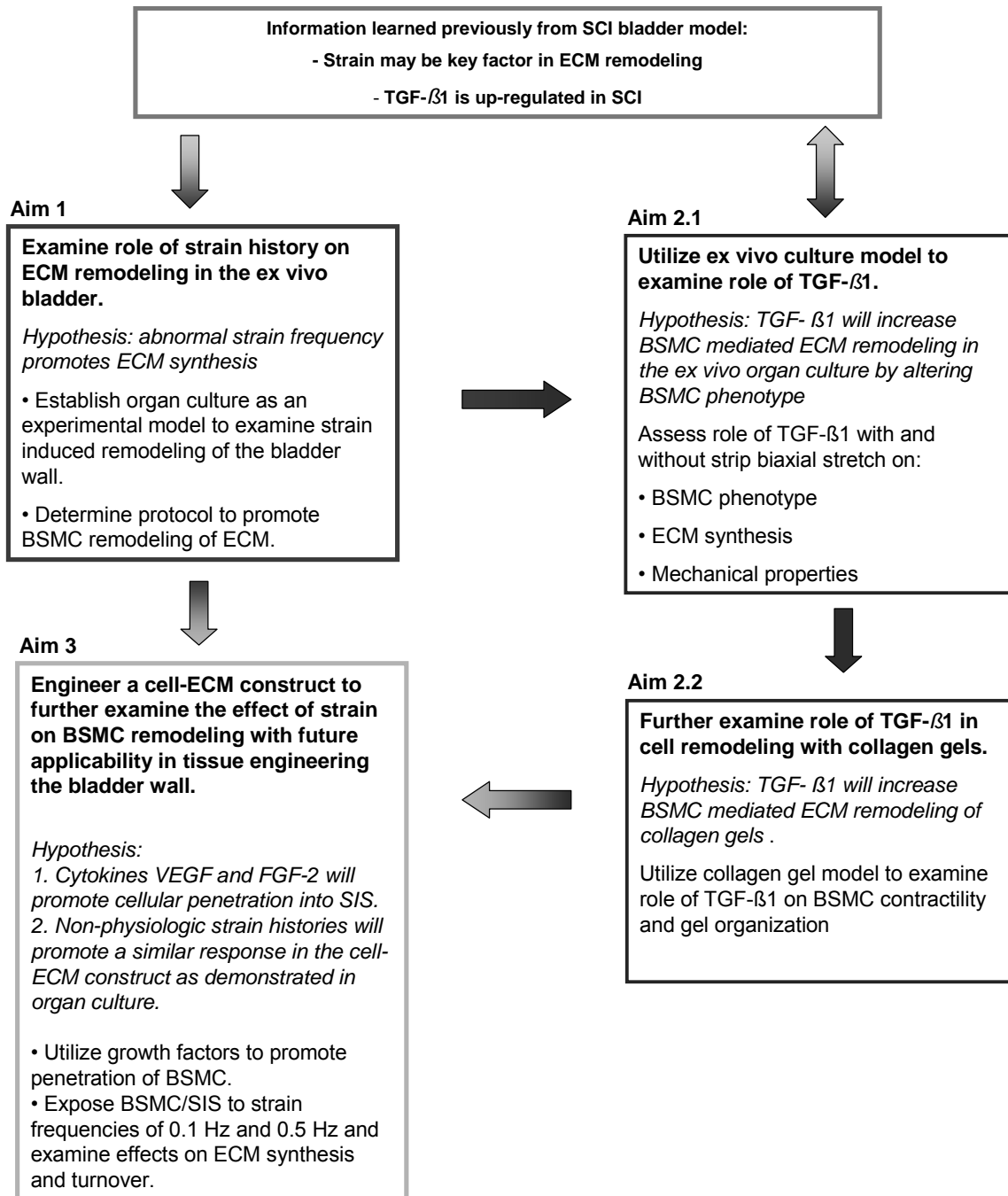


Figure 1-16. Flowchart of specific aims based upon previous studies of the SCI affected bladder. These aims sought to test the overall hypothesis that BSMC respond to altered strain histories with tissue remodeling marked by changes in ECM composition resulting from a shift in BSMC phenotype.

2.0 THE EFFECTS OF TISSUE LEVEL STRETCH ON URINARY BLADDER WALL EXTRACELLULAR MATRIX REMODELING

2.1 INTRODUCTION

Urinary bladder wall (UBW) pathologies resulting from bladder outlet obstruction diabetes mellitus, spinal cord injury and related neurogenic disorders, commonly lead to substantial tissue remodeling marked by hypertrophic BSMC and altered ECM components. This remodeling results in changes in bladder biomechanical and structural properties leading to altered bladder function. In vivo studies of bladder outlet obstruction have demonstrated increases in bladder vascularization [114] and weight [115], as well as alterations in smooth muscle contractility [116]. In the rat streptozotocin induced diabetes model, increases in bladder capacity, cross sectional area, and hypertrophic smooth muscle have been identified as indicators of remodeling [117]. The UBW also undergoes remodeling with rapid changes in ECM composition and smooth muscle hypertrophy following spinal cord injury [112]. Previous studies have revealed that during the initial areflexic phase of spinal cord injury the bladder undergoes profound remodeling that appears to be a compensatory mechanism for the increased wall stretch resulting from over-distension [112, 113]. Remodeling in the UBW results in biomechanical changes and ultimately the ability of the organ to normally fill and void [55].

The normal urinary bladder is composed of approximately 70% smooth muscle with the remaining 30% being ECM proteins, predominantly collagen types I and III with a loose network of elastin fibers [117, 118]. The majority of the elastin found in the bladder is in the vasculature, with small additional amounts found surrounding individual bladder smooth muscle cells [119], within the connective tissue connecting smooth muscle bundles [120], and in the urothelium and lamina propria [121]. While in most soft tissues a certain amount of turnover of the ECM constituents is expected, elastin is generally assumed to be metabolically stable with negligible turnover rates [122].

In the aforementioned bladder pathologies, the balance of smooth muscle and ECM components is altered leading to either a highly compliant and over distended bladder (as seen in early stages of spinal cord injury [54] or diabetes [123]), or a non-compliant, fibrotic bladder (as seen in late stages of spinal cord injury [64] or in bladder outlet obstruction [124]). These studies indicate that maintenance of the ratios of ECM and smooth muscle is essential to normal bladder function. Thus, understanding the remodeling process in the diseased state is crucial in treatment and developing methods to restore the bladder function.

Although much information can be obtained by studying bladder tissue remodeling in vivo, the multiple effects of innervation, immune responses, and heterogeneous wall deformation and stress associated with filling and voiding are difficult to separate. Ex vivo organ culture models have been established to examine UBW development [67], cancer [70, 71, 125], metabolism [66], and bladder outlet obstruction [68, 69]. Capolicchio et al. examined ECM gene response in an ex vivo model of rat bladder outlet obstruction and found that collagen I, III, and XII gene expression is up-regulated under stretch injury [68]. In an additional organ culture study using the same rat bladder outlet obstruction model, mechanical stretch along with PDGF-

BB were stimulators of SMC hypertrophy after 24 hours of distension [69]. These studies demonstrate that an ex vivo model of the UBW is feasible and useful in examining a strain-induced remodeling.

However, the modes of mechanical stimulation that are responsible for bladder remodeling in response to strain remain unknown. In order to more firmly establish our understanding of UBW remodeling events, it is necessary to have an understanding of the mechanisms that trigger these events. In particular, while it is intuitive that mechanical forces and deformations likely drive the remodeling processes, definitive studies have yet to be performed for the UBW. Thus, while the primary function of the bladder is mechanical, our understanding of the remodeling process and the role of mechanical stimulatory factors for the bladder remains surprisingly limited.

The objective of the present study was to accomplish the endpoints of Specific Aim 1: determine the effect of strain history on ECM remodeling of the ex vivo organ cultured bladder. Which were to establish organ culture as an experimental model to examine strain induced remodeling of the bladder wall and to determine the strain history protocol to promote BSMC remodeling of ECM. Thus, this study determined the effects of varied, continuously cycled strain histories on ECM production in the ex vivo rat bladder as a first step toward full understanding of the remodeling process. In particular, we speculate that strain history plays a pivotal role in determining the responses of the UBW. An ex-vivo organ culture system was utilized to remove the potentially confounding effects of innervation and humoral factors from strictly mechanical strain effects. Resulting changes in ECM components were quantified.

2.2 PROTOCOLS

2.2.1 Ex vivo organ culture

Bladders were extracted from female Sprague-Dawley rats (150-300 g) following euthanasia with CO₂. Bladders were opened and strips 9- 10 mm in the circumferential direction x 12-14 mm in the longitudinal direction were excised. Strips were attached on the longitudinal ends with custom-made tissue grip springs. Samples were then mounted in a custom-made tension bioreactor (Fig 1D) and stretched in the longitudinal direction for 7 or 14 days under sterile conditions in RPMI-1640 (Invitrogen) media supplemented with 10% FBS (Invitrogen) and 1% PenStrep (Invitrogen) at 37 degrees and 5% CO₂. Bladder samples were stretched to 20% under either 0.5 Hz, “1 hour” (stretched to 20% over an hour then released over 10 seconds), or “8 hour” (stretched to 20% over 1 hour, held for 7 hours, then released over 10 seconds). Freshly excised bladder strips (referred to as “Native”) and free-floating, statically cultured bladder strips (referred to as “Static”) served as controls. The 0.5 Hz group was chosen based upon previous studies wherein BSMC were stretched on distensible membranes [126]. The 1 hour group was chosen to mimic rat bladder voiding, and the 8 hour group was chosen to mimic SCI bladders that were expressed 3-4 times daily. See Table 2-1 and Figure 2-1 for stretch protocol descriptions and waveforms.

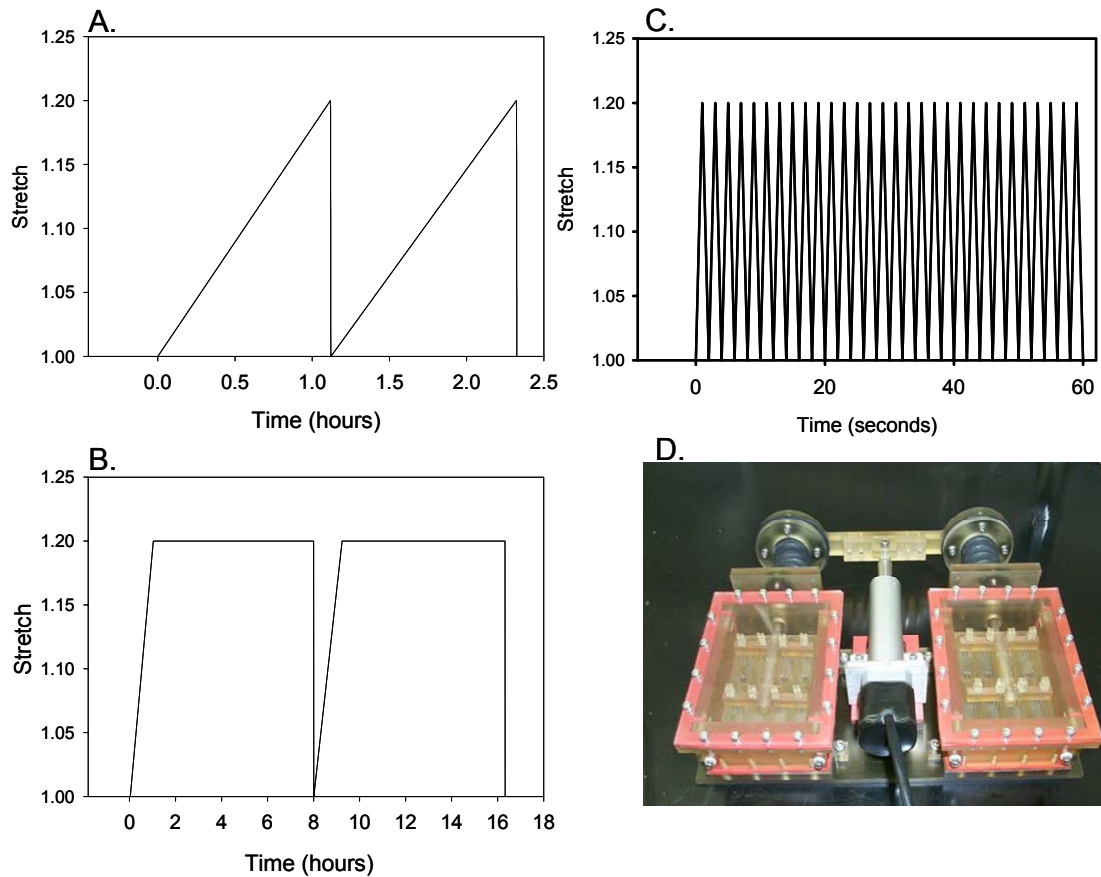


Figure 2-1. Sample waveforms for (A) two cycles of “1 hour cycle”, (B) two cycles of “8 hour cycle” and (C) several cycles of “0.5 Hz cycle” in the *ex vivo* rat bladder strips. (D) A photograph of the tension bioreactor.

Table 2-1. Stretch Protocols

Protocol name	Description
Native	Freshly excised tissue
Static	Statically cultured tissue
0.5 Hz	Cyclically stretched to 20% from its initial length at 0.5Hz, for 7 or 14 days
1 hr	Stretched to 20% from its initial length over 1 hour then released over 10 seconds, repeated for 7 or 14 days
8 hr	Stretched to 20% from its initial length over 1 hour, held for 7 hours, then released over 10 seconds, repeated for 7 or 14 days

2.2.2 Tissue strains experienced in the tension bioreactor system

In order to determine the strains experienced by the ex vivo bladder strips in the tension bioreactor system, a custom designed strip biaxial testing device was utilized as described previously [127]. Briefly, the testing apparatus consisted of a small bath secured to a computer controlled translation stage to which one end of the specimen could be mounted via a bar attached to the moving bath and the other end of the specimen mounted via a fixed bar. The bath was then moved with a linear actuator such that the bladder strip was stretched to 20% from its initial length. Tissue strains were measured by tracking 4 markers placed in a square on the middle of the bladder specimen. Additionally, to determine any plastic deformation that occurred over the length of time in culture, measurements were taken by hand of the length and width of each sample before and after culture.

2.2.3 Collagen and elastin assessment

Collagen and elastin concentrations were determined based on techniques adapted from Brown et al [128], which have previously been used to quantify ECM synthesis of ovine vascular smooth muscle cells under cyclic mechanical flexure [129]. Soluble collagen was extracted from tissue samples using a solution of 0.5 M acetic acid (Sigma) and 1 mg/mL Pepsin A (Sigma). Each sample was placed in a microcentrifuge tube and incubated in 1 ml of extraction solution overnight (~16 h) on a rocker table operating inside a refrigerator at 2–8°C. In order to determine the amounts of highly cross-linked collagen in the tissue samples, samples were denatured in a pepsin/acetic acid solution at 80 °C for 1.5 hours. Following denaturation,

samples consisted of solubilized collagen which was measured separately from the pepsin/acetic acid digested collagen. Elastin was extracted using a hot oxalic acid treatment. The supernates from the oxalic acid treatments were loaded onto Centricon RC/YM-3 centrifugal filter units (Millipore, Bedford, MA) and centrifuged at 3000g for an additional hour. The concentrate was then be re-suspended in cold (<5°C) Elastin Precipitating Reagent (UK Biocolor). Soluble collagen from the collected media samples at days 2, 4, 7, 9, 11, and 14 was precipitated with 4 M NaCl. Fresh media was used as the control. Following the extraction steps, the collagen and elastin extracts were assayed according to the guidelines provided with the Sircol™ and Fastin™ assay kits, respectively (UK Biocolor).

2.2.4 Matrix metalloproteinase (MMP) activity

Since the pepsin soluble collagen found in the tissue may be either newly formed collagen or degraded collagen, the culture media was assayed for both collagen and bulk matrix metalloproteinase activity. MMP activity was assayed from the conditioned media at days 2, 4, 7, 9, 11, and 14 utilizing a similar method to Aitken et al 2006 [130]. Net activity was assayed using the EnzCheck collagenase/gelatinase assay kit (Invitrogen). DQ-gelatin fluorescein conjugate (0.1 mg/mL) was incubated in Tris buffer (50 mmol/L) with conditioned media for 2 hours. The MMPs then released the quenched activity of the FITC from the FITC-gelatin. The released FITC was measured on a fluorescent microplate reader at 495 nm absorption and 525 nm excitation. Collagenase produced in *Clostridium histolyticum* provided in the kit was used as a positive control. Negative controls were performed with 20 µmol/L of 1,10-phenanthroline to inhibit the MMP activity. Background from unconditioned media was subtracted from all

samples. Data are reported as a summed total of activity from each day media was changed (2, 4, and 7 days for 7 day groups and from 2, 4, 7, 9, 11, and 14 days for 14 day groups).

2.2.5 Histological assessment

Following 7 or 14 days in culture, bladder samples were fixed in 10 % neutral buffered formalin overnight and transferred to Hank's Buffered Saline Solution (HBSS, Invitrogen) for storage. Once all samples were collected, they were embedded in paraffin, cross-sectioned, and stained with Elastic Trichrome. Stained specimens were imaged at 400x. Additionally, immunohistochemistry was performed on 3 representative sections from each sample group. Following paraffin embedding and sectioning, slides were deparaffinized and antigen retrieval was performed using a sodium citrate buffer (Sigma). Samples were then washed 3x in Tris Buffered Saline (TBS, Sigma) and blocked with 0.3% BSA in TBS for 1 hour. Then, samples were incubated with an anti-elastin primary rabbit polyclonal antibody (1:400, Abcam Inc.) for 1 hour at room temperature. Following the primary antibody incubation, samples were incubated for 1 hour in FITC labeled goat polyclonal anti-rabbit IgG-H&L (1:400, Abcam Inc). Samples were thoroughly rinsed in TBS and incubated in 300 nM 4',6-diamidino-2-phenylindole dilactate (DAPI, Invitrogen) for 10 minutes. Samples were rinsed in TBS and imaged on a Leica DMRB fluorescence microscope. Negative controls for elastin antibody staining were a primary antibody delete, and positive controls were the blood vessels in the tissue.

2.2.6 Statistical analysis

All numerical data are presented as mean \pm s.e.m. Statistical analyses of these data were performed using SigmaStat 3.0 software package (Chicago, IL). A one-way analysis of variance was used on all samples followed by a Tukey test for pair-wise comparisons. Following these tests, p-values of less than or equal to 0.05 were considered significant.

2.3 RESULTS

2.3.1 Realized tissue deformations

Analysis of the strains experienced under the strip biaxial organ culture revealed that the bladder strips underwent nearly pure strip biaxial stretch in the center portion of the sample. Stretch ratios in the longitudinal direction were measured to be 1.196 ± 0.007 while the entire strip was stretched to 1.20 from its initial length. Stretch ratios in the circumferential direction were 1.040 ± 0.014 , with negligible shear observed. Measurement of the bladder strips following organ culture showed that some permanent set occurs affecting both the longitudinal and circumferential directions. The permanent set occurring in the longitudinal direction of the 3 stretched groups (0.5 Hz, 1 hour, and 8 hour) increased the length by 1.45 ± 0.65 mm resulting in an average stretch ratio between 1.17 and 1.18 instead of the original 1.20. There also was a shortening in the circumferential direction by 2.11 ± 0.70 mm. In the static culture group, dimensions of the bladder strips decreased by 1.33 ± 0.57 mm and 1.66 ± 0.54 mm in the longitudinal and circumferential directions, respectively. This shortening was most likely

resultant from the unrestrained bladder strip curving back to its native shape of the UBW. Overall, the experimental system was able to subject the UBW tissue strips to a predictable and consistent strain pattern, with small effects of tissue attachment and permanent set.

2.3.2 Collagen remodeling in the tissue

Indications of UBW remodeling were seen in the dynamic organ culture conditions evidenced by the collagen assays. A significantly larger amount of pepsin-soluble collagen (non-fibrillar collagen) was detected in the native tissue (actual value 2.510 +/- 0.151 mg) compared to the 0.5 Hz and 1 hr groups at 7 days and the 1 hr and 8hr groups at 14 days (Fig. 2-2A). Additionally, there was a significantly greater amount ($p=0.017$) of soluble collagen found in the 0.5 Hz group at 14 days compared to the same group at 7 days. Pepsin insoluble collagen (fibrillar collagen) concentration was not statistically different ($p=0.256$) among any of the groups following 7 days in culture (Fig 2-2B). The actual value of the insoluble collagen in the native rat bladder was found to be 30.784 +/- 3.214 mg. In contrast to the 7 day results, after 14 days in culture there was a significant increase in pepsin insoluble collagen ($p=0.033$) in the 1 hr group compared to the amount found at the 7 day time point (Fig 2-2B).

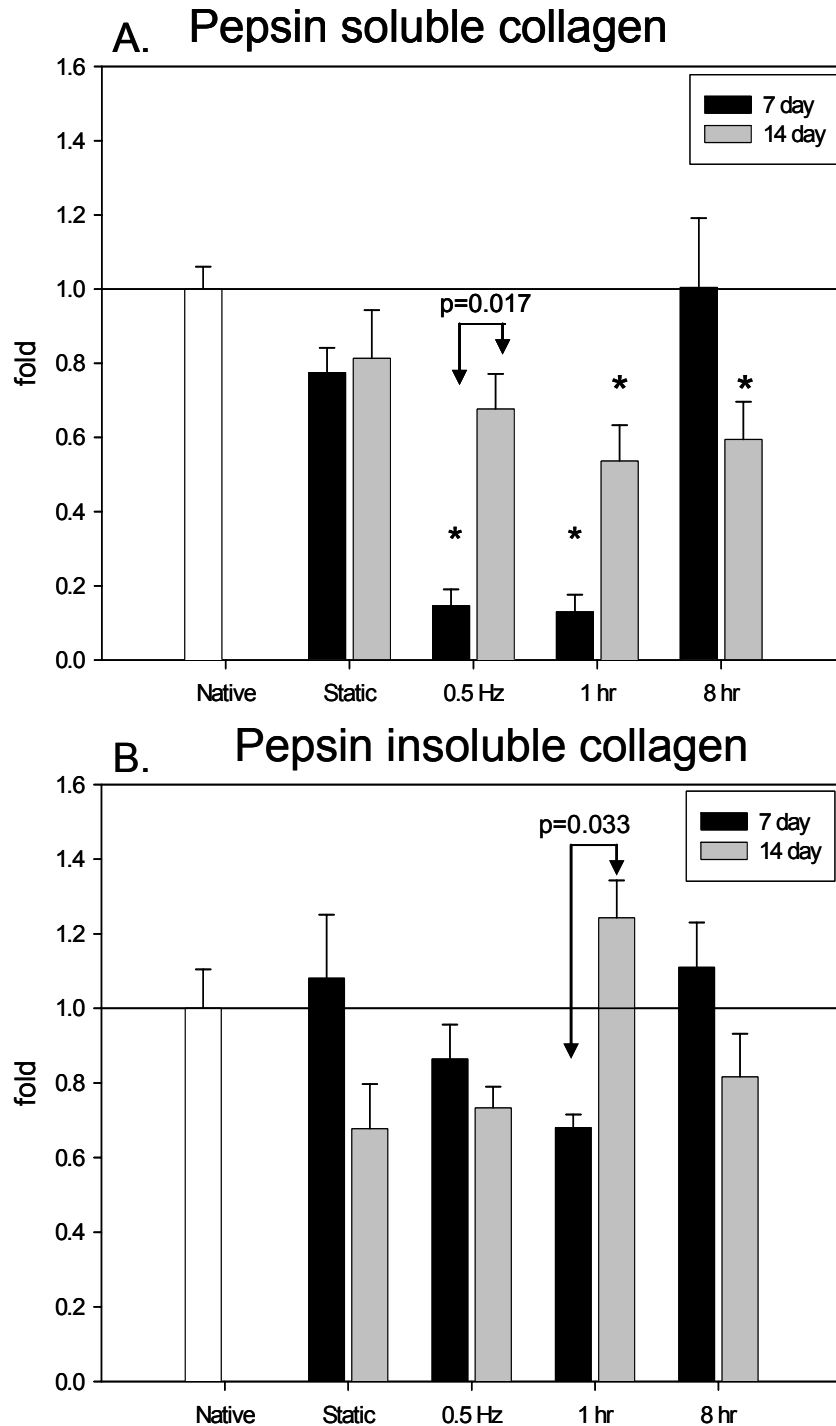


Figure 2-2. Total collagen concentration (pepsin insoluble and soluble) of cultured bladder strips following 7 and 14 days in culture. (A) Pepsin soluble collagen at 7 and 14 days. The 0.5 Hz and 1 hr groups are significantly different $p < 0.01$ than all other groups. The Native group is significantly higher than the 0.5 Hz and 1 hr groups at 7 days and the 1 hr and 8 hr groups at 14 days * $p < 0.05$. (B) Pepsin insoluble collagen at 7 and 14 days. There were no statistically significant differences in insoluble collagen between the groups except for between the 7 and 14 day time points in the 1 hr group ($p = 0.033$). All data are presented as mean \pm sem with $n = 5$ or 6 per group.

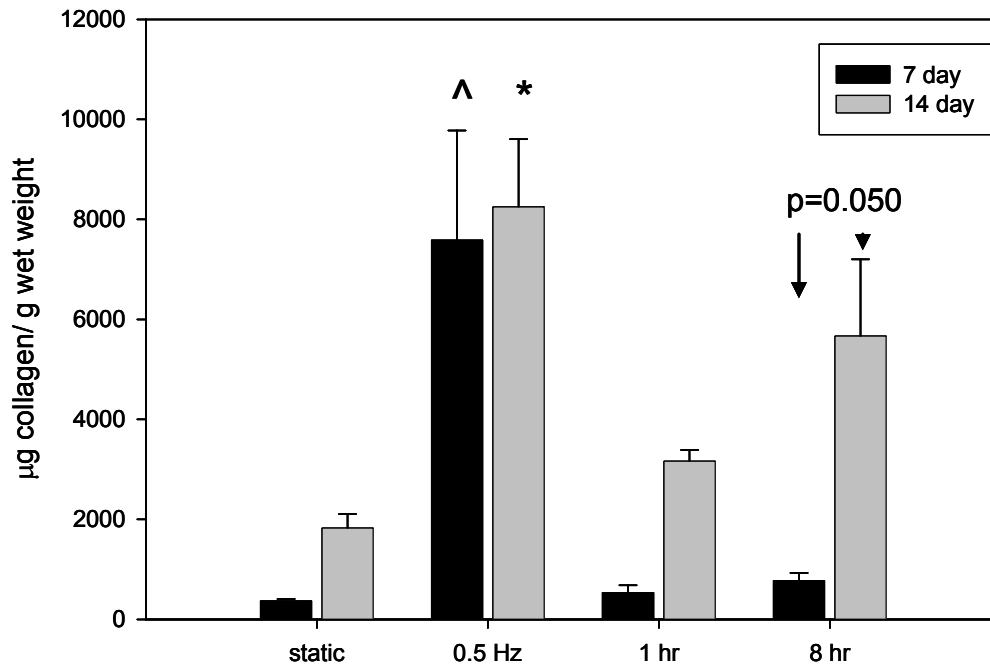
2.3.3 Collagen turnover

These assay results were summed from each day of collection. After 7 and 14 days in culture, the soluble collagen found in the media of the 0.5 Hz group was nearly 20 fold higher than that of any other group (Fig 2-3A). Similarly, at 14 days in culture, the MMP activity of the 0.5 Hz group was found to be significantly greater ($p < 0.05$) than that of any other group (Fig 2-3A). However, in the 8 hr group, a significant difference was observed ($p = 0.050$) between the 7 and 14 day groups (Fig 2-3A).

2.3.4 Elastogenesis

Elastin assays along with histology and immunohistochemistry revealed that elastogenesis occurred. Histological analysis (Fig 2-4) showed that bladder strips in the organ culture system remain viable and structurally intact for up to 7 days in culture. Smooth muscle bundles in circumferential and longitudinal layers surrounded by collagen were visible in all samples. Samples exposed to stretch appeared to be thinner than the fresh and statically cultured samples in histological sections. A large amount of elastin fibers, (Fig 2-4E, arrows), was observed in the 0.5 Hz group that could not be found in any other groups. Furthermore, immunohistochemical staining with the antibody to elastin showed large amounts of positive staining in the 0.5 Hz group (Fig 2-5B) while the only positive staining for elastin in all other groups was found only in the blood vessels (Fig 2-5 A).

A. Collagen in media



B. MMP activity in media

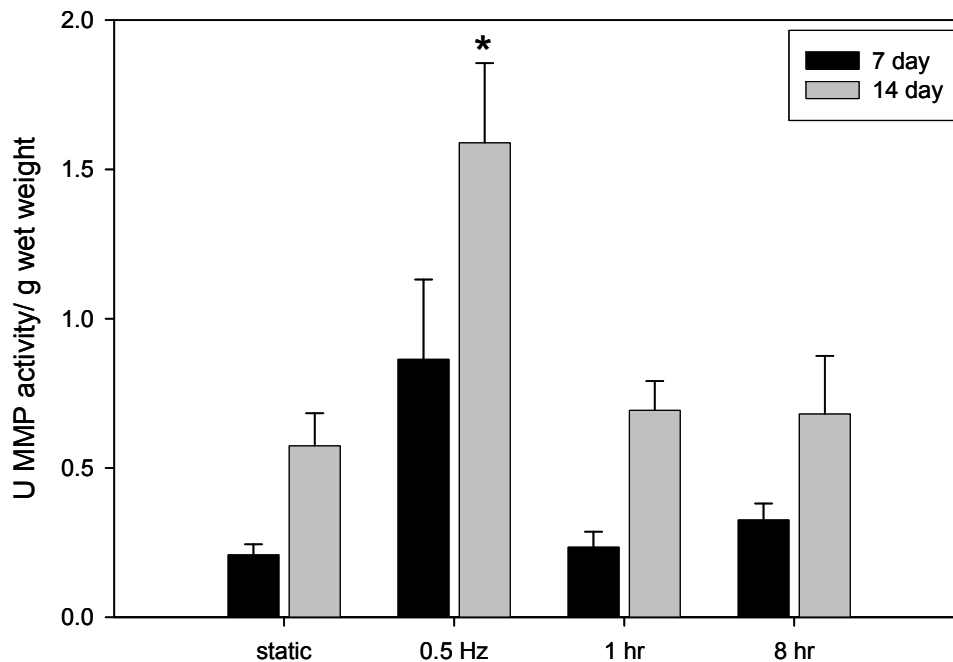


Figure 2-3. Soluble collagen and MMP activity found in the culture media (A) 7 and 14 day soluble collagen found in the media. Significantly more soluble collagen was found in the 0.5 Hz group media than in all other groups, $^{\wedge}p < 0.05$. The soluble collagen in the media from 8 hour group at 14 days was significantly greater than the soluble collagen from the 8 hour group at 7 days, $p = 0.050$. (B) 7 and 14 day MMP activity found in the media. Significantly more MMP activity was found in the 0.5 Hz group media at 14 days than in all other groups, $*p < 0.05$. All data are presented as mean \pm sem with $n = 4$ for 7 day groups and $n = 5$ or 6 for 14 day groups.

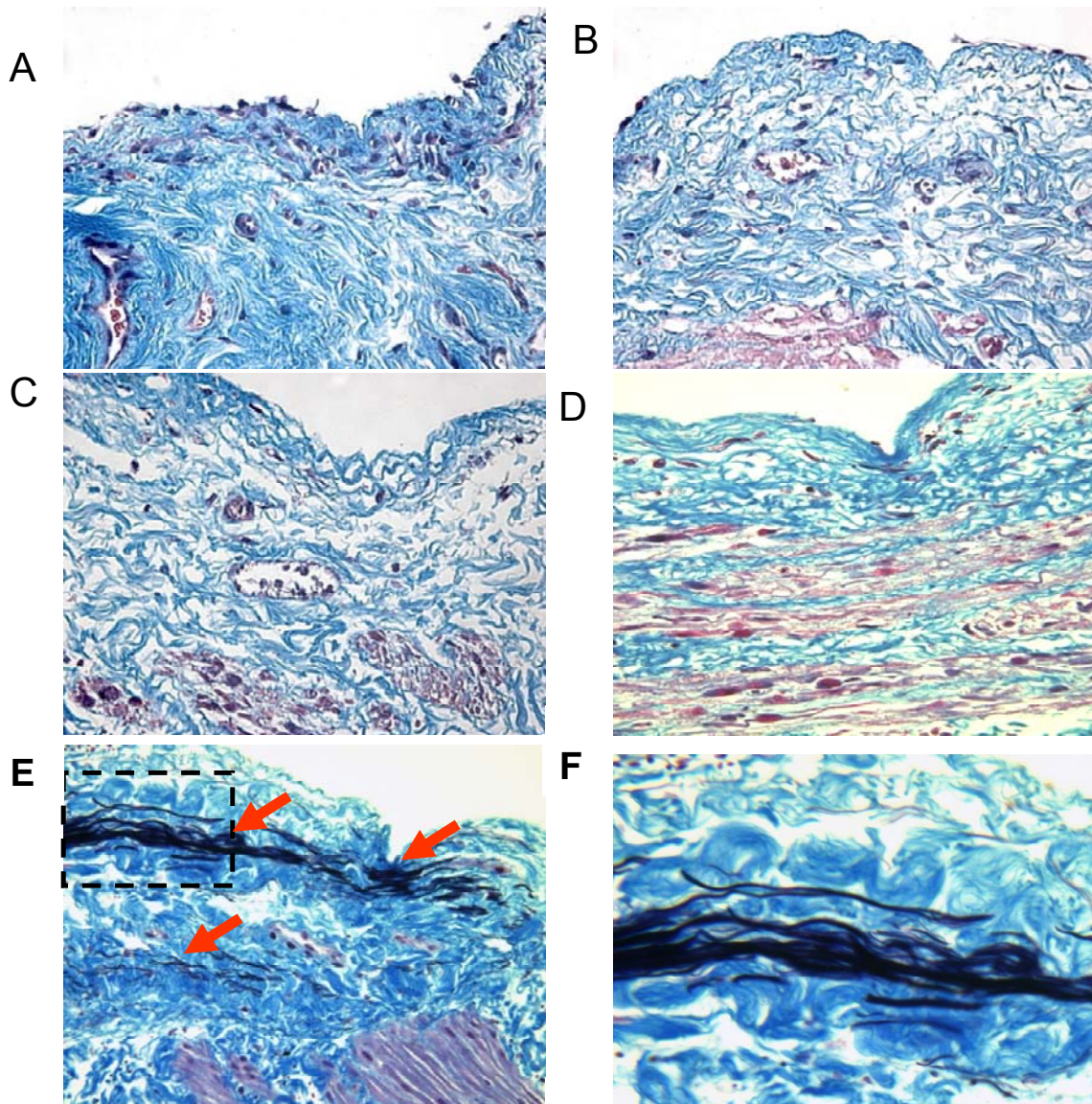


Figure 2-4. Elastic trichrome staining of cross sections of (A) fresh tissue, (B) 7 day statically cultured tissue, (C) 7 day 1 hr cycle, (D) 7 day 8 hr cycle, (E) 7 day 0.5 Hz cycle, (F) portion of 7 day 0.5 Hz magnified to display the elastin. Images are reduced from 400x. Red arrows in (E) indicate areas of elastin formation. Blue represents collagen, black represents elastin, purple represents cell nuclei, and red represents cytoplasm.

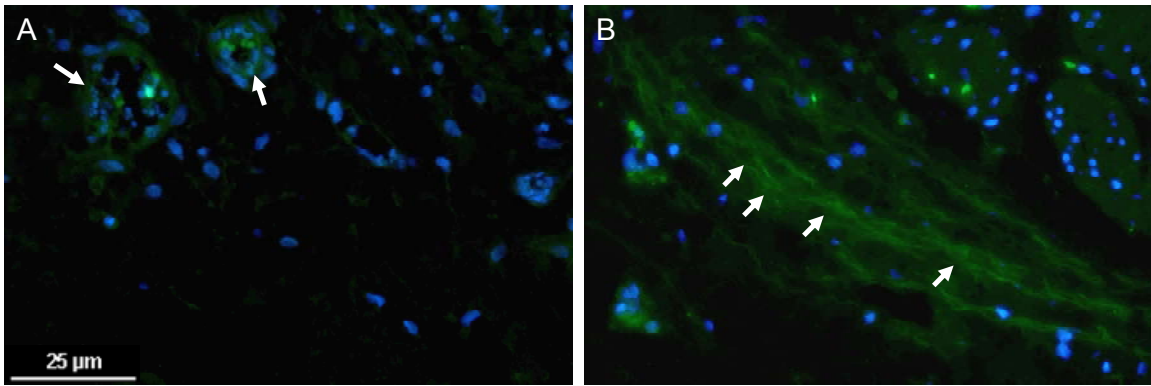


Figure 2-5. Immunohistochemistry with antibody to elastin and DAPI nucleoli staining (blue). (A) Overlaid image of static culture specimen, note elastin (green) is only seen around blood vessels (arrows). (B) Overlaid image of 0.5 Hz group at 7 days, note the large portion of fibrillar elastin (green).

Quantitatively, after 7 days in culture, elastin in the 0.5 Hz group was 6 fold greater than in the native tissue (actual value native tissue: 239.267 +/- 34.584 μg) (Fig 2-6). There was no change in elastin composition between the native tissue and the static, 1 hr and 8 hr groups (Fig 2-6). A similar trend was seen at the 14 day time point. Again, there was a significantly greater amount of elastin found in the tissues stretched at the 0.5 Hz cycle compared to all other groups (Fig 2-6). This up-regulation of elastin in the cyclic group is indicative of elastogenesis and confirmed the results found by histology and immunohistochemistry.

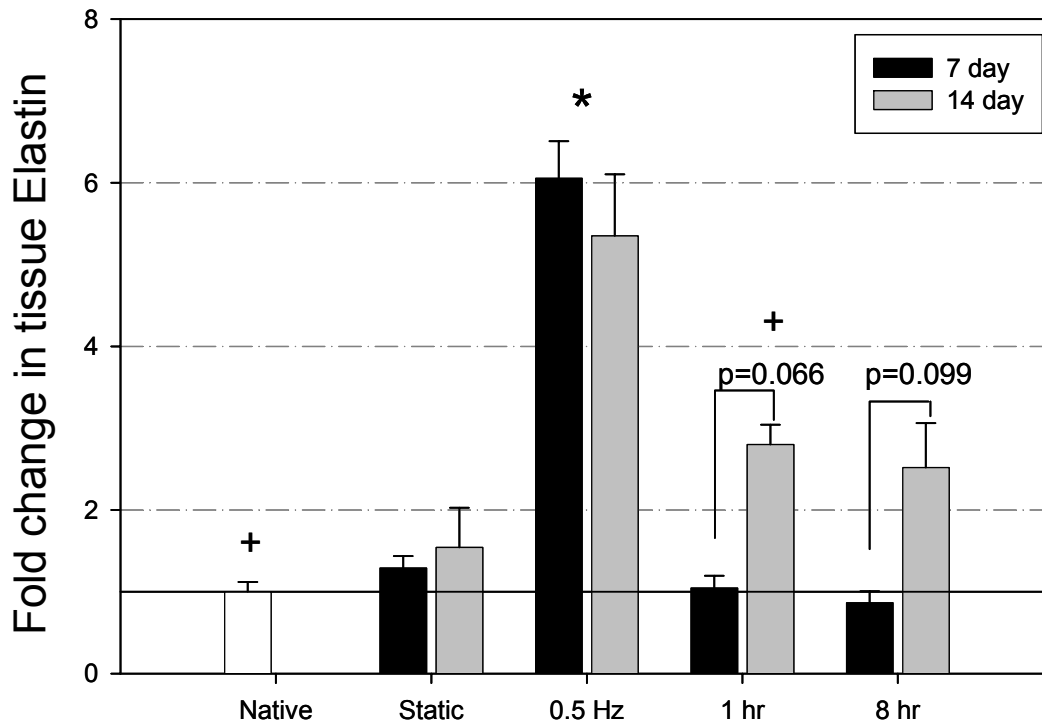


Figure 2-6. Elastin concentration of bladder samples following 7 and 14 days in culture. Data are presented as mean \pm sem with $n=5$ or 6 for each group. The 0.5 Hz group at both 7 and 14 days was significantly greater, $*p<0.001$, compared to all other groups. The 1 hour group at 14 days was significantly greater, $+p<0.05$, compared to native tissue.

2.4 DISCUSSION

2.4.1 Bladder wall tissue remodeling

This is the first study to the authors' knowledge that examines the UBW in a dynamic ex vivo system, which demonstrated significant ECM remodeling, and in particular profound fibrillar elastogenesis. While it is known that the bladder wall undergoes profound remodeling resulting

from pathologies such as spinal cord injury or obstruction, there have been few studies examining the role of strain in the remodeling process. This study has isolated the effect of strain on the UBW, and has shown that strain is capable of inducing collagen turnover and biosynthesis as well as elastin production and assembly into fibrils after only 7 days in culture. Furthermore, this study has shown that the strain history of the UBW influences the remodeling process greatly, with small changes in collagen synthesis under physiological strain histories, and large changes in both collagen turnover and elastogenesis under a non-physiological strain history.

2.4.2 Strain induced alterations in collagen biosynthesis

The changes in both soluble and insoluble collagen in the tissue indicated that there is collagen turnover occurring dependent on the stretch protocol. MMP results from the media are positively correlated to the collagen found in the media ($R^2=0.98$ for 7 days and $R^2=0.75$ for 14 days) thus indicating that a portion of the soluble collagen that was found in the media may be enzymatically degraded collagen. However, since there was nearly a *20 fold* increase in the media collagen at 0.5 Hz at 7 days compared with only a 4 fold increase in the media MMP under the same conditions, it is possible that there may also be newly formed collagen in the media or fragmentation of broken-down collagen that has not been entirely degraded by the MMPs.

In a previous study, MMPs have been found to increase in an ex vivo model of bladder outlet obstruction after 24 hours of static distension, and bladder smooth muscle cells responded to static distension with an increase in ERK-1,2 [130]. These findings contrast the results from the present study wherein MMP activity was only increased in the 0.5 Hz group, not in the 8 hr cycle, which is more similar to static distension. The present study looked at the cumulative long

term effects of stretch in the ex vivo organ; however, even at the 48 hour media collection, the MMP values in the 0.5 Hz group were over 2 fold greater than those of any other group (data not shown). The reason for the contrast between our results and others may be due to our organ culture preparation involving cutting the sample into a strip that may induce a different microenvironment than found in the intact bladder.

Additionally, the soluble collagen is decreased in the 1 hr group at 7 days, but there was a significantly higher amount of insoluble collagen in the same group at 14 days. These results indicate that collagen production is occurring over time and a portion of it is likely being incorporated into the tissue. Compared to pathological conditions, this increase in collagen concentration in the 1 hr group at 14 days is on the same order of magnitude observed in the rat bladder following spinal cord injury at 10 weeks (1.24 and 1.68 fold, respectively [64]). Moreover, increased amounts of collagen, or fibrosis, is found in the non compliant bladder resulting from non-neurogenic pathologies such as the obstructed bladder or radiation therapy [47]. In these previous in vivo studies, bladder fibrosis occurred after the pathological condition persisted on the order of months. The 1 hour loading condition in the present study gave rise to collagen deposition at 14 days, which was not seen at 7 days, thus indicating that for collagen remodeling to occur, longer-term loading may be necessary.

2.4.3 Strain induced elastogenesis in the UBW

The most extensive tissue remodeling seen in the ex vivo bladder strips occurred in the 0.5 Hz group. The increase in elastin concentration of the 0.5 Hz group at both 7 and 14 days (5-6 fold compared to native tissue) is indicative of elastogenesis occurring in response to this high strain

rate. This increase in elastin concentration is similar to the increase seen in the spinal cord injury affected bladder. At 1.5 weeks following spinal cord injury, the rat bladder contained nearly 4 fold more elastin than in the normal bladder, and at 3 weeks following spinal cord injury, the rat bladder contained 5.19 fold more elastin than the normal bladder [64].

While the Fastin elastin assay measures all forms of elastin (tropoelastin and mature elastin), fibrillar elastin was seen in the Elastic Trichrome staining and immunohistochemistry of the cross sectioned samples. Patches of elastin were found throughout the tissues in the 0.5 Hz group; however, the large fibrillar bundles were located primarily near the lamina propria above the detrusor muscle. In pathological conditions, the majority of newly formed elastin is found intra- and interfascially in the detrusor muscle [36, 53, 112, 131]. In the organ culture system presented in this study, the bladder smooth muscle cells in the detrusor are preserved in the RPMI 1640 culture media, while the urothelium are not viable in the system and slough off the bladder strip within in the first day of culture as observed with histological sectioning (data not shown).

Based on our present understanding, definitive evidence for the origin of the elastin produced is lacking in part due to the third major cell type found in the UBW, the myofibroblast. The media used in this system contains the D isomer of valine that should not support fibroblast growth [132]; however, histological sectioning of our bladder strips shows these suburothelial myofibroblasts in the regions of the lamina propria where the large amounts of fibrillar elastin are located. At present, the bladder myofibroblasts have not been shown to play a role in bladder ECM regulation and have been shown to play a role in electrical signal transduction in the bladder [3]. Since the bladder smooth muscle cells make up the vast majority of cells in the bladder, and it has been shown previously that bladder smooth muscle cells have the capability to

produce elastin in the non-compliant bladder [2], it is reasonable to postulate that tropoelastin molecules are produced in the detrusor under the non-physiologic stretch frequency of 0.5 Hz. Furthermore, the elastin molecules may be assembled into fibrillar elastin in the thick collagenous matrix of the lamina propria since elastin molecules produced by smooth muscle cells need an ECM in order to be assembled [68].

A potential explanation for the extensive fibril formation found in the 0.5 Hz group may be due to the effects of the high stretch frequency on the binding sites on the elastin proteins. In a previous study by Jesudason et al. [133], cyclic stretch at 0.33 Hz on an elastin rich ECM was found to have a protective effect against elastase activity while a much slower frequency of ~0.08 Hz was found to increase elastase degradation. The authors explained that the binding sites on the elastin were protected at the higher stretch frequency while the binding sites were exposed at the lower frequency [133]. Therefore, it is plausible that the elastin produced in the tissue at 0.5 Hz was protected by the high stretch frequency thus allowing it to form what appears to be dense fibrillar elastin within the lamina propria. The 1 and 8 hour groups are stretched at a much lower frequency, potentially exposing any newly formed elastin to degradation. However, after 14 days in culture, the elastin in the 1 and 8 hour groups is increased compared to the native group and the 1 and 8 hour groups at 7 days. It is possible that with prolonged stretch, the cells are producing elastin; yet there was no visible fibrillar elastin in the 14 day histology of the 1 and 8 hour groups.

2.4.4 Stretch frequencies

The 1 hour and 8 hour stretch protocols in this study were chosen based upon approximations of in vivo bladder pathologies in the rat model; however, the results do not precisely mimic remodeling found in vivo. During normal voiding, bladder tissue is stretched between 10-20% multi-axially. In the present system, the bladder strips are stretched strip biaxially with strain applied in the longitudinal direction. In the native rat bladder, the bladder is stretched multi-directionally during filling; however the most stretch occurs in the longitudinal direction (observation during cystometry). It has been shown previously that the majority of the bladder smooth muscle bundles are oriented longitudinally in the rat bladder [112]. By stretching the bladder to 20% in the longitudinal direction, a contractile response may be elicited, further mimicking the native bladder as it stretches for filling and contracts for voiding [4]. Ideally, to determine the forces generated by this contractile response in the organ culture system, load cells would be used for real time measurement of the bladder strips during stretch. The addition of load cells to our bioreactor set up is not trivial; however, this option will be explored in our future studies.

In diseased states such as spinal cord injury or bladder outlet obstruction, the bladder may be over-distended to 25% stretch or more. The rates of voiding also vary greatly between normal and diseased states i.e., in the normal rat, the bladder fills over 1-1.5 hours and voids over 10 s between 18 – 24 times daily, and in the spinal cord injury rat the bladder fills over 1 hour but only voids 3-4 times daily [134]. Previous studies of these physiological conditions showed remodeling of the bladder, specifically in the spinal cord injury pathology (similar to our 8 hour cycle) [35], indicated by alterations in ECM proteins, hypertrophy, and biomechanical

properties. However, the non-physiological loading state of 0.5 Hz produced a model most closely mimicking UBW remodeling in the disease state. The 0.5 Hz frequency stimulated the largest amount of tissue remodeling indicated by the large quantity of elastin produced in the tissue and the large quantity of collagen and MMPs released into the culture media.

2.4.5 Influence of strain history

The 0.5 Hz frequency in this study was chosen to deliver a non-physiologic strain history to the bladder strips based upon information from isolated cell studies on smooth muscle. Smooth muscle cells isolated from the bladder have been shown to express up-regulated ECM genes, specifically collagen types I and III and fibronectin, under high frequency stretch protocols ranging from 0.1-1 Hz. Stretch frequency ranges have been shown to alter cellular gene expression for contractile proteins alpha-smooth muscle actin and calponin as well as collagen types I and III [126] [135]. At a stretch frequency of 0.5 Hz, collagen type I was up regulated in bladder smooth muscle cells while at a stretch frequency of 0.4 Hz, collagen types I and III along with fibronectin were up regulated [126]. There are currently no studies that have examined the effect of the 0.5 Hz frequency in bladder smooth muscle cells with regard to elastin production. However, under static pressure bladder smooth muscle cells produced a larger amount of elastin than cells under atmospheric pressure [136]. Additionally, vascular smooth muscle cells seeded on a collagen gel produced elastin when stretched at 0.5 Hz [137]. The aforementioned studies suggest that remodeling in the UBW may depend on the frequency of strain; however, future studies will also examine the effects of the magnitude of strain in this ex vivo system. These previous studies along with data obtained in the current study indicate the need to examine both

physiological and non-physiological stretch frequencies in order to have an understanding of bladder function in disease.

2.4.6 Examining the limits of ex vivo organ culture

In order to further examine the role of strain on ECM remodeling, two pilot studies were performed examining 1) larger strain of 40% and 2) a physiologic fast cyclic stretch frequency of 0.1 Hz. The physiologic fast cyclic may be considered physiologic because the bladder wall undergoes rhythmic contractions 1-5 times a minute. The 0.1 Hz frequency may approximate these peristaltic contractions. For the larger strain experiment, 6 bladder strips were prepared as described in the protocol section 2. These 6 bladders were stretched for 7 days to 40% stretch at 0.5 Hz. Following the stretch the same outcome measures were utilized. These experiments showed that by stretching at 0.5 Hz to 40 % there was significantly more collagen in the tissue compared to the 20% stretch at 0.5 Hz (Figure 2-7). Additionally, stretching to 40% did change the amount of elastin in the tissue with a significant increase compared to the native and a significant decrease compared to the 20% 0.5 Hz tissue (Figure 2-7). These results indicate that ECM composition in the rapidly cycled bladder groups is not only frequency dependent but also stretch dependent.

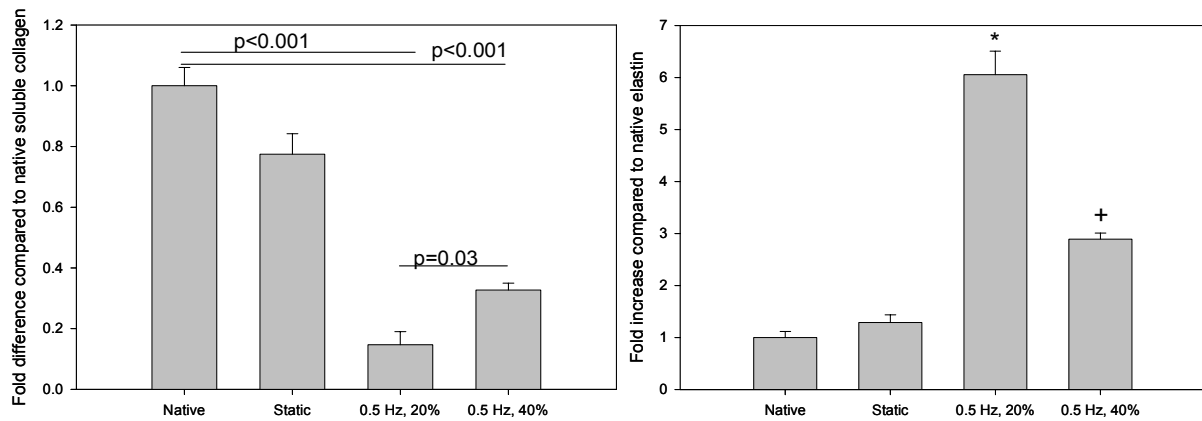


Figure 2-7. A. Soluble collagen following 7 days organ culture. Significance determined by one way ANOVA followed by Student Newman Keuls test for multiple comparisons. B. Fold increase over native elastin concentration. Data are presented as mean +/- sem, n=5-6 per group. *p<0.001 compared to native. +p<0.001 compared to native.

2.4.7 Implications for engineered smooth muscle tissues

In many of the aforementioned urinary bladder pathologies (bladder outlet obstruction, diabetes mellitus, and spinal cord injury or related neurogenic disorders) wherein remodeling of the ECM occurs, the chronic disease state ultimately leads to the need for bladder replacement. The field of tissue engineering has made significant strides in improving upon traditional methods of UBW replacement. Replacements are usually comprised of autologous cells that have been seeded on either a biodegradable polymeric scaffold [138] [139] or xenographic decellularized matrix, such as small intestinal submucosa (SIS) [140, 141] or bladder acellular matrix (BAM) [100, 142]. The recent findings of an initial clinical study by Atala et al. [99] showed significant and exciting success utilizing autologous urothelial and smooth muscle cells on a composite matrix implanted into patients with myelomeningocele. The patients' bladder capacities and compliance were increased; however, functionality of the bladder could not be determined.

Studies utilizing these methods have shown regenerated urothelium [82], smooth muscle fibers and multiple blood vessels [82], in addition to minimizing inflammatory reactions up to 22 weeks [143].

Yet, despite these encouraging results, incomplete and disorganized bladder smooth muscle regeneration has been observed 22 weeks post-implantation [143]. Typically, smooth muscle cells were observed to aggregate into small, irregular muscle bundles and did not achieve the large-scale tissue structures observed in the native bladder [143]. In another study, smooth muscle cells were arranged only longitudinally compared to the circumferential and longitudinal orientations found in the native UBW [82]. The above cited studies underscore that in-vivo remodeling by itself cannot be completely relied on to form a fully functional implant, and there is a need to develop approaches that promote appropriate ECM formation prior to implantation. Cues from tissue remodeling in pathological conditions may lead to better methods for functional tissue engineering of the bladder.

The present study has demonstrated that the cells in the urinary bladder may be manipulated via varied stretch protocols and frequencies ex vivo to produce large quantities of the ECM proteins, collagen and elastin. These ECM proteins, particularly elastin, are of great interest in tissue engineering other smooth muscle tissues such as the airway and vasculature wherein the elastin is crucial to proper tissue function. The present study suggests that bladder smooth muscle cells may be manipulated via mechanical stretch on a synthetic or ECM-derived scaffold to produce the proper ratios of elastin and collagen for smooth muscle tissue engineering applications.

2.4.8 Summary

This study has demonstrated that the ex vivo bladder wall responds to certain strain histories by upregulated collagen and elastin assembly. Specifically, fibrillar elastin was produced under a cyclic strain of 0.5 Hz (an increase of over 5-fold the amount found in the native bladder), while collagen was both synthesized and degraded within the bladder tissue at the same 0.5 Hz frequency. These results exemplify the effectiveness of utilizing an ex vivo organ culture model to understand strain-induced bladder wall remodeling, separating the effects of innervation and the tension associated with bladder filling from contractile forces. Furthermore, ex vivo organ culture of the bladder provides a means to understand strain-induced tissue remodeling that may be exploited in the future to tissue engineer UBW replacements.

3.0 THE EFFECT OF EXOGENOUS TGF- β 1 ON EX VIVO BLADDER EXTRACELLULAR MATRIX COMPOSITION AND SMOOTH MUSCLE CELL PHENOTYPE

3.1 INTRODUCTION

The urinary bladder wall undergoes extensive structural remodeling following pathologies which cause over distension and loss of controlled voiding. Following spinal cord injury (SCI) the bladder increases in size tremendously (Figure 3-1). The bladder smooth muscle hypertrophies, elastin content increases, and the biomechanical properties of the wall change material class, from isotropic to anisotropic [64]. It is unclear at present whether the detrusor is adaptive and compensating to an increase in volume from continual filling and irregular voiding, or whether the clinical symptoms of this increased volume and irregular voiding are due to the remodeling itself, which may occur as a result of the lack of innervation. As seen in the SCI affected bladder, the remodeling process appears in two phases. In the first phase, the bladder is areflexic and in the second phase spontaneous contractions begin to occur. In the areflexic phase the bladder is flaccid and tends to be over distended due to intermittent voiding [54]. Adam et al suggested that hypertrophy, or increase in bladder muscle mass, is due to sustained distension of the bladder wall [69]. While with the present data it is impossible to know the sequence and/or relationship of remodeling events, it is helpful to utilize in vitro organ culture models to examine the role of

molecules involved in or responsible for portions of the remodeling process. TGF- β 1 is one such molecule.

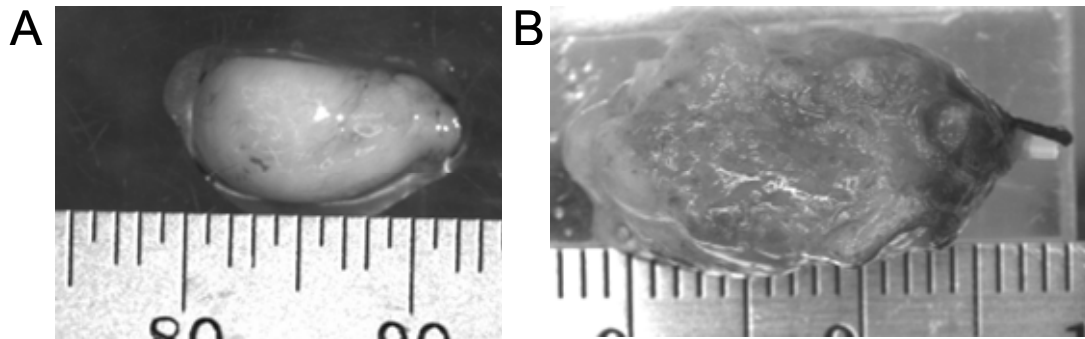


Figure 3-1. Photographs of excised bladders from A. Normal and B. SCI rats. Small ruler increments are in mm.

3.1.1 Role of TGF- β 1 in disease state and fibrosis

TGF- β 1 is a molecule often implicated in fibrosis and remodeling many tissues under pathological conditions. In the urinary bladder TGF- β 1 has gone largely overlooked in the disease state. Our laboratory has shown previously that TGF- β 1 gene expression is up-regulated only 3 days following SCI in the rat urinary bladder and continues to be up-regulated out to 21 days post-SCI (Figure 3-2). The TGF- β 1 expression also correlates with expression of tropoelastin, lysyl oxidase, and IGF-1. In other studies, TGF- β 1 has induced hypertrophy, up-regulated collagen, and inhibited proliferation of BSMCs [144]. TGF- β 1 has been known to modulate cellular phenotype in fibrosis [145], and it has been shown to regulate the RHAMM protein as well as CTGF in the fibrotic bladder [68, 146]. Gene expression for TGF- β 1 was also found to be up-regulated in a streptozotocin induced diabetic rat model [34]. Furthermore, TGF- β up regulation has been found repeatedly in rat models and in patients who have bladder outlet

obstruction [144], and it has also been found up regulated in the bladders of human patients with interstitial cystitis, urothelial cancer, and prostate cancer [147]. TGF- β 1 has also been administered to rabbit bladders and caused the fibroblasts within the lamina propria to differentiate into smooth muscle bundles [148]. Additionally, TGF- β 1 administered to human BSMC lead to an increase in stress fibers with a reduction of connexin-43 gap junctions [147]. Based upon these previous studies from our laboratory and others, it stands to reason that TGF- β 1 may be a key regulator of tissue fibrosis and hypertrophy in the SCI affected bladder.

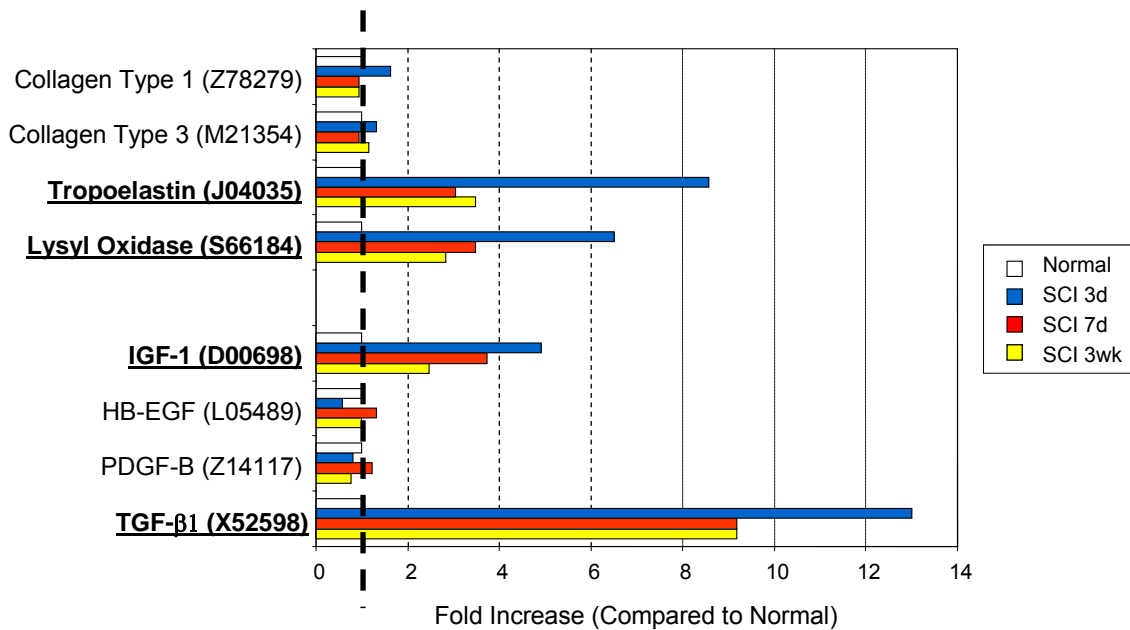


Figure 3-2. Gene array expression of key genes involved in ECM remodeling of the SCI bladder. [35].

3.1.2 Cellular phenotype shift

The BSMCs are the most prevalent cell type in the urinary bladder wall. These cells require the maintenance of a contractile phenotype, commonly characterized by the expression of h-caldesmon (h-CaD) and alpha-smooth muscle actin (α -SMA), in order to function properly to sustain muscular tone and produce coordinated contractions when signaled by stretch. In certain

pathological conditions, it has been reported that the BSMCs may experience a phenotypic shift from a more contractile to a more synthetic phenotype. In tissue culture on polystyrene plates, the BSMCs only retain their contractile phenotype for a limited number of cell passages, marked by a decrease in expression of h-CaD. Furthermore, in the vascular literature, a phenotypic shift of the SMC is thought to occur early on in culture as the cells begin to proliferate [138]. Since the nature of virtually all SMC in the body is to remain in a contractile, non-proliferative state, tissue culture of primary SMC shifts the cells into a proliferative and sometimes synthetic state. In the disease states of the bladder, there has been much controversy whether or not the BSMC hypertrophy or proliferate. Hypertrophic smooth muscle cells express larger amounts of α – SMA in comparison to normal, not hypertrophied cells [149].

There has been an area of research recently that examines phenotypic shift in cells occurring in myofibroblasts. In the disease state, these myofibroblasts will shift from their normal, quiescent phenotype to an active, synthetic phenotype. The synthetic phenotype in the myofibroblast is characterized through increased expression of α –SMA and increased collagen production simultaneously [150]. In a collagen gel model, myofibroblasts contract collagen gels to a greater degree than fibroblasts [151]. Additionally, myofibroblasts with the addition of TGF- β 1 become more contractile [151].

The phenotypic shift occurring within BSMCs are not as clear. Firstly, the BSMCs retain a contractile phenotype in the healthy bladder. Second, the BSMC become synthetic in any unnatural state, i.e. in tissue culture or a pathological condition. One theory is that the bladder smooth muscle cells differentiate toward myofibroblasts or a wound healing phenotype in the neurogenic bladder. This is supported via alterations in contractile proteins and synthesis of collagen [47]. However, this evidence is not consistent in all disease states. Evidence of a

phenotypic shift in smooth muscle cells has been found in the cardiovascular system [152], the kidney [153], and the airway [149, 154]. Mechanical stretch experiments on isolated BSMC have also shown that increased stretch will alter the BSMC phenotype by modulating cellular shape and actin reorganization [155]. Leask et al has shown that TGF- β 1 can modulate the cells toward a more synthetic phenotype [145]. Throughout the literature, the phenotypic shift of the BSMC does not appear to have concrete, common, characteristics other than that the cells become functionally less contractile. There is thus a need to further explore the effect of mechanical stretch and TGF- β 1 on the phenotype of the BSMC to understand the shift that may occur in the disease state.

The overall goal of the present study presented in this chapter was to accomplish the scientific endpoint of Specific Aim 2.1. This endpoint was to assess the role of TGF- β 1 with and without strip biaxial stretch on BSMC phenotype, ECM synthesis, and mechanical properties and compare these outcome measures to established data on the SCI rat bladder. The present study provides further evidence that TGF- β 1 is an important biological factor in the remodeling process.

3.2 PROTOCOL

3.2.1 Dynamic ex vivo organ culture

Bladder strips were excised from female Sprague Dawley rats (2-3 mos.) and mounted in the tension bioreactor as described in Chapter 2. Nine bladder strips were stretched at 0.5 Hz , 20%

stretch for 7 days. Another nine bladder strips were statically floating in the bioreactor. To all groups, 1 ng/mL TGF- β 1 (R&D Systems) in RPMI 1640 media supplemented with 10% FBS and 1% PS. Media was changed daily.

3.2.2 ECM assays

At the end of culture time, bladder samples were removed and snap frozen in liquid nitrogen for biochemical assays or fixed in 10% neutral buffered formalin. Soluble collagen was assayed from the tissue and the media according to methods in Chapter 2. Elastin was also assayed with methods described in Chapter 2

3.2.3 RT-PCR

Messenger RNA extraction and RT-PCR were performed by the Pitt Genomics and Proteomics Core Laboratories, Pittsburgh, PA. Samples following culture at 0.5 Hz, n=3 per group, were snap frozen with liquid nitrogen and stored at -80 degrees C. mRNA extraction was isolated using RNeasy kit. Ribonucleic acid concentration and purity were determined spectrophotometrically. The integrity of the RNA samples was confirmed by RNA integrity numbers that were greater than 5.0 according to the Bioanalyzer 2100 and the RNA Nano 6000 LabChip kit (Agilent Technologies, Santa Clara, Calif). Ribonucleic acid samples (1 μ g) were reverse transcribed to create complementary deoxyribonucleic acid (cDNA) at 42°C for 1 hour with the Superscript III First Strand Synthesis Kit (Invitrogen) and a Rotorgene thermal cycler (Corbett Life Sciences, Sydney, Australia). The cDNA samples were then amplified (40 cycles: 90°C for 15 seconds and 60°C for 60 seconds) with the SYBR Green Master Mix (Invitrogen)

and custom designed PCR primer sets for type I collagen, type III collagen, and tropoelastin in the Rotorgene thermal cycler (Table 3-1). Each sample was normalized to its amplification of Beta glucuronidase (beta gus). Furthermore, for comparison purposes the native group was averaged and used to normalize expression in the test group. Time permitted for only the 0.5 Hz group and the native bladders to be tested.

Table 3-1 *PCR primers*

	Sense	Anti-Sense
Type I collagen	5'- TCCTTTCTCCACCCCTC -3'	5'- TCCTGTGTCTTTGGGGGA - 3'
Type III collagen	5'-GTCTTATCAGCCCTGGTT C-3'	5'-CCAGTATTCTCCGCTCTTGAGT-3'
Tropoelastin	5'-CCTGTCCCTGACTCCCATTA-3'	5'-CAGTGTGAGAAGTCGTCGGA-3'
Beta glucuronidase	5' -GCCTTCATT TTGCGAGAGAG - 3'	5' -ACGGTCTGCTTCCCATACAC -3'

3.2.4 Mechanical testing

Due to extreme preconditioning from stretching the bladder strips in the longitudinal direction in culture for 7 days, mechanical testing was performed using a strip-biaxial testing system as described previously [127]. With this set up, the bladder strips were mounted to the bars of the testing device using the stainless steel spring grips that were also used to stretch the sample in culture. Four graphite markers were placed in a square in the center of the specimen. For passive and inactive testing, the bladder strips were stretched to 1.2 or 1.3 (for more compliant groups) while the deformation of the flexible bar was monitored. For decellularized testing, the bladder

strips were stretched until the tension stretch curve moved out of the linear elastic region, (on average to 1.35).

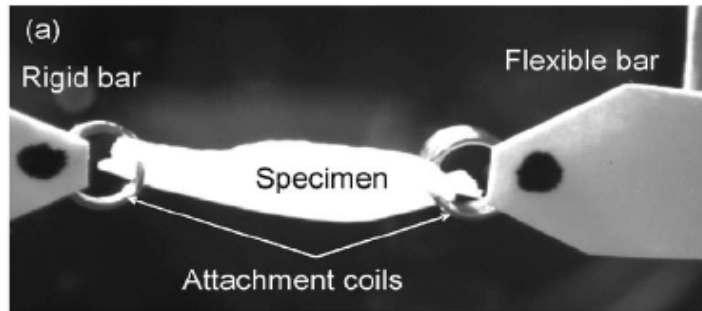


Figure 3-3. Mechanical testing set up [127]

Table 3-2. Mechanical testing conditions for bladder strips following culture

Testing case	Conditions
Active	Testing under physiologic conditions, Kreb's solution at 37 degrees C, bubbled O ₂ , stretched to 20% prior to the addition of XmM carbachol. Active contraction was measured by bar deformation.
Passive	Testing under physiologic conditions, 37 degrees C, bubbled O ₂
Inactive	Testing in room temperature PBS following an overnight in modified Kreb's.
Decellularized	Testing under inactive conditions following week long decellularization protocol.

3.2.5 Bladder decellularization

Following inactive mechanical testing bladder strips were decellularized according to a modified protocol from Nagatomi et al. Briefly, bladders were immersed in hypotonic Tris buffered saline (pH 8.0; Sigma) with 0.1 M Phenylmethanesulfonyl fluoride (PMSF, Sigma) for 28 hours. Second, the bladders were transferred into new solution with the Tris buffered saline, PMSF, and

the addition of 1% Triton X-100 (Sigma) for 44 hours. Finally, the bladders were transferred into new Tris solution with PMSF and 0.1% SDS (BioRad) for 28 hours. At the end of the decellularization process, the bladder strips were rinsed in PBS for 30 min and then tested at room temperature in PBS.

3.2.6 Immunohistochemistry

Sections of bladder tissue from 10-day, post-surgical spinalized female Sprague-Dawley rats were obtained from a previous study.[54] Three bladders from each test group were fixed in 10% neutral buffered formalin overnight and then transferred to PBS until processing could be performed. Samples were paraffin embedded and sectioned en face. Three slides per sample were used for each antibody stain. Slides were deparaffinized in 2 changes of xylene followed by a graded ethanol re-hydration. Antigen retrieval was performed using a Citrate EDTA buffer (10mM Citric Acid, 2 mM EDTA, 0.05% Tween 20, pH 6.2) at 95 degrees C for 30 minutes. All sections were blocked in 2% BSA for 1 hour prior to antibody application. For the TGF- β 1 antibody staining, 5 μ m sections were incubated with an anti-TGF- β 1 primary rabbit polyclonal IgG antibody (1:200; Santa Cruz Biotechnology, Santa Cruz, CA) and visualized with a streptavidin-Cy3 goat anti-rabbit IgG secondary antibody (1:1000; Jackson ImmunoResearch Laboratories, West Grove, PA). For the alpha-SMA staining, sections were incubated in a monoclonal anti-actin, α -Smooth Muscle-FITC antibody produced in mouse (1:250, Sigma Aldrich). For the h- and general CaD staining, sections were incubated in either a monoclonal anti-caldesmon antibody produced in mouse (1:100, Sigma Aldrich) or a monoclonal anti-caldesmon (smooth) antibody produced in mouse (1:100, Sigma Aldrich). The sections were then incubated with a rat biotinylated adsorbed anti-mouse IgG (1:500, R&D Systems). Finally, the

sections were rinsed in PBS and incubated with streptavidin-Cy3 (1:250, Sigma Aldrich). Following staining, the TGF- β 1 sections and the caldesmon sections were incubated for 10 minutes in 4',6-diamidino-2-phenylindole, dihydrochloride (DAPI; Invitrogen). Slides were then visualized using a Leica DM IRB fluorescence microscope. All images were taken at the same exposure time for each group of antibody staining.

3.2.7 Statistics

All data are expressed as mean \pm standard error of the mean (SEM), except for gene expression data, which is expressed in mean \pm standard deviation. Data were analyzed by either the Student's t-test or a one-way analysis of variance (ANOVA) followed by the Holm-Sidak method to detect statistical differences using SigmaStat software (Systat Software). $p < 0.05$ was considered statistically significant

3.3 THE EFFECT OF TGF- β 1 IN EX VIVO ORGAN CULTURE

3.3.1 TGF- β 1 antibody staining of normal, SCI-10 day, and cultured bladder strips

As shown in section 4-3 there was more abundant staining of TGF- β 1 in the SCI 10 day bladder (Figure 3-4 D) compared to the native bladder (Figure 3-4 A). Additionally the 0.5 Hz stretched bladder (Figure 3-4 C) also expressed more positive staining for TGF- β 1 compared to the native bladder. The two experimental groups to which TGF- β 1 was added to the media had positive staining throughout the smooth muscle bundles and blood vessels (Figure 3-4 E,F). The statically cultured bladders without the addition of TGF- β 1 had no positive staining for the TGF- β 1 antibody (Figure 3-4 B).

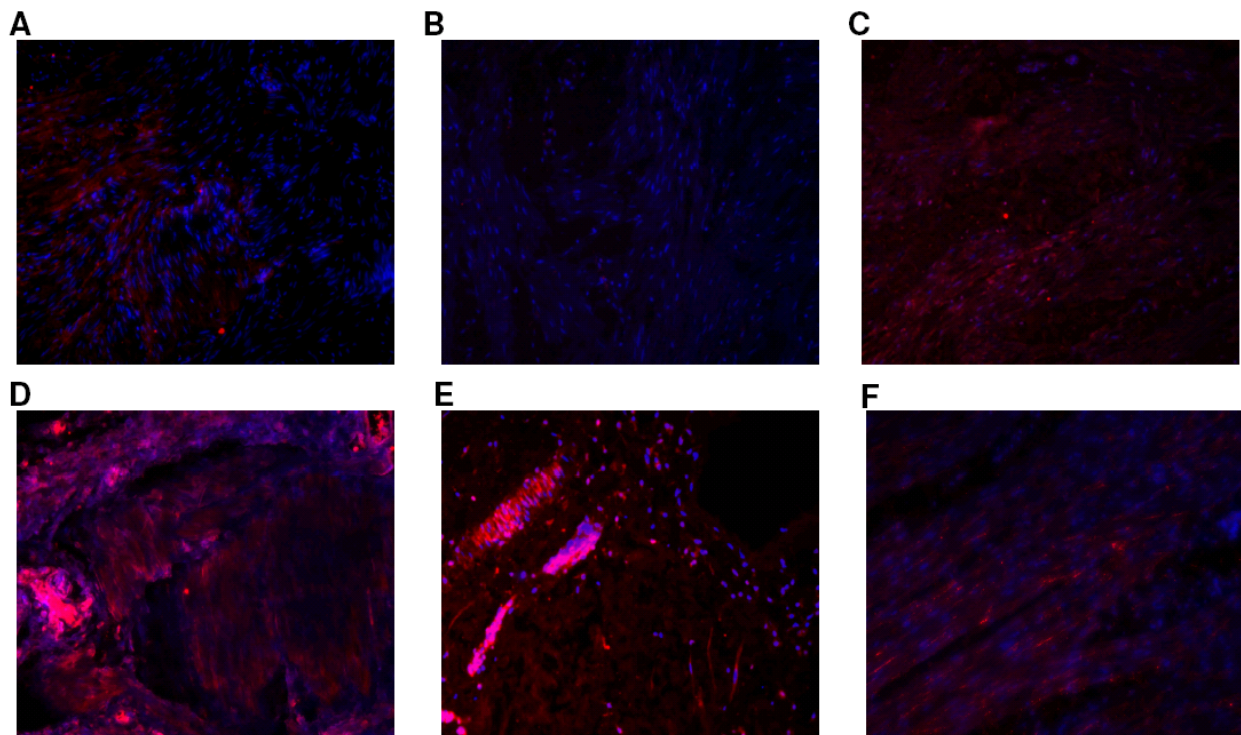


Figure 3-4. TGF- β 1 antibody staining on en face bladder sections. A. Normal native bladder, B. Static culture 7 days, C. 0.5 Hz culture 7 days, D. 10-day SCI bladder, E. Static culture + TGF- β 1 7 days, F. 0.5 Hz culture + TGF- β 1 7 days. Blue represent cell nuclei. Images are reduced from 200x.

3.3.2 Collagen and elastin in the cultured bladders

As shown in section 2.3, the 0.5 Hz cycling of bladder strips at 20% stretch produced significantly higher quantities of elastin compared to the native bladder and statically cultured bladders. The addition of 1 ng/mL of TGF- β 1 did not alter elastin protein content in either the static or cyclically stretched culture groups compared to normal culture media treated groups (Figure 3-5). The cyclically stretched group with the addition of TGF- β 1 still produced a significantly greater amount ($p < 0.01$) of elastin compared to the native bladder (Figure 3-5). RT-PCR was performed only on the native and the 0.5 Hz bladder group. The RQ values showed that the amount of tropoelastin gene expression was not significantly different between the native bladder and the bladders cycled at 0.5 Hz at 7 days (Figure 3-7).

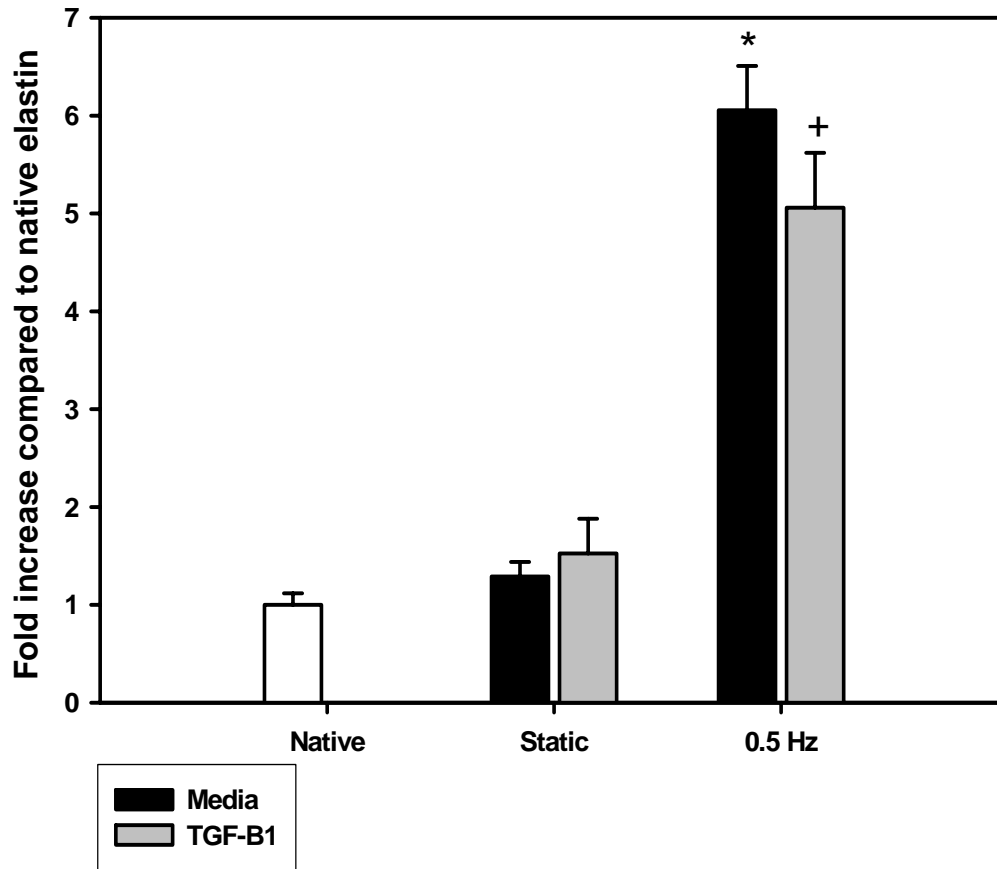


Figure 3-5. Fold increase in elastin compared to the native bladder. Data are presented as mean \pm s.e.m. $n=6$ per group. * $p<0.001$ compared to native, + $p<0.01$ compared to native.

There were significant differences in the amount of soluble collagen found within the bladder tissue when TGF- β 1 was added to the culture media in the 0.5 Hz stretch group (Figure 3-6). There was significantly less soluble collagen found in the tissue in the 0.5 Hz group with regular media compared with the native bladder. In the media of the cultured bladder strips, there was a significantly greater amount of collagen when TGF- β 1 was added to the culture in the static group compared to the static group with regular media (Figure 3-6 B). There were also large amounts of collagen found in the media of both 0.5 Hz groups. RT-PCR data further indicate that gene expression for both collagen type I and collagen type III is significantly down regulated in 0.5 Hz cultured bladders at 7 days compared to normal native bladders (Figure 3-7).

This indicated that the collagen found in the media was likely broken down collagen in the 0.5 Hz case. Further RT-PCR analysis would be necessary to determine the origin of the collagen in the media in the other test groups.

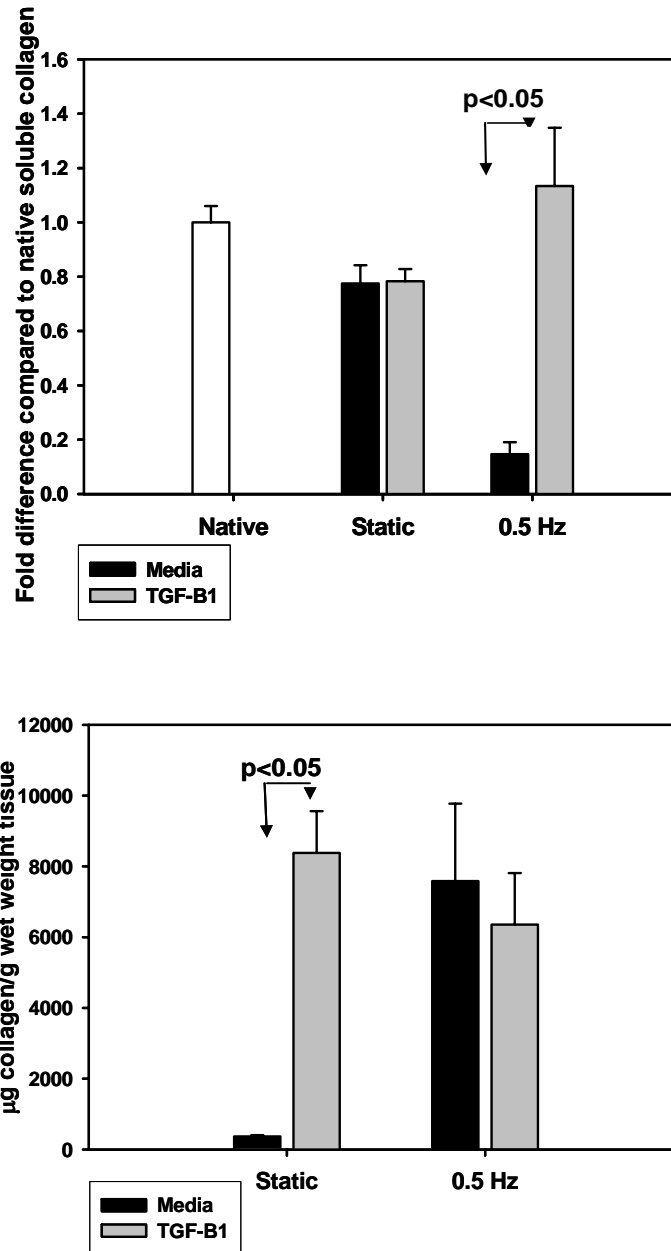


Figure 3-6. Soluble collagen protein found in A. bladder tissue of native and cultured bladders and B. media assay of soluble collagen. Data are presented as mean +/- sem with n=5-6 per group.

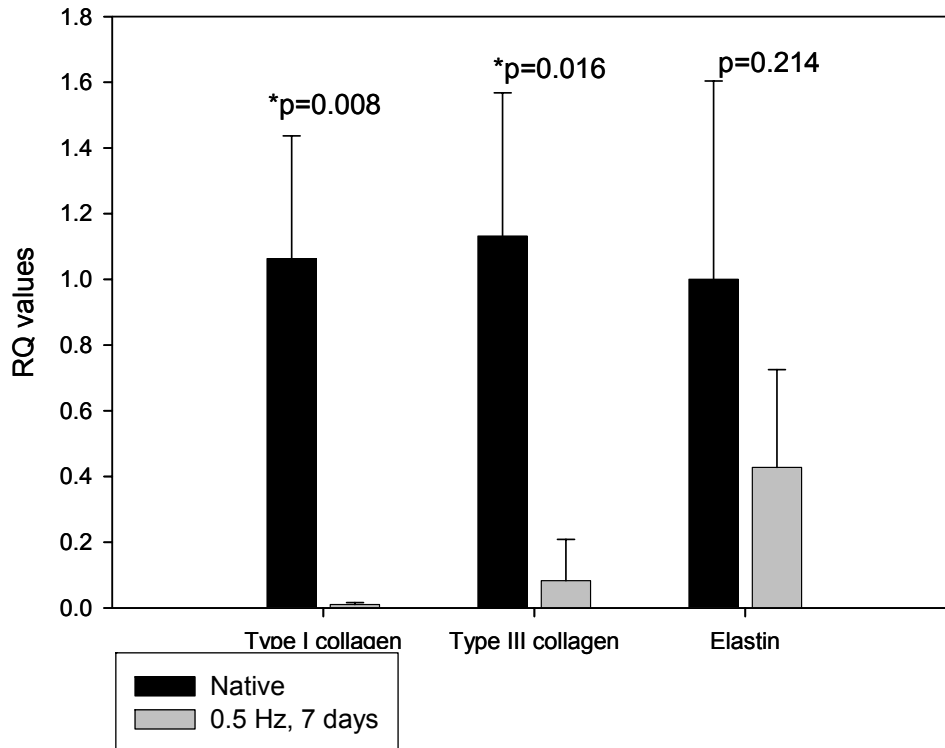


Figure 3-7. *RQ values of RT-PCR gene expression for Type I collagen, Type III collagen, and elastin from native (black) and 0.5 Hz cultured bladders (gray). Data are presented as mean +/- st.dev. n=3 per group.*

Elastic trichrome staining of bladder segments revealed dense patches of elastin in the 0.5 Hz cycled bladders with more disperse elastin seen in the 0.5 Hz + TGF-β1 bladders (Figure 3-8). Interestingly, the statically cultured bladders with the addition of TGF-β1 had no clear lamina propria marked by the blue collagen staining above the smooth muscle bundles in all other groups. It appears that smooth muscle bundles made up the entirety of the cultured tissue with a larger portion of ECM separating what may have formerly been the collagenous lamina propria (Fig 3-8 C).

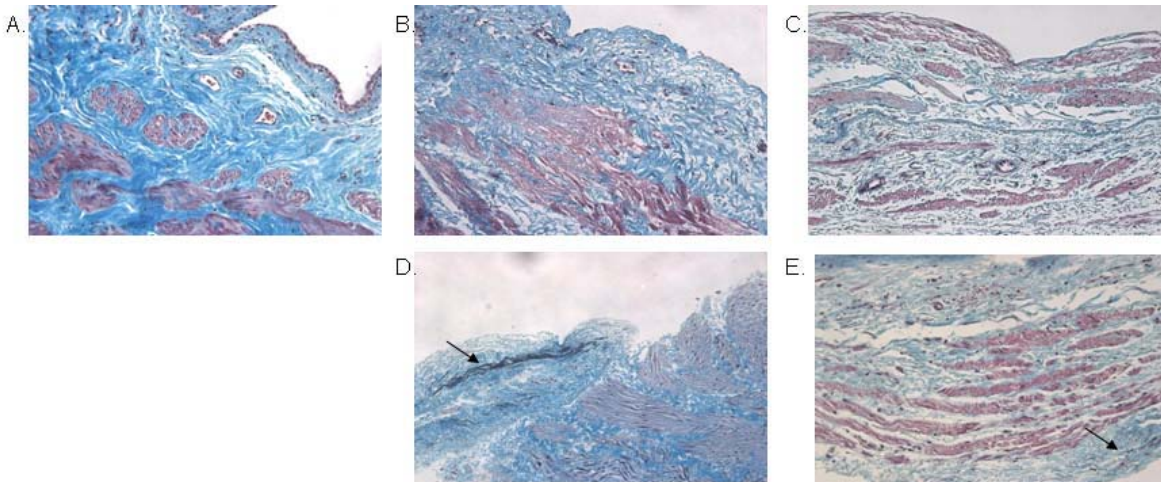


Figure 3-8. Elastic trichrome staining of A. native bladder, B. statically cultured bladder, C. statically cultured bladder + TGF- β 1, D. 0.5 Hz cultured bladder, E. 0.5 Hz cultured bladder + TGF- β 1. Images are reduced from 200x. Red/purple are smooth muscle cells, blue staining is collagen, black staining is elastin.

3.3.3 Mechanical properties of cultured bladder tissue

The addition of carbachol for active testing only promoted a coordinated active contraction of the bladder strips in the freshly excised native bladders. Strip biaxial mechanical testing showed that all test groups retained some passive tone compared to inactive testing (Figs 3-9 and 3-11 A). Static and cycled bladders with the addition of TGF- β 1 to the media exhibited greater compliance under passive and inactive testing indicated by the long toe region in the tension vs. stretch curves (Figs 3-9) and the statistically significantly ($p < 0.05$) lower tension values at a stretch of 1.2 (Fig 3-11 A). In the decellularized tissue the static group had the largest tension values at a stretch of 1.2 that were significantly greater than all other groups ($p < 0.05$). Furthermore, the 0.5 Hz groups with and without the addition of TGF- β 1 exhibited significantly lower ($p < 0.05$) tension values at a stretch of 1.2 compared to all other groups indicating increased compliance in these decellularized bladder strips (Fig 3-10 B).

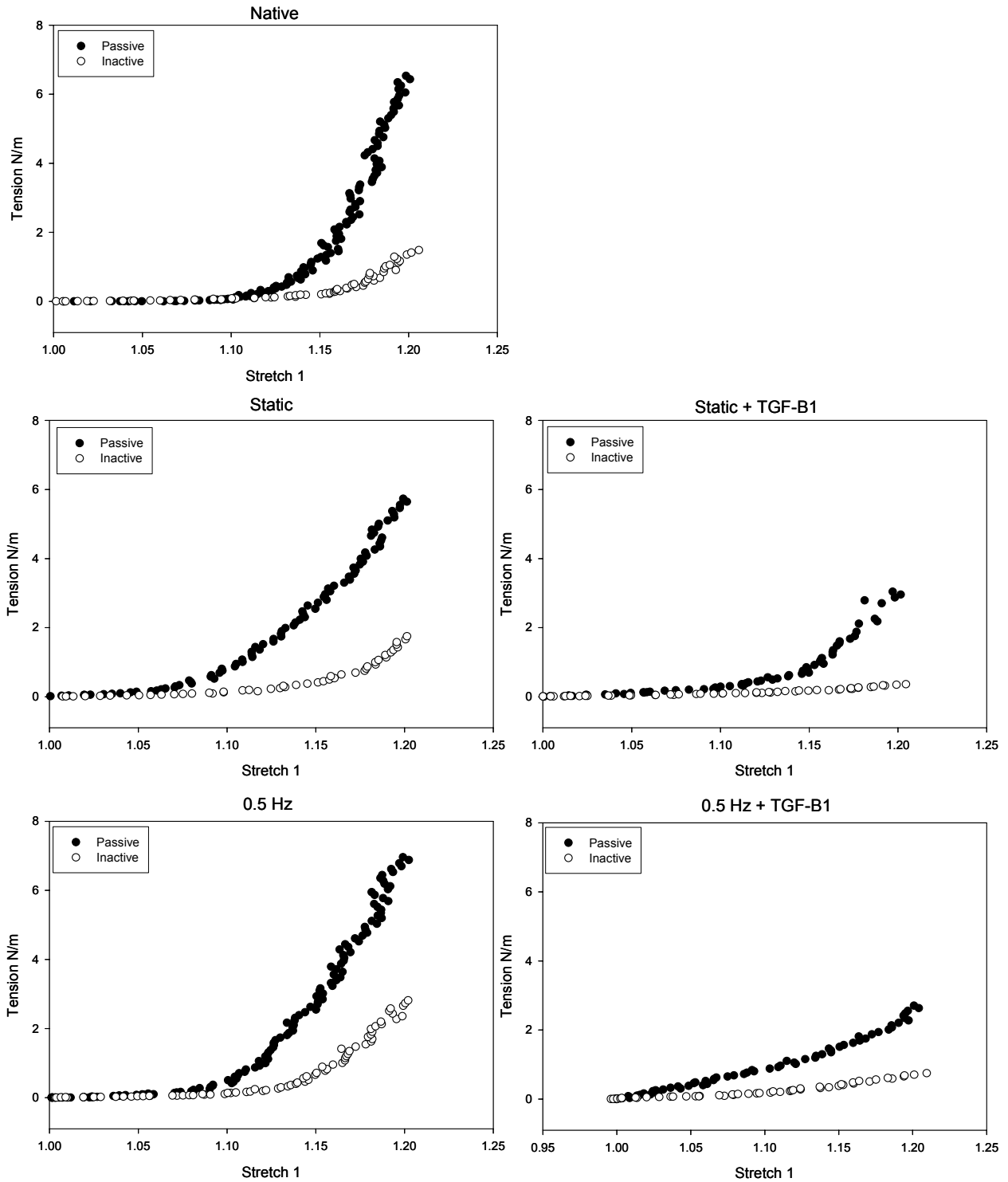


Figure 3-9. Representative tension vs. stretch curves of passive testing and inactive testing.

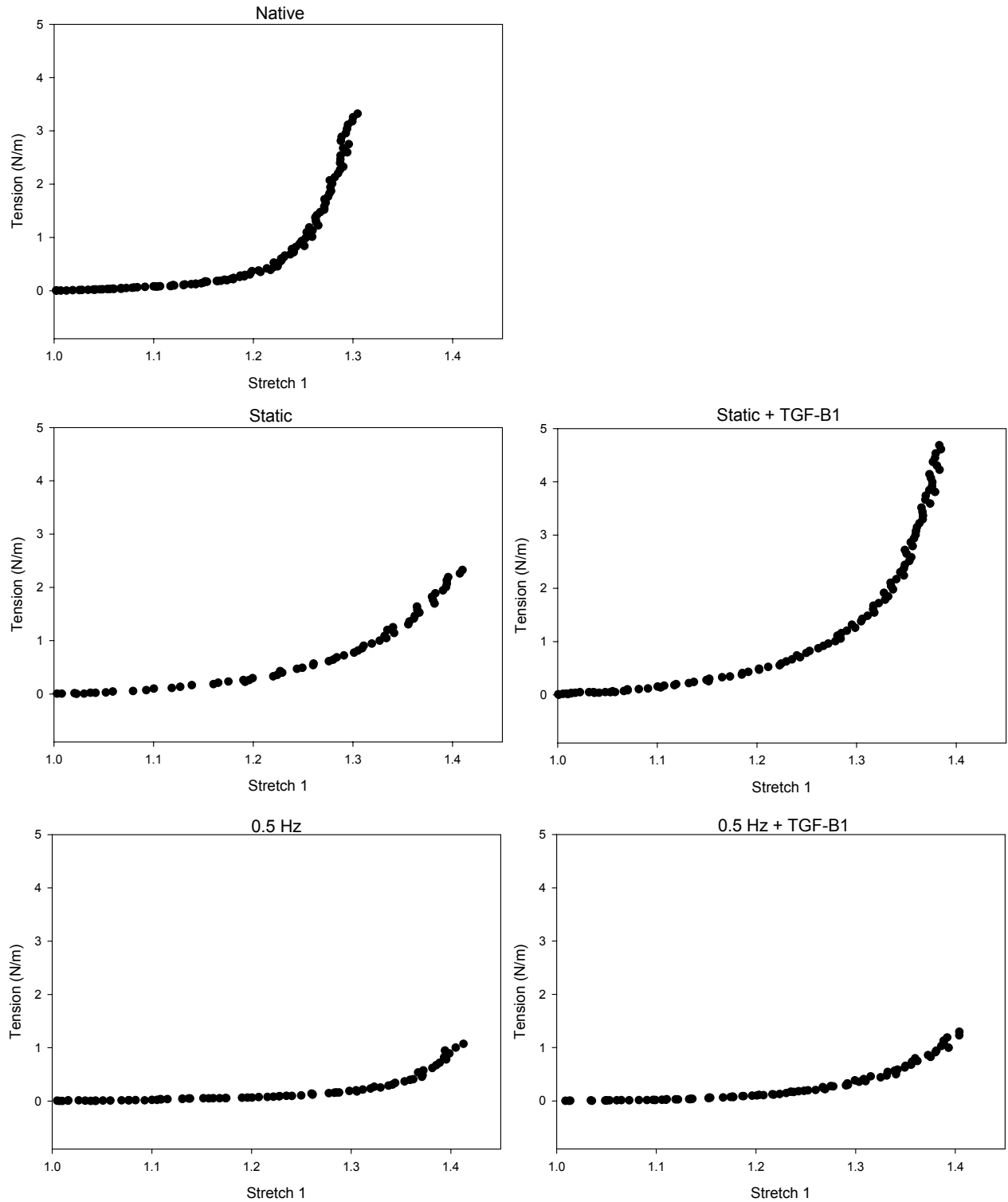


Figure 3-10. Representative tension vs. stretch curves of decellularized bladder tissue

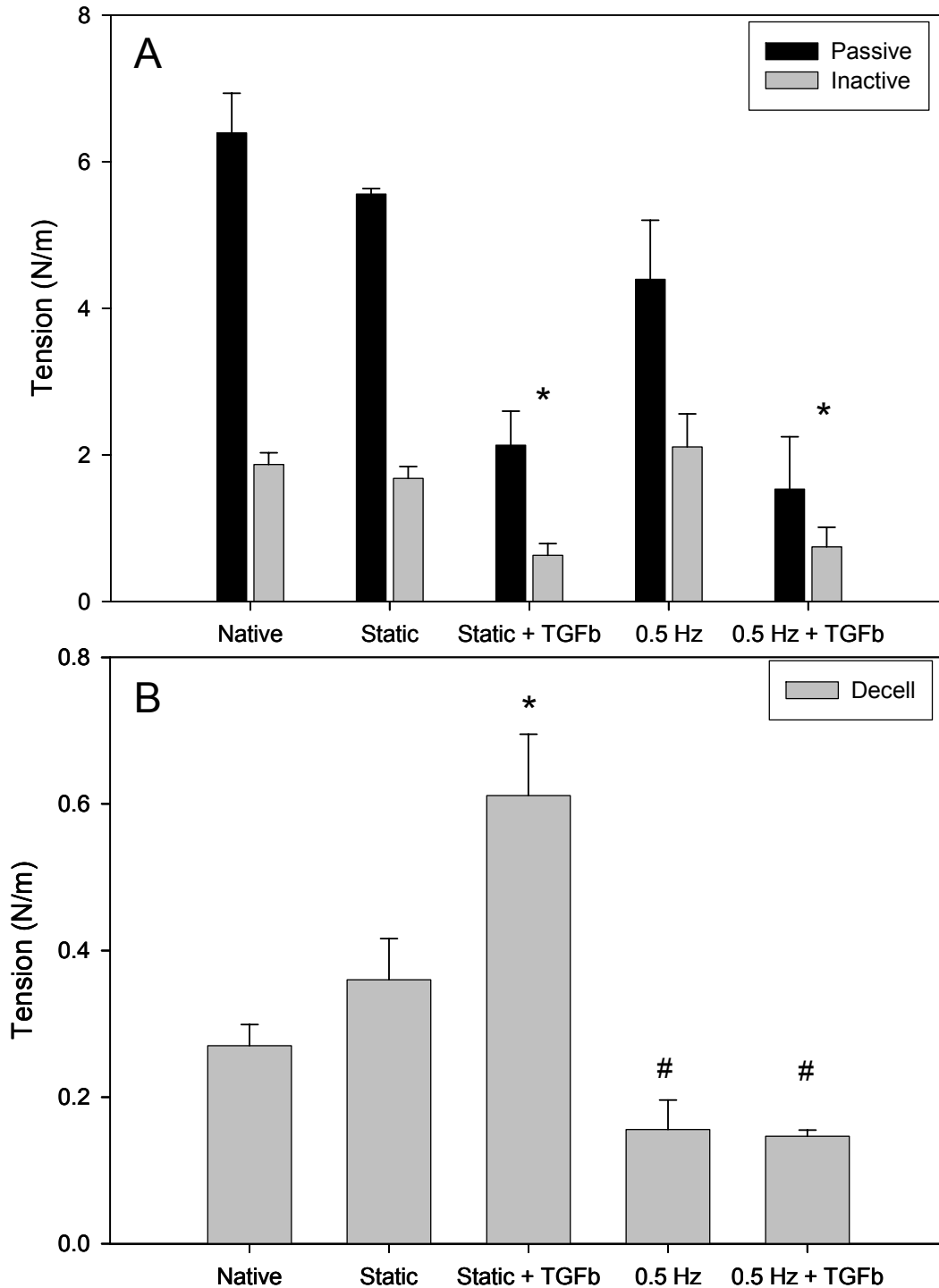


Figure 3-11. Tension values at 1.2 stretch from strip biaxial biomechanical testing. A. Tension values from passive testing and inactive testing. B. Tension values following decellularization of the bladder strips. All data are presented as mean \pm se.m. with $n=4$ per group. In graph A, * indicates that the TGF- β 1 groups are significantly statistically lower ($p<0.05$) than all other groups within each testing mode. In graph B, * indicates significantly greater ($p<0.05$) than all other test groups, and # indicates significantly lower than native and static groups but not from each other.

3.3.4 BSMC phenotype

En face bladder sections stained for markers of alpha smooth muscle actin (α -SMA), general caldesmon (CaD), and smooth caldesmon (h-CaD) showed that the native bladder positively expressed the contractile phenotype. The 10-day SCI bladders expressed greater levels of α -SMA, CaD, and h-CaD than the normal bladders (Figures 3-12, 13, 14 A and D). Additionally, the 0.5 Hz cultured bladders expressed greater levels of α -SMA, CaD, and h-CaD than the normal bladders (Figures 3-12, 13, 14 C and A). The α -SMA appeared in stress fibers while the CaD and h-CaD appeared throughout the cells cytoplasm. These levels for the 0.5 Hz group appear to be equivalent to the staining in the 10-day SCI bladders for all three contractile markers. The statically cultured bladder strips treated with and without TGF- β 1 expressed little to no CaD, and h-CaD (Figures 3-13,14 B and E). Statically cultured bladders with and without the addition of TGF- β 1 expressed small amounts of α -SMA (Figure 3-12 B and E). The dynamically cultured bladders with the addition of TGF- β 1 to the media expressed lower levels of α -SMA, CaD, and h-CaD than the dynamically cultured bladders with regular media (Figures 3-12,13,14 F). Furthermore, the dynamically cultured bladders with the addition of TGF- β 1 appeared to express even lower levels of the contractile proteins than the native normal bladder sections for all groups (Figures 3-12,13,14 F and A). However, the statically cultured bladders with the addition of TGF- β 1 expressed larger amounts of α -SMA than the statically cultured bladders in media alone yet no differences were apparent between the culture groups for h-Cad and Cad staining (Figures 3-12,13,14 B and E).

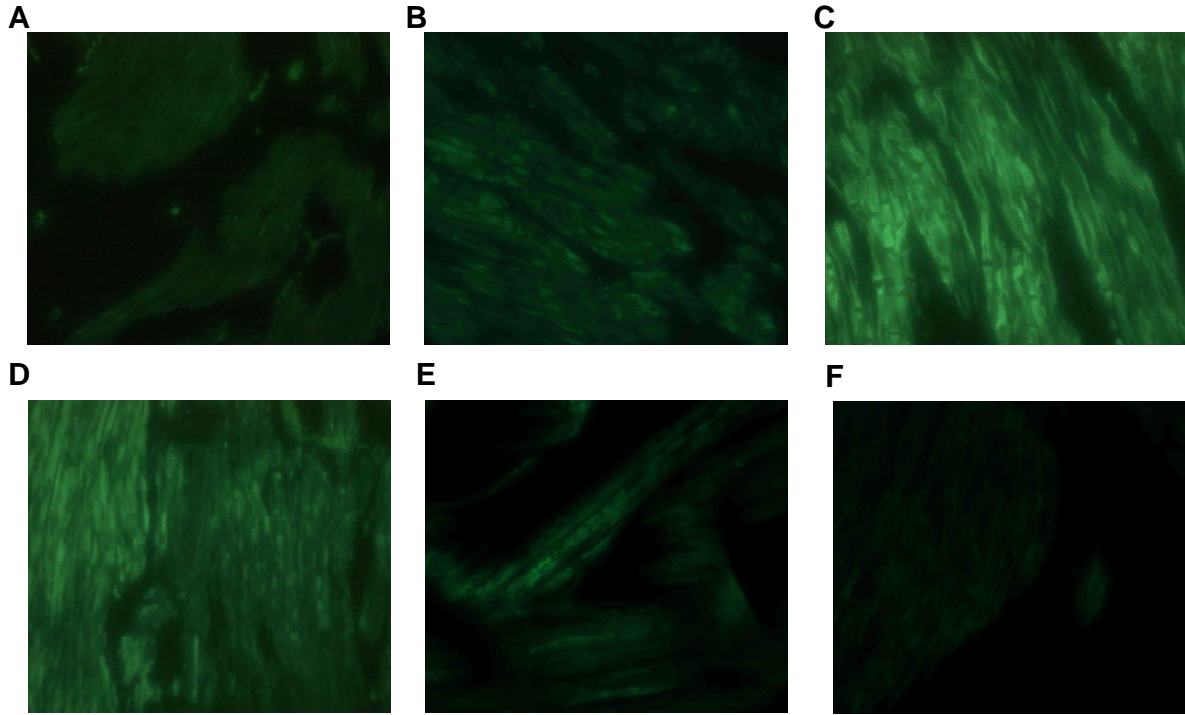


Figure 3-12. Representative images from alpha smooth muscle actin (green) staining of en face sections of A. Normal native bladder, B. Static culture 7 days, C. 0.5 Hz culture 7 days, D. 10-day SCI bladder, E. Static culture + TGF- β 1 7 days, F. 0.5 Hz culture + TGF- β 1 7 days. Images are reduced from 400x.

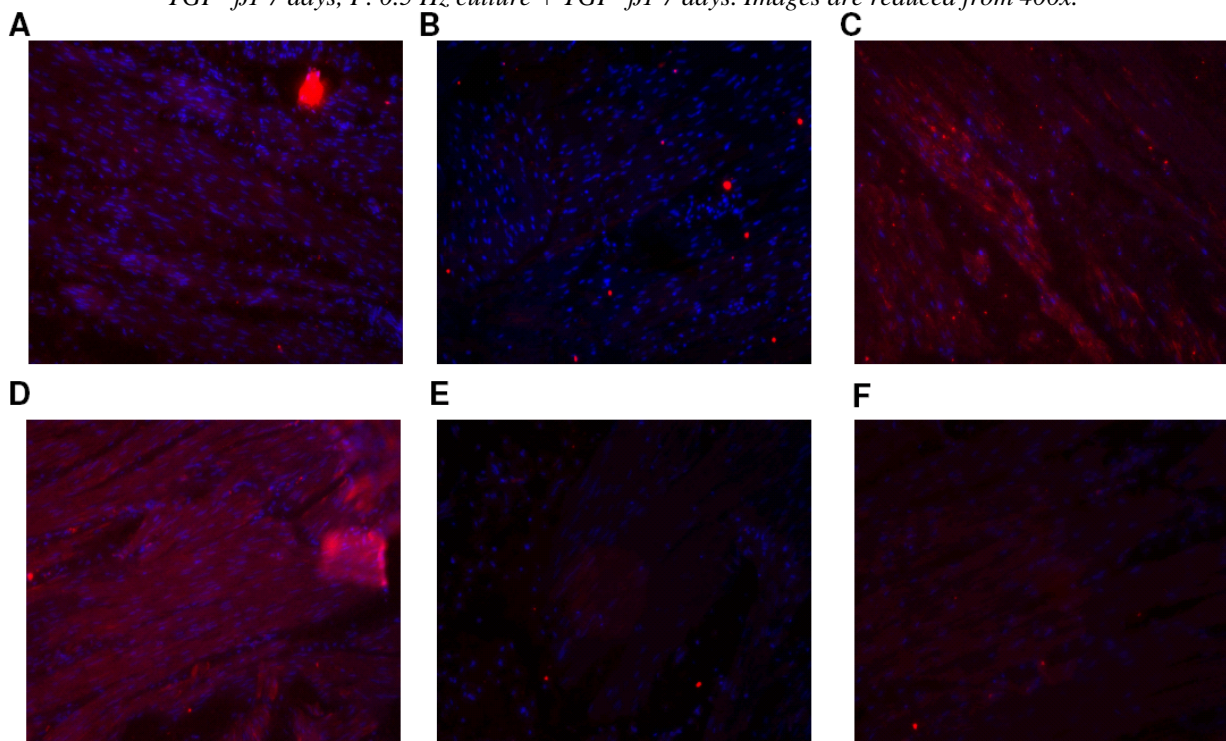


Figure 3-13. General caldesmon (red) and nuclei (blue) staining of en face sections of A. Normal native bladder, B. Static culture 7 days, C. 0.5 Hz culture 7 days, D. 10-day SCI bladder, E. Static culture + TGF- β 1 7 days, F. 0.5 Hz culture + TGF- β 1 7 days. Images are reduced from 200x.

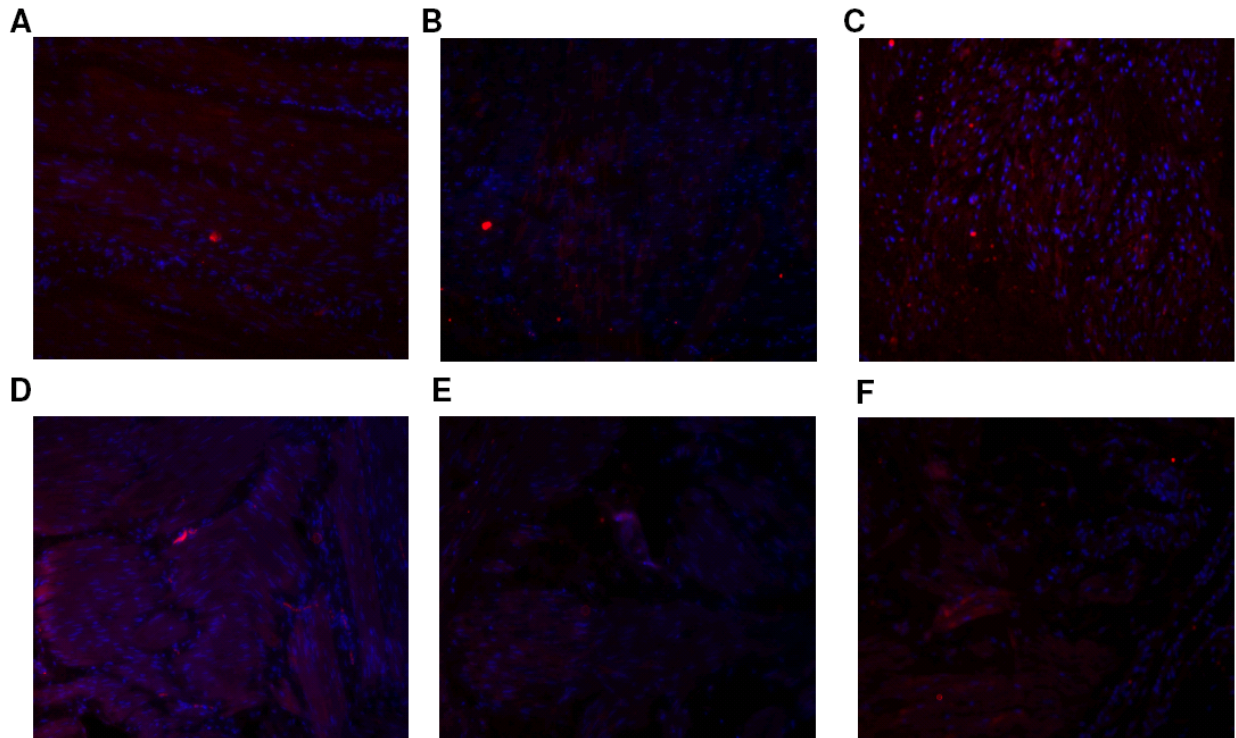


Figure 3-14. *h-caldesmon (smooth) (red) and nuclei (blue) staining of en face sections of A. Normal native bladder, B. Static culture 7 days, C. 0.5 Hz culture 7 days, D. 10-day SCI bladder, E. Static culture + TGF-β1 7 days, F. 0.5 Hz culture + TGF-β1 7 days. Images are reduced from 200x.*

3.4 DISCUSSION

3.4.1 Alterations in ECM composition and mechanical properties

The present study further confirmed that mechanical stimulation has a profound affect on the elastin content of the bladder strips in culture. However, the addition of TGF-β1 to dynamic culture did not affect the elastin content within the samples. Since TGF-β1 has been shown previously to stabilize the tropoelastin and lysyl oxidase molecules, this result was somewhat

surprising [145]. However, it is possible that since TGF- β 1 was up-regulated in the 0.5 Hz culture without any additional TGF- β 1 added the tropoelastin was already stabilized, and the elastogenic capabilities of the BSMC within the bladder strips were already maximized. The addition of TGF- β 1 to static culture did not promote any elastogenesis compared to all other groups. This finding suggests that the stimulus for elastogenesis was mechanical stimulation at the 0.5 Hz frequency. Although there is a wide milieu of molecular mechanisms that may be altered in the bladder following SCI, the present study indicated that TGF- β 1 alone may not be responsible for the early change in elastin composition in the SCI bladder.

The structural role of the elastin in the cultured bladders was exhibited in mechanical testing under a decellularized state. The 0.5 cyclically stretched bladders are significantly more compliant than all other groups, but not significantly different from each other. This may indicate that the elastogenesis in the cycled bladders plays a structural role in the biomechanical properties of the bladder; however, the tensions at a 1.2 stretch level appear to be governed by the SMC with both passive tone and inactive tone. Native bladders are stretched to larger stretch levels when filled, approximately 2.0 at maximum filling. The lamina propria has been reported previously to play a mechanical role at the beginning of filling and toward the end of bladder filling while the detrusor smooth muscle governs bladder biomechanics in between [24].

TGF- β 1 did have an impact in the collagen composition of the cultured bladders. TGF- β 1 is most commonly known as a promoter of collagen production leading to fibrosis of many organs [156]. The addition of TGF- β 1 to cultures of human BSMC increased both collagen type I and III protein expression at three different concentrations [156]. Other studies have shown that the diseased bladder produced primarily type III collagen under several disease conditions [157]. Our laboratory found previously, that dynamic culture of bladder strips at 0.5 Hz up-regulated

the expression of MMPs (See chapter 2). TGF- β 1 has also been shown to reduce MMP activity [145], which may have also led to the increase of soluble collagen within the tissue of the 0.5 Hz bladder strips compared to the marked decrease in soluble collagen that was found in the 0.5 Hz group in regular media. However, in contrast, MMP-2 has been shown to be up-regulated in airway SMC when treated with TGF- β 1 [158]. Therefore, while an increase in collagen protein levels was observed, mechanical properties did not necessarily follow the same pattern. Mechanical analysis of the bladder strips with and without treatment of TGF- β 1 revealed that strips exposed to TGF- β 1 with and without mechanical stimulation were more compliant than strips cultured in regular media under passive and inactive testing. However, the increased compliance in the passive testing conditions for both TGF- β 1 treated groups may have been due to the decrease in BSMC contractile proteins CaD and h-CaD. The caldesmons are actin associated proteins thought to modulate contraction by mediating phosphorylation of the myosin [159]. The increased compliance in the inactivated bladder strips treated with TGF- β 1 in static culture may have been due to the increase in smooth muscle bundles in the lamina propria. As stated in Chapter 1, the lamina propria governs bladder compliance during initial stages of filling [2]. The increase in cells in this region likely altered the mechanical properties of the tissue in the inactivated state. The increased compliance in the dynamically cultured bladder strips with TGF- β 1 may have been due to the decrease in stress fibers within the tissue. Even though inactive testing does not allow for smooth muscle tone, the BSMC remain in the tissue and the biomechanical properties of the tissue may be dependent on the cell matter that is remaining. When the bladder strips were decellularized the statically cultured bladders with the treatment of TGF- β 1 was significantly less compliant than all other groups. This finding showed that the actual ECM within the bladder strips was altered with the addition of TGF- β 1 to the culture.

3.4.2 Phenotype

Culture of bladder strips at 0.5 Hz, 20% without the addition of TGF- β 1 for 7 days mimicked the phenotype of the BSMC that was seen in the SCI bladders at 10 days. Increases in all contractile protein markers were seen compared to the normal native bladder. Furthermore, expression of TGF- β 1 was up-regulated in the 0.5 Hz group similarly to the 10 day SCI bladders. While no hypertrophy of the BSMC was seen in the cultured bladders, an increase in these contractile proteins, particularly h-CaD has been seen previously in hypertrophied smooth muscle [159].

Increases in l-CaD along with a reverted fetal cell marker phenotype in SM1 and SM2 [160] or in concert with increases in SM-A myosin heavy chain [161] have been seen previously following bladder obstruction. Varied changes in α -SMA and calponin expression have been observed in obstructed bladders [162]. Increases in thin filament proteins, calponin, caldesmon, and tropomyosin have been observed in the diabetic bladder [163].

In the present study, exogenous TGF- β 1 added to culture decreased contractile proteins CaD and h-Cad. However, in static culture, the α -SMA appeared to be unchanged with the addition of TGF- β 1. An increase in alpha-SMA expression has been reported previously in static culture of isolated BSMC as well as aortic smooth muscle cells with the addition of TGF- β 1 to culture [144]. TGF- β 1 has also been shown previously to increase cell hypertrophy in an isolated BSMC study [156]. Furthermore the addition of TGF- β 1 to culture of BSMC increased α -SMA expression but decreased connexin gap junctions [147]. The present study showed that the presence of mechanical stimulation clearly has an affect on the cellular phenotype of the BSMC within organ cultured bladder strips. The addition of TGF- β 1 may have caused more cellular

migration in the statically cultured bladder strips, or it may have caused the fibroblasts within the lamina propria to form bundles of what appeared to be smooth muscle. However, phenotypic staining showed no difference between these bundles and those in the bulk of the detrusor in the static + TGF- β 1 group. The decrease in contractile phenotype with the addition of TGF- β 1 to culture was further demonstrated by the passive and inactive mechanical testing where the TGF- β 1 groups were significantly more compliant than all other groups.

3.4.3 Relation to SCI affected bladders

The present study showed distinct similarities between the 10 day SCI bladder and the bladders cultured at 0.5 Hz. Similarities were seen previously in elastogenesis and collagen content (Chapter 2). The present study highlighted more similarities in TGF- β 1, α -SMA, hCaD, and general CaD expression. Furthermore, similarities were seen in mechanical testing. Previous testing of SCI 10 day decellularized tissue under biaxial mechanical testing exhibited increased compliance compared to normal bladders [7]. In the present study, strip biaxial mechanical testing demonstrated increased compliance in the decellularized tissue cycled at 0.5 Hz. Although it remains to be understood exactly why the specific 0.5 Hz frequency promotes similar remodeling in both ECM composition and phenotypic change, it does appear that organ culture of bladder strips under mechanical stimulation may serve as an experimental model to examine cellular remodeling.

The addition of TGF- β 1 to culture decreased bladder tone and caused more soluble collagen to be produced in the cultured bladders. The increase in collagen in these groups may be similar to the fibrosis seen in later stage SCI pathology [64]. There is no data to date that specifically shows the phenotype of long-term SCI detrusor BSMC, so it is unclear whether the

change in phenotype that was seen in the present study can be correlated to changes in the SCI bladder. However, the addition of TGF- β 1 can clearly play a role in remodeling of the bladder detrusor. The previous studies from our laboratory showed that TGF- β 1 expression remains up-regulated out to 3 weeks post SCI while indicators of fibrosis do not appear until later [64]. The precise kinetics of how the TGF- β 1 signals the cells of the detrusor to promote collagen synthesis is unclear to date and may be the focus of future studies. With the knowledge to date we can speculate that the addition of TGF- β 1 to dynamic ex vivo organ culture of the bladder may mimic the SCI bladder at a later stage due to the decrease in contractile phenotype of the cells and the increase in collagen production compared to the other cycled bladders.

3.4.4 Limitations

Ideally in experiments examining the effect of cellular response to a growth factor, the experiments are carried out in little to no serum to differentiate effects that may be due to the multitude of serum proteins. In the present study, high fetal bovine serum (10%) was used in order to maintain cell survival in the organ culture strips. Additionally, cultures of the bladder strips were only carried out to 7 days due to a trend toward migration of the BSMC out of the tissue seen at later time points (Chapter 2). A perfused bioreactor with oxygenated media may be the focus of future designs to examine later time points. Additionally, active contraction was not able to be measured due to the length of culture time only BSMC tone was able to be measured. It may be possible to examine earlier time points following mechanical stimulation to determine not only when the phenotypic shift occurs, but also if the phenotypic shift alters the contractility of the detrusor.

3.4.5 Summary

The present study highlights the complexity of molecular signaling that occurs in bladder wall remodeling. The ex vivo system described in this study may be utilized in future research to examine the TGF- β 1 signaling cascade in the bladder that likely leads to fibrosis and stiffening following SCI. For other fibrotic diseases such as scleroderma, there have been studies underway to utilize antibodies to TGF- β 1 to prevent fibrosis [145]. With further study, the addition of TGF- β 1 antibodies to the diseased bladder may prevent stiffening of the bladder wall at early time points following SCI. Furthermore, the present study highlighted the importance of cellular phenotype on changes collagen synthesis. Further examination of the affect of TGF- β 1 on BSMC behavior is discussed in Chapter 4.

4.0 THE EFFECT OF TGF- β 1 ON BSMC MEDIATED COLLAGEN GEL REMODELING

4.1 INTRODUCTION

The previous chapter described the impact of TGF- β 1 on ECM composition and cellular phenotype in organ culture of the bladder. While it was noted that change occurred in the soluble collagen within the bladder strips, we were unable to quantify any changes in collagen architecture within the bladder. Our laboratory has shown previously that the bladder smooth muscle bundles hypertrophy following SCI such that the alignment changes from mostly longitudinal to both longitudinal and circumferential (Figure 4-1) [54]. With this change in directionality, it is probable that the collagen fibers also change in orientation. However, this change has never been quantified in vivo. Previous studies have isolated BSMC from neurogenic bladders and found that the BSMC possess increased proliferation, reduced cell adherence, and decreased contractility [164]. Additionally, BSMC become synthetic and produce large quantities of ECM proteins in the pathologic bladder. These components of tissue remodeling both the biochemical and biophysical are the result of changes in the bladder cell phenotype [35, 68]. As shown in the previous chapter, the phenotype of the BSMC may be altered with the addition of TGF- β 1.

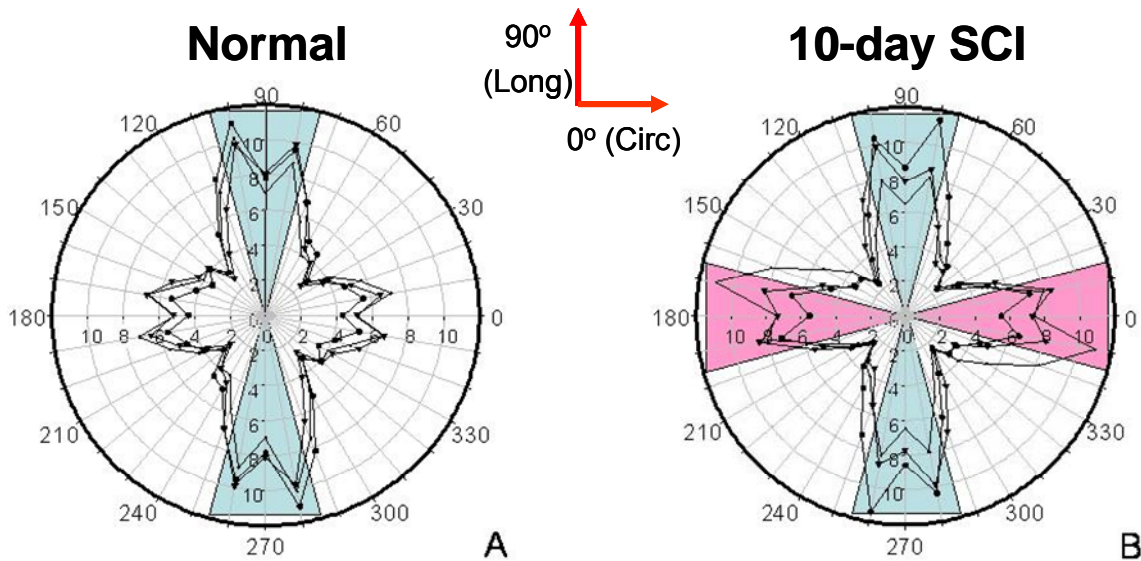


Figure 4-1. Polar plots of directionality of smooth muscle bundles in normal A. and SCI B. bladders. [54]

The importance of TGF- β 1 in bladder fibrosis and disease was detailed in the previous chapter. Additionally, TGF- β 1 has also been implicated in other organs disease remodeling response. For this reason TGF- β 1 has been utilized in isolated cell studies to examine its effects on a number of cell functions. Particularly when examining the impact of TGF- β 1 on cellular response, a simplified experimental model may be utilized. Furthermore, the effect of TGF- β 1 may be examined in a low serum case in a cell culture setting that was not possible in the organ culture studies due to decreases in organ strip survival. The present study in this chapter focused on exploring the effect of TGF- β 1 on collagen type I gel contraction and organization of the collagen fibrils within the gel.

4.2 PROTOCOL

4.2.1 Cell culture

Rat BSMCs were derived from female Sprague-Dawley rats (2-3 months old) according to a method by [165]. Briefly, the mucosal layer of the bladder was removed, and the remaining tissue was minced. The minced bladder tissue was placed in RPMI 1640 (Invitrogen) medium containing 0.1% collagenase Type I-A (Sigma) and 0.2% trypsin (Invitrogen) in a Petri dish then incubated at 37 degrees for 30 minutes. The mixture was then filtered through a 100 um cell strainer and centrifuged at 1200 rpm for 3 minutes. Supernatant was discarded and the pellet was then re-suspended in complete media. Cells were cultured in RPMI 1640 medium (Invitrogen, Carlsbad, CA) supplemented with 10% fetal bovine serum (FBS; Hyclone, Logan, UT) and 1% antibiotic/antimycotic (Invitrogen, Carlsbad, CA). They were grown in cell culture flasks and a humidified atmosphere containing 5% CO₂ at 37°C. Upon confluency, cells were rinsed with 1× Hank's Balanced Salt Solution (HBSS; Invitrogen) twice and trypsinized with 0.12% trypsin-EDTA (Invitrogen). The cells were either passaged or counted with a hemocytometer for use in the experiments at three cell populations of 5×10^4 , 1×10^5 , and 2.5×10^5 cells (per collagen gel). All cells were used between passages 5 and 10 to minimize changes in phenotype from in vitro culturing. Prior to seeding, cell purity was assessed by confirming positive staining for antibodies to α -SMA and calponin. Cultures with approximately 99% cell purity were used for the experiments.

4.2.2 TGF- β 1

Lyophilized TGF- β 1 (R&D Systems, Minneapolis, MN) was reconstituted in a filter-sterilized 4 mM HCl solution containing 0.1% bovine serum albumin (BSA) at 1 μ g/ml. The reconstituted solutions were frozen at -20°C for no more than three months prior to use. 1 ng/ml was used in all of the experiments.

4.2.3 Anchored collagen gels

Anchored collagen gels were utilized based on a previous protocol (Parekh et al, submitted). The collagen solution was cast in silicone molds (601 A/B mixture, Wacker Silicone, Lansing, MI) that were placed on glass coverslips in Petri dishes. Steel mesh anchors (Small Parts, Miami Lakes, FL) were previously glued on to the glass coverslips with a silicone adhesive to provide uniaxial anchoring of the collagen gels. The type I collagen gels, from the commercial product PureCol at 3 mg/ml (Inamed, Fremont, CA), were prepared as previously described to yield a final concentration of 2.4 mg/ml. 150 μ l of collagen solution was polymerized in each mold in a humidified, 37°C chamber for one hour. BSMCs were then placed on top of the collagen gels inside the molds in 400 μ l complete medium. The dishes were incubated for 30 minutes to ensure BSMC adhesion. The silicone molds were removed, and 7 ml of culture medium, either control (2% FBS) or supplemented with 1 ng/ml TGF- β 1, was added to each Petri dish. The dishes were incubated for 30 minutes to allow the medium to equilibrate.

The collagen gels with the highest seeding population of 2.5×10^5 cells routinely tore off one of the anchors by 24 hours with TGF- β 1; therefore, these collagen gels were evaluated at 18 hours. Collagen gels were imaged at 0, 2, 4, and 18 or 24 hours using a dissecting microscope (Nikon, Melville, NY) and digital camera with capture software (PixeLINK, Ottawa, Ontario, CA). The contraction of the anchored collagen gels was calculated based on the change in surface area when compared to $t=0$. Collagen gel areas were measured with SigmaScan software (Systat Software, Richmond, CA) using a ruler for calibration. Comparisons were made for the control versus TGF- β 1 cases. Collagen gel seeding and contraction calculation are shown in Figure 4-2.

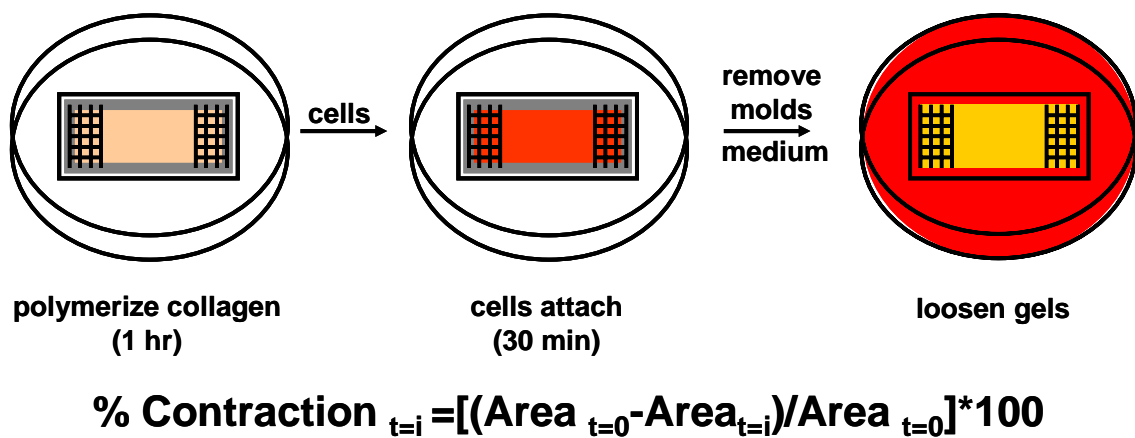


Figure 4-2 Schematic of anchored collagen gels and calculation of % contraction of the gels.

4.2.4 Immunohistochemistry

For TGF- β 1 staining, sections of bladder tissue from control and 10-day, post-surgical spinalized female Sprague-Dawley rats were obtained from a previous study [54]. 5 μ m cross- and lateral-sections were incubated with an anti-TGF- β 1 primary rabbit polyclonal IgG antibody (1:200; Santa Cruz Biotechnology, Santa Cruz, CA) and visualized with a streptavidin-Cy3 goat anti-rabbit IgG secondary antibody (1:1000; Jackson ImmunoResearch Laboratories, West Grove, PA). Samples were visualized with 20 \times fluorescent microscopy and captured with a digital camera and software (Olympus, Center Valley, PA). TGF- β 1 was quantified for control and SCI bladders in both orientations based on the ratio of TGF- β 1 fluorescent area to total detrusor tissue area per section using Metamorph software (Universal Imaging, Downingtown, PA).

For caldesmon staining, 1×10^5 BSMCs were seeded on glass coverslips in Petri dishes in a similar manner as the collagen gels (i.e., liquid volume spread out on an approximately equivalent surface area). To mimic the collagen gel protocol, the dishes were incubated 30 minutes to allow for BSMC attachment, 7 ml of control medium or medium with TGF- β 1 was added, and the dishes were incubated for another 30 minutes to allow the medium to equilibrate. After 4 hours, the coverslips were rinsed with HBSS and fixed with 2% paraformaldehyde (Sigma). The coverslips were incubated with either an anti-caldesmon primary mouse monoclonal IgG1 antibody (1:100; Sigma) or an anti-caldesmon (smooth) primary mouse monoclonal IgG1 antibody (1:100; Sigma) that bind either both caldesmon isoforms or the high molecular weight form, h-CaD, respectively. The coverslips were incubated with a biotinylated

rat adsorbed horse anti-mouse IgG secondary antibody (1:500; Vector Laboratories) and visualized with a streptavidin-Cy3 conjugate secondary antibody (1:250; Sigma). Caldesmon was visualized using 400× fluorescent microscopy with a digital camera and software (Leica, Bannockburn, IL).

4.2.5 Small angle light scattering (SALS)

The anchored collagen gels were fixed in formalin at either 18 (for 2.5×10^5 cells) or 24 hours (for 5×10^4 and 1×10^5 cells). The SALS technique was then performed on the collagen gels to ascertain collagen fibril organization. The technique is well-developed and has been described previously [166] and has been used to quantify collagen gel reorganization (Parekh submitted). A 4 mW HeNe laser light (Uniphase, Manteca, CA) with a wavelength of 632.8 nm was passed through the collagen gel samples at a spatial resolution of approximately 250 μm . The internal planar fibrillar architecture of the collagen gels causes a scattering of the laser light that is collected on a projection screen. The resulting angular distribution of scattered light, $I(\Phi)$, can be used to quantify the fibrillar architecture of the collagen gels in terms of the preferred fibril direction, Φ_c , and the orientation index, OI, of collagen fibrils. SALS video images of the laser light scattering were collected, digitized, and analyzed with custom software. The $I(\Phi)$ is interpreted by the software as a distribution of fibril angles corresponding to the positions within each collagen gel. This analysis gives the Φ_c , the centroid of the distribution $I(\Phi)$, which is symbolized as a vector, and the OI, which is defined as the angle that contains 50% of the total fibrils. Therefore, randomly oriented fibril networks result in large OI values while highly

oriented fibril networks result in small OI values. The collagen gels were evaluated based on 704 individual OI values at each point throughout the collagen structures then averaged to represent the physical remodeling of each collagen gel. This area of evaluation was chosen to encompass the majority of the collagen gel but ignored the free edges and areas near the steel mesh anchors to avoid edge effects (Fig. 4-2). The fibril orientation of these collagen gels was used for comparison between controls and TGF- β 1 cases. In order to confirm that changes in reorganization were due to changes in the collagen gel architecture, BSMCs were treated with 0.25% trypsin for four days to detach all of the cells. Images were taken before and after with the dissecting microscope to compare the effect of the BSMCs on the collagen gels.

4.2.6 Cell morphology

Cell morphology on the collagen gels was imaged and captured using 100 \times phase contrast microscopy with a digital camera (Nikon) and Metamorph software (Universal Imaging, Downingtown, PA), respectively at 4 and 18 or 24 hours depending on the cell seeding density.

4.2.7 Statistics

All data are expressed as mean \pm standard error of the mean (SEM). Data were analyzed by either the Student's t-test or a one-way analysis of variance (ANOVA) followed by the Holm-Sidak method to detect statistical differences using SigmaStat software (Systat Software). $p < 0.05$ was considered statistically significant. Data generated using multiple cultures of BSMCs were pooled together.

4.3 THE EFFECT OF TGF- β 1 ON COLLAGEN GEL CONTRACTION AND ORGANIZATION

4.3.1 TGF- β 1 expression in SCI bladders

Fluorescent antibody staining for TGF- β 1 confirmed previous results wherein SCI bladders expressed greater amounts of TGF- β 1 than normal bladders [35]. In the present study, TGF- β 1 area of staining was 5 fold greater in the cross sections and 2 fold greater in the lateral sections of SCI bladders than normal bladders (Figures 4-3, 4). The larger area of staining is diffuse throughout the bladder smooth muscle tissue (Figure 4-3).

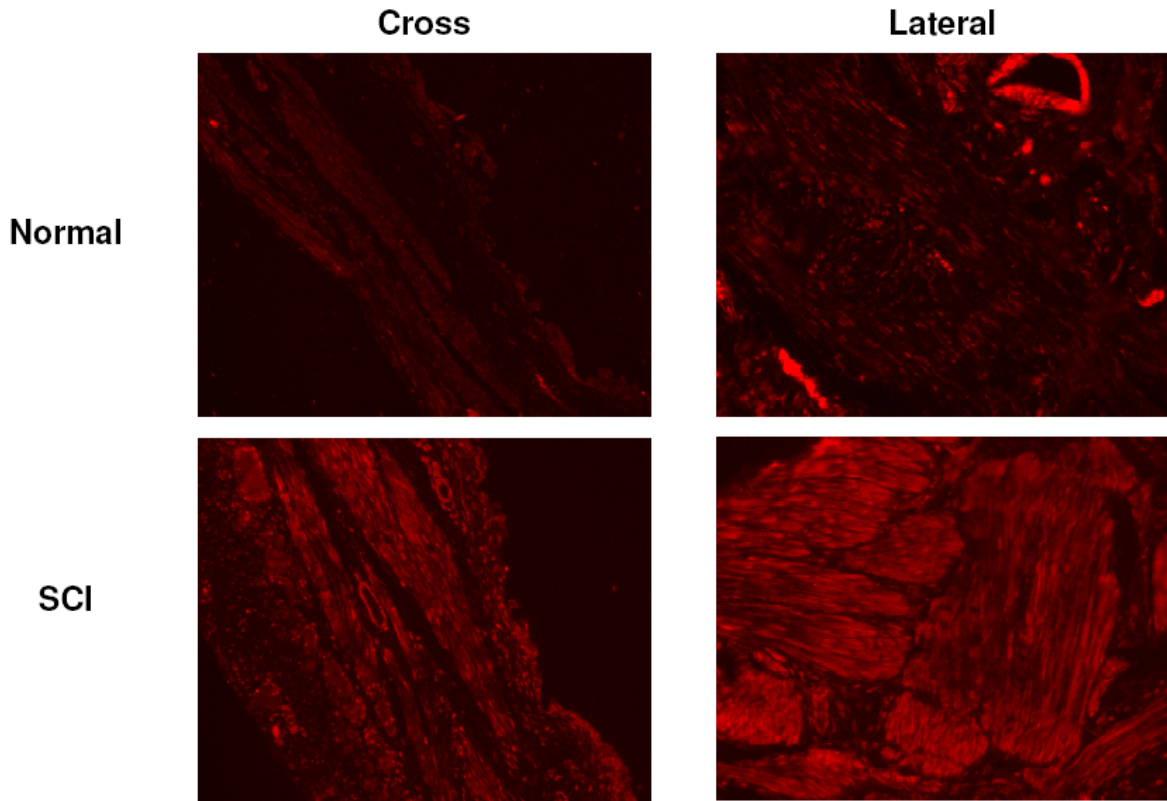


Figure 4-3. Fluorescent antibody labeling of TGF- β 1 in normal and 10 day post-surgical SCI bladders in both cross- and lateral-sections indicates greater TGF- β 1 expression in the SCI smooth muscle tissue. Bright structures are blood vessels.

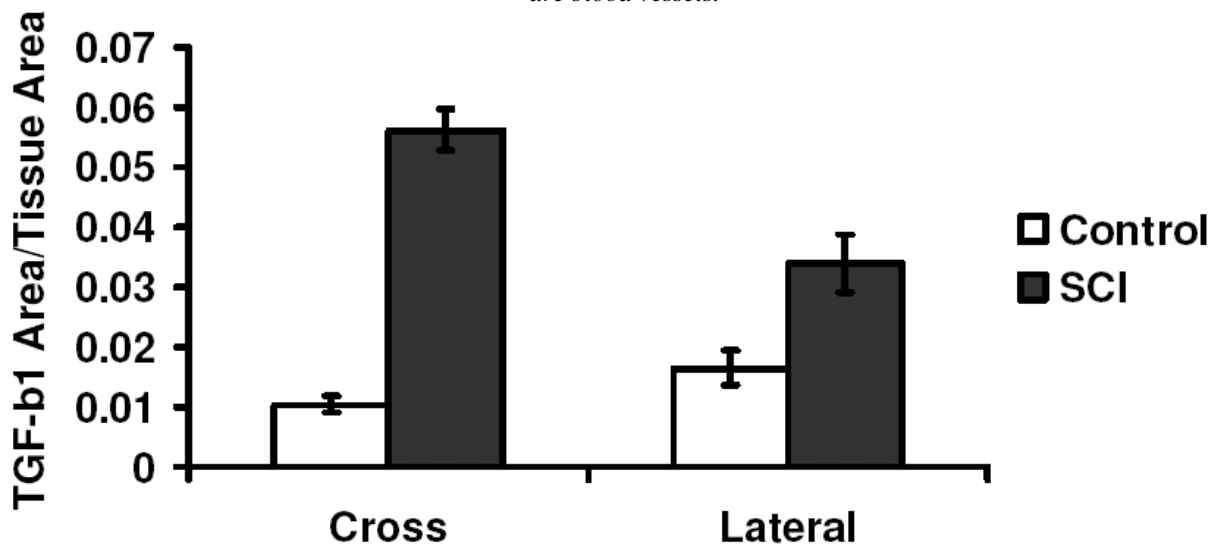


Figure 4-4. TGF- β 1 expression is quantitatively greater in the SCI tissue in both the cross- and lateral-sections. Expression was calculated as the ratio of total fluorescent area to total smooth muscle area. $n=48$ for all cases but the lateral control case which was $n=44$. Values represent mean \pm SEM and * indicates $p<0.005$.

4.3.2 TGF- β 1 decreases contraction of collagen gels at early time points

For all three cell populations, the BSMCs contracted over time (Figure 4-5). At 2 hours, 2.5×10^5 BSMCs contracted the collagen gels by 11.0% versus 2.6% and 4.0% for 5×10^4 and 1×10^5 BSMCs, respectively ($p < 0.05$). Collagen gel contraction remained higher at 4 hours for 2.5×10^5 BSMCs versus 5×10^4 and 1×10^5 BSMCs, 19.1% versus 4.1% and 7.6%, respectively ($p < 0.05$). However, at 24 hours, no significant differences were found among the three groups; contraction was 20.3%, 20.0%, and 24.4% for 5×10^4 , 1×10^5 , and 2.5×10^5 BSMCs, respectively.

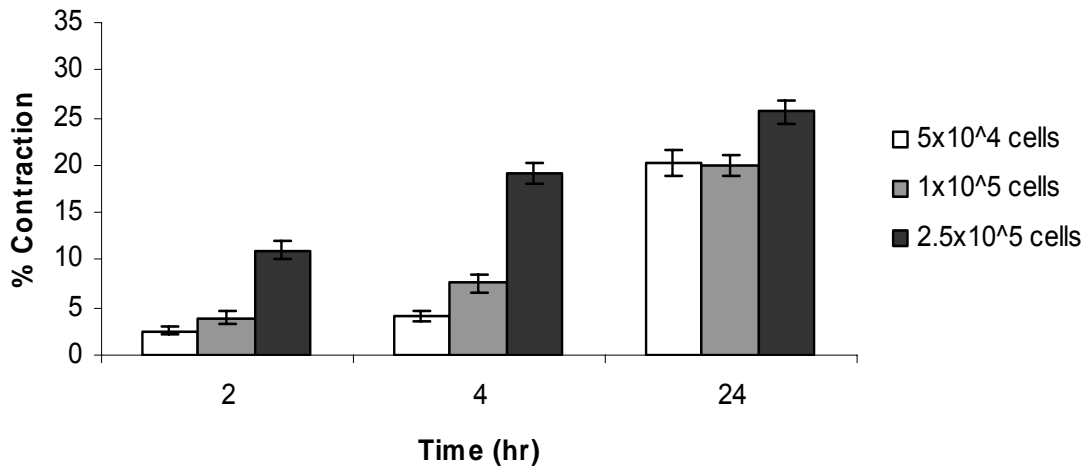
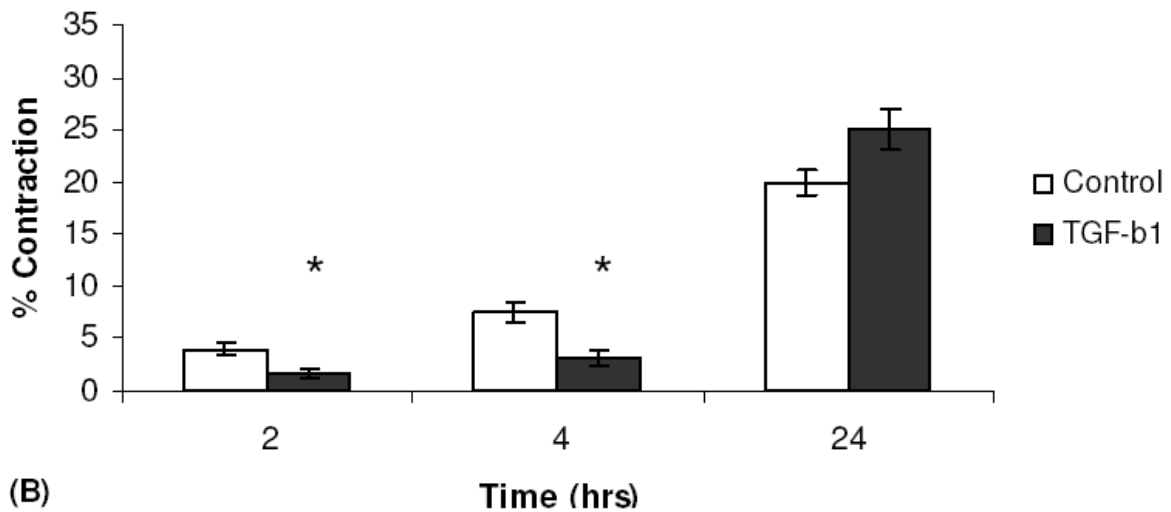
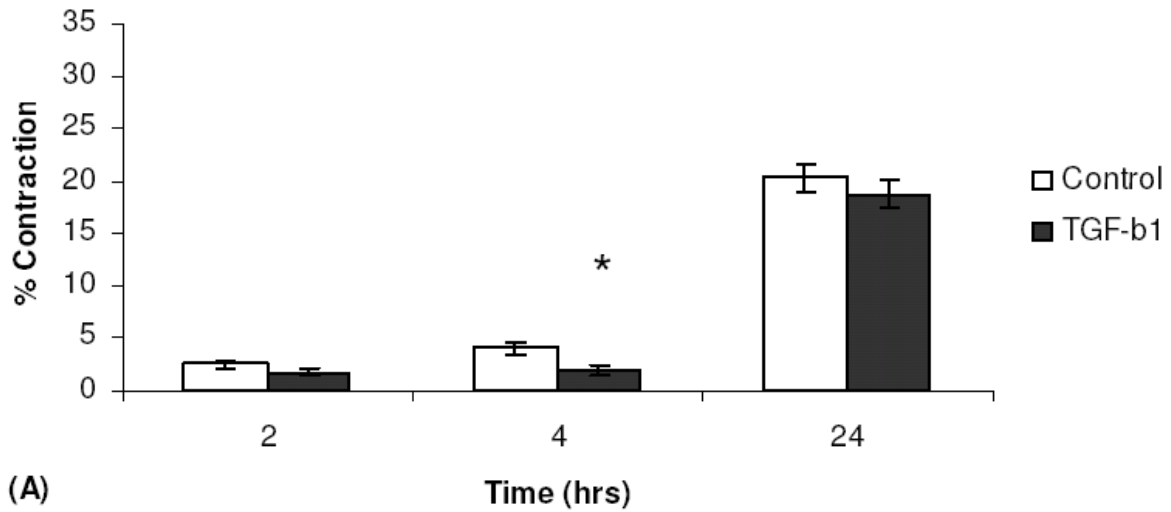


Figure 4-5. Basal BSMC contraction of anchored collagen gels is greater for the highest population of cells at 2 and 4 hours. All anchored collagen gel assays were performed using the three cell populations in control conditions (RPMI 1640 and 2% FBS). $n=13-18$, $16-21$, and $9-17$ for 5×10^4 , 1×10^5 , and 2.5×10^5 BSMCs, respectively. Values represent mean \pm SEM and * indicates $p < 0.05$.

With the addition of TGF- β 1 to culture, cellular contraction of the collagen gels was significantly inhibited for all three cell populations at both 2 and 4 hours following seeding (Figure 4-6). Positive staining for general caldesmon was seen in both regular media and TGF- β 1 treated groups (Figure 4-7). Slight phenotypic differences were visualized in the expression of

h-caldesmon following 4 hours of exposure BSMC exposure to TGF- β 1 on glass coverslips (Figure 4-7). Following light microscopy imaging, BSMC were trypsinized from the surface of the collagen gels. Figure 4-12 shows the trypsinized gels. The gels retained their contracted shape and visible white regions of collagen alignment following the removal of the cells (Figure 4-12).



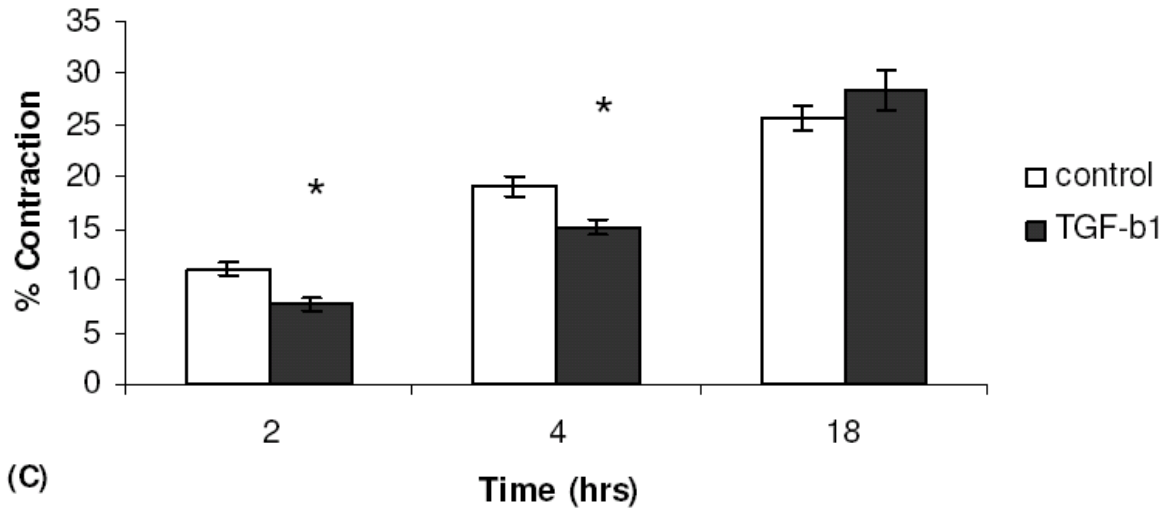


Figure 4-6. *TGF-β1* inhibits contraction of anchored collagen gels by (A) 5×10^4 , (B) 1×10^5 , and (C) 2.5×10^5 BSMCs. Anchored collagen gel contraction was assessed in control conditions with and without 1 ng/ml *TGF-β1*. $n=8-18$, $10-21$, and $7-17$ for 5×10^4 , 1×10^5 , and 2.5×10^5 BSMCs, respectively, for the control and *TGF-β1* cases. Values represent mean \pm SEM and * indicates $p < 0.05$.

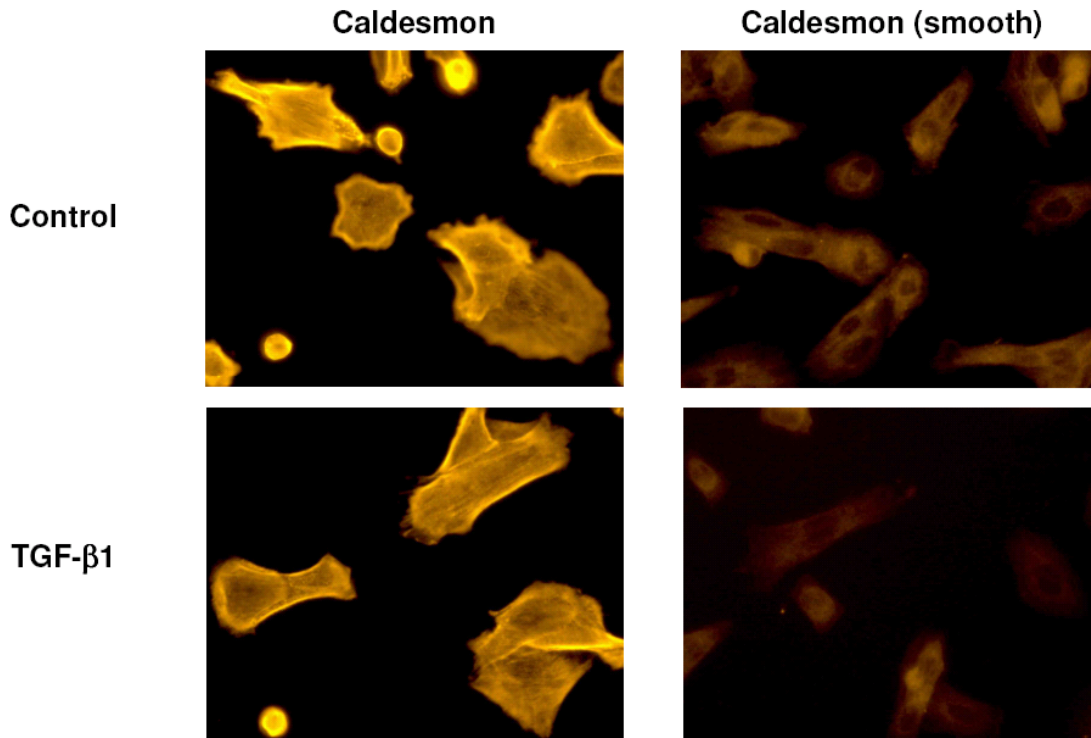


Figure 4-7. *Fluorescent antibody labeling of caldesmon (both isoforms) and h-CaD in BSMCs after 4 hours on glass coverslips for control and TGF-β1 cases. Caldesmon labels intensely in the actin cytoskeleton and cytoplasm for both cases, whereas h-CaD staining is less intense, cytosolic, and further diminished in the TGF-β1 case.*

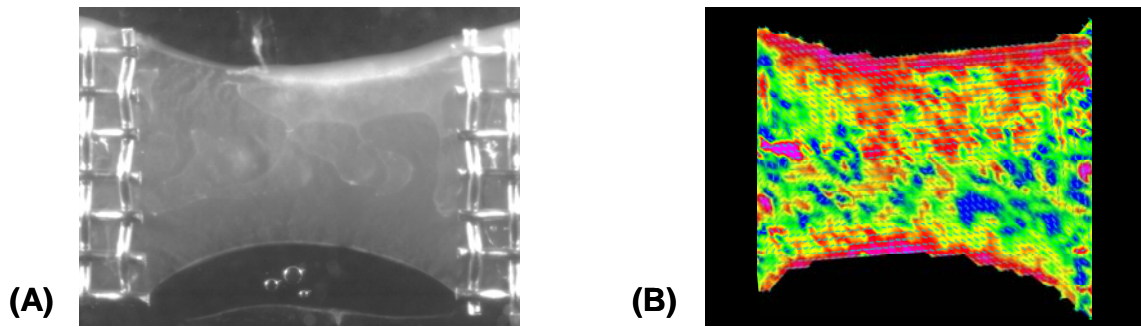


Figure 4-8. (A) An example of a contracted anchored collagen gel between the steel mesh anchors 5×10^4 BSMCs after 24 hours. (B) SALS image of the same collagen gel. Dotted box depicts area of analysis containing the 704 OI values averaged to represent the physical remodeling or reorganization of each collagen gel. Areas of red depict highly oriented fibril networks (corresponding to small OI values), whereas areas of blue indicate randomly oriented fibril networks (corresponding to large OI values).

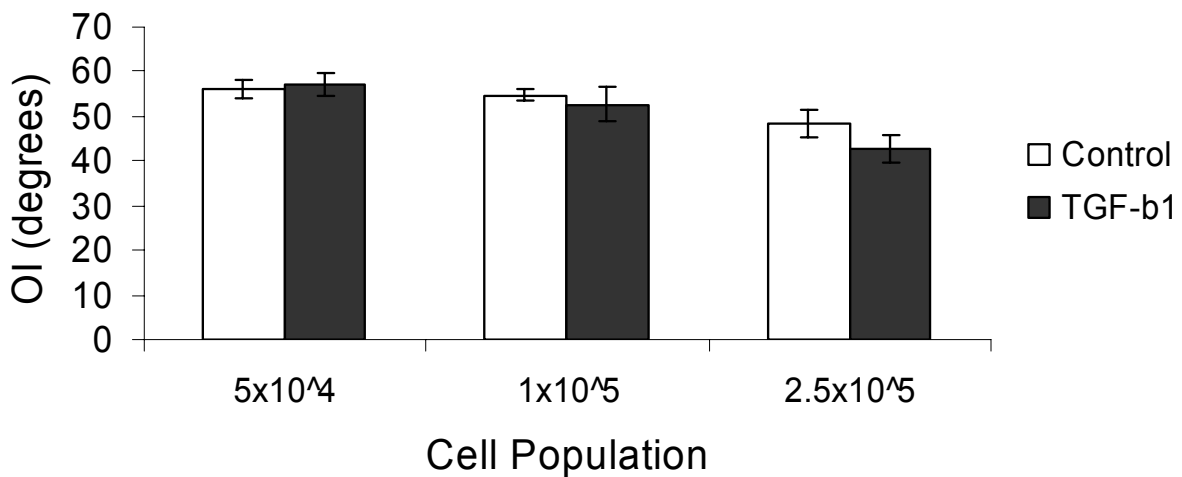


Figure 4-9. TGF- β 1 increases collagen gel alignment and orientation (smaller OI values) for 2.5×10^5 BSMCs. 2.5×10^5 BSMCs physically remodel and organize the collagen gels (smaller OI values) more than the other two BSMC populations (not shown statistically on graph). OI values were assessed after 24 hours of contraction for the 5×10^4 and 1×10^5 BSMCs and 18 hours for the 2.5×10^5 BSMCs. $n=4-7, 5,$ and $8-9$ for $5 \times 10^4, 1 \times 10^5,$ and 2.5×10^5 BSMCs, respectively, for the control and TGF- β 1 cases. Values represent mean \pm SEM and * indicates $p < 0.005$.

4.3.3 TGF- β 1 alters collagen reorganization

SALS scanning showed that contracted collagen gels had aligned collagen fibrils along the edges indicated by the pink regions of the SALS scans (Figure 4-8). The addition of TGF- β 1 increased the organization of collagen gels at the highest cell population (Figure 4-9). Representative SALS scans show the areas of higher alignment (red and pink) in the TGF- β 1 treated higher cell populations (Figure 4-10).

4.3.4 TGF- β 1 causes BSMC bundling

The regions of higher alignment in Figure 4-10 c right panels appear to correspond to the white regions seen in Figure 4-10 c left panels. Light microscopy images of the BSMC on the collagen gels with and without the addition of TGF- β 1 are shown in Figure 4-11. These images showed that the addition of TGF- β 1 to the middle and high cell populations causes bundling of the BSMC on the surface of the gel. Further SALS scanning showed that these regions of cellular bundling corresponded to regions of high collagen alignment within the gel (Figure 4-10).

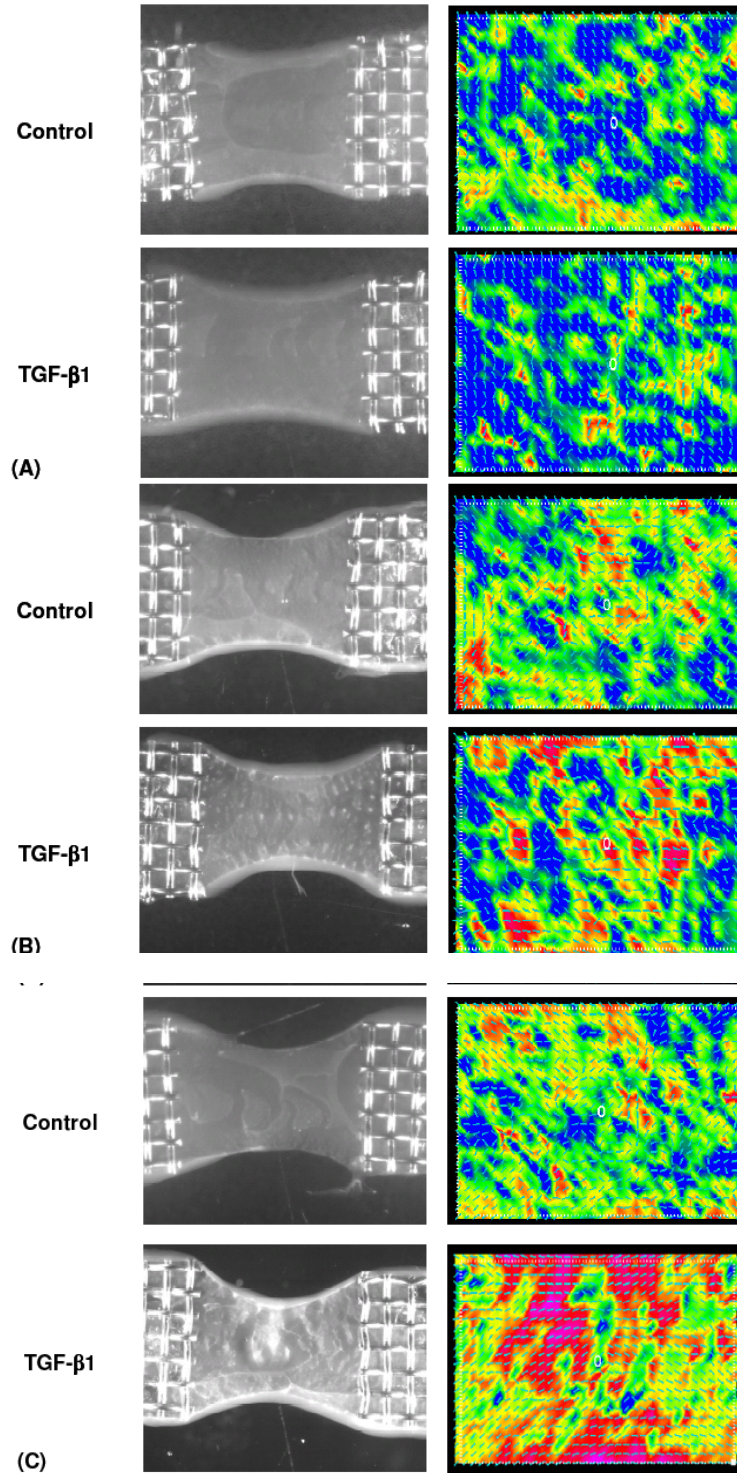
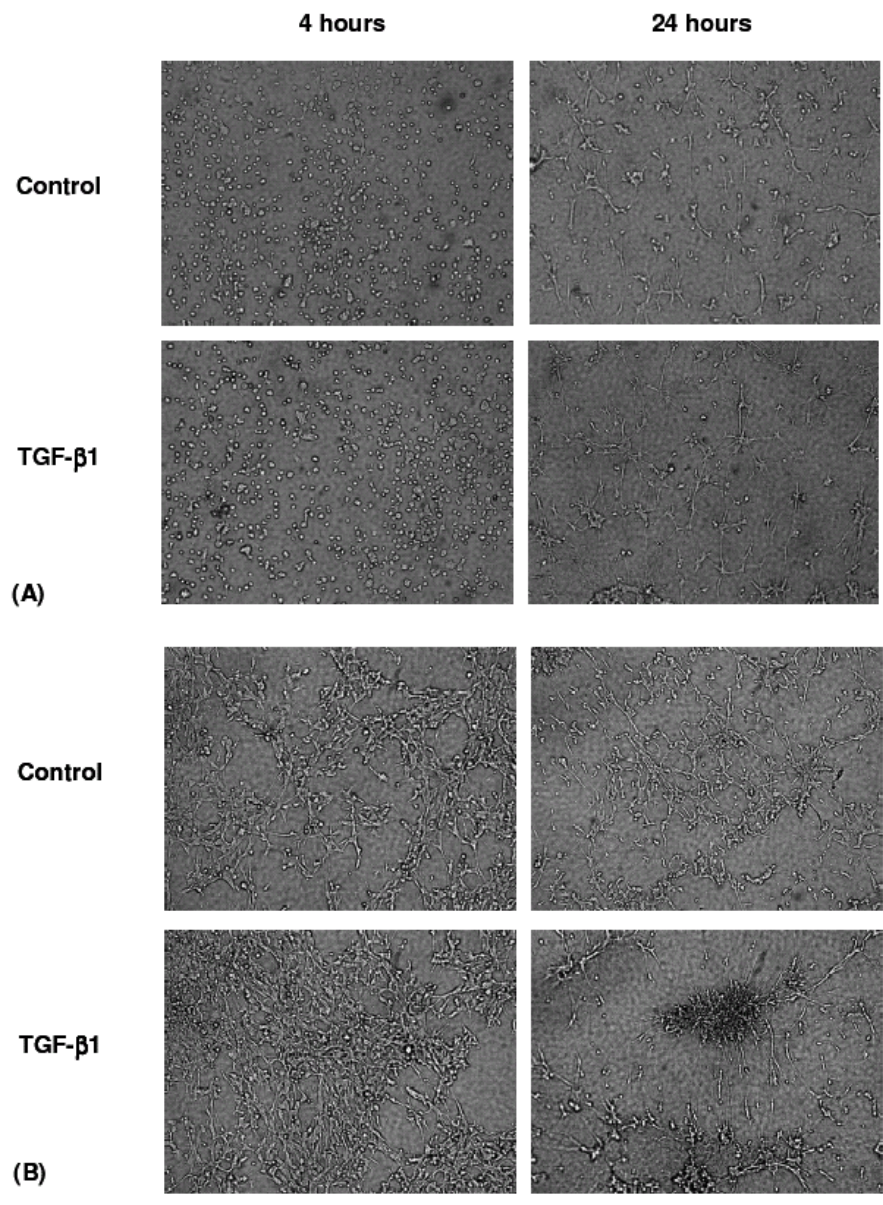


Figure 4-10. Contracted anchored collagen gels and accompanying SALS images for control and TGF- β 1 cases for (A) 5×10^4 BSMCs at 24 hours, (B) 1×10^5 BSMCs at 24 hours, and (C) 2.5×10^5 BSMCs at 18 hours. Highly aligned areas of collagen fibrils (red) increase with increasing cell populations and are more prominent at higher cell populations. TGF- β 1 induces the formation of white patches on the collagen gels (B, C).



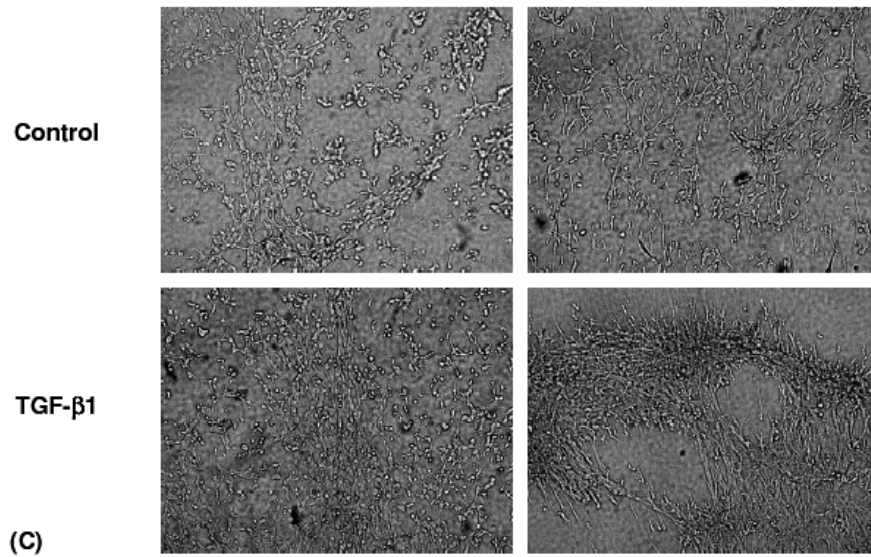


Figure 4-11. Cell morphology on anchored collagen gels for (A) 5×10^4 , (B) 1×10^5 , and (C) 2.5×10^5 BSMCs at 4 and 24 hours for control and TGF- β 1 cases. Spreading depends on cell population with a higher number of cells spreading faster on the collagen gel surfaces at 4 hours and maintaining this morphology at 24 hours in the control cases. By 24 hours, the majority of BSMCs are spread and elongated in the control conditions. However, TGF- β 1 induces cell bundles or aggregates (B, C) which correspond to white patches on the collagen gels and regions of high collagen fibril alignment.

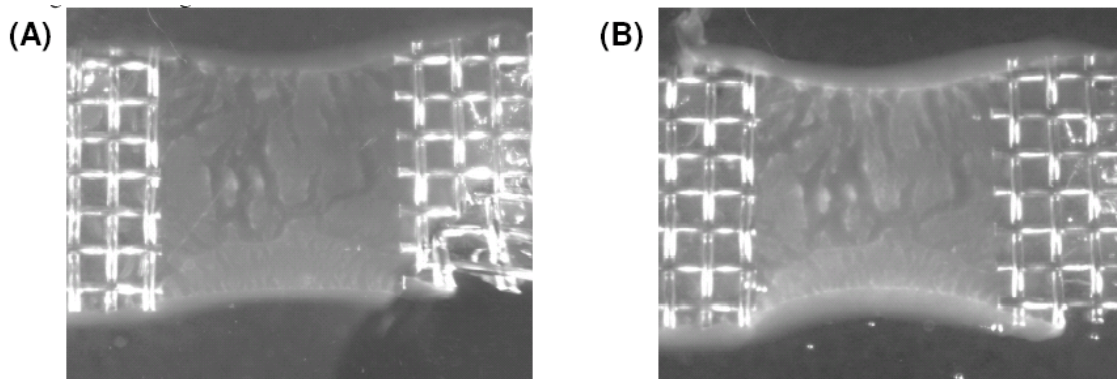


Figure 4-12. An anchored collagen with 2.5×10^5 BSMCs after (A) 18 hours of contraction and followed by (B) 4 days of trypsinization shows that the changes in collagen gel architecture caused by the BSMC aggregates are conserved.

4.4 DISCUSSION

4.4.1 Influence of TGF- β 1 on gel contraction and cellular phenotype

As discussed in chapter 3, the contractile phenotype of BSMC within the organ cultured bladder strips was decreased following culture with the addition of TGF- β 1 to the media daily. The study discussed in this chapter further demonstrated this phenotypic shift of the BSMC with the addition of TGF- β 1. TGF- β 1 decreased BSMC mediated gel contraction at early time points. Additionally, TGF- β 1 decreased expression of the contractile marker h-CaD. At the highest cell population, TGF- β 1 eventually increased gel contraction at 18 hours with the gels torn off of the anchors at 24 hours. The increase in gel contraction appears to have been due to the cells forming rudimentary bundles on the collagen gels. These rudimentary bundles have been observed previously when TGF- β 1 was infused into a rabbit bladder in vivo [148]. This change in gel contraction may have also been due to the effects of the TGF- β 1 being metabolized by the high cell population at a faster rate than in the low and middle cell populations. As stated in a previous section, the contractile phenotype of the BSMC does diminish over time in culture. Cells utilized in this study were seeded from passages 4-8. In preliminary studies from our laboratory, the contractile phenotype marked by the expression of h-CaD is diminished at passages greater than 10. The cells in culture are automatically pushed toward a less contractile phenotype, but this predisposition was minimized as much as possible by using the cells at

relatively low passage numbers. The antibody staining for h-Cad was further diminished with the addition of TGF- β 1 giving further evidence of a phenotypic shift.

4.4.2 Influence of TGF- β 1 on collagen gel organization

The collagen alignment of the BSMC was again much lower than alignment found utilizing other cell types (Parekh submitted); however, the OI values seem to be consistent with smaller contraction under basal conditions. Although the addition of TGF- β 1 to the BSMC on the collagen gels diminished the cellular contractile phenotype and decreased the rate of collagen gel contraction at 2 and 4 hours, an increase in collagen alignment was seen compared to the collagen alignment found within the BSMC seeded gels in regular media. It was also observed that these values were not consistent throughout the collagen gels. The increased areas of alignment corresponded to the areas of the BSMC rudimentary bundles even after extensive trypsinization. These areas of high alignment were evidence that TGF- β 1 has local physical remodeling effects on the BSMC. Localized physical remodeling of the gels was further observed by the collagen gels tearing off of the anchors at the high cell population at 18 hours. It is possible that instead of the cells regaining a contractile phenotype as the effects of TGF- β 1 diminished, the BSMC formed such tight bundles that holes appeared in the collagen gels. This local physical remodeling of the collagen orientation by the BSMC may be akin to the remodeling that our laboratory has observed previously in the SCI affected bladder at 10 weeks [54].

4.4.3 Implications

The overall changes in cellular phenotype with the addition of TGF- β 1 may be of great importance to understanding the vast changes in ECM seen in various pathologies affecting the bladder wall. While the precise role of a phenotypic shift in the bladder under SCI or any pathology is not currently understood, we can speculate based upon our current findings that the phenotypic shift alters the relationship between the cells and the ECM causing dysfunction. This shift in phenotype may be chemically modulated by TGF- β 1. It is important to note that the behavior of the BSMC on the collagen gel may have implications for engineered tissues. The regulation of ECM synthesis by both biochemical and biophysical factors must be closely monitored in order to engineer a tissue with proper ECM and BSMC organization and composition.

5.0 IN VITRO MECHANICAL CONDITIONING OF BSMC SEEDED ON SIS

5.1 INTRODUCTION

The most successful approaches to tissue engineering the urinary bladder wall utilize biodegradable scaffolds seeded with autologous cells. Although this technique has proven successful in increasing bladder capacity and decreasing the pressure build up that ultimately leads to kidney damage, problems remain with lack of proper tissue organization post-implantation, impairing the bladder's ability to maintain its full function. Small intestinal submucosa (SIS) has been utilized previously to engineer the urinary bladder wall with and without cell seeding. These previous studies have shown that in order to maintain graft size, seeding of the SIS prior to implantation is necessary [105]. In order to engineer a functional tissue replacement for the bladder wall with controlled ECM production and proper BSMC alignment for contraction, mechanical stimulation may be necessary. However, mechanical stimulation of cell seeded SIS is difficult due to the long periods of time it takes for BSMC to penetrate the SIS so that it may be stretched.

5.1.1 Previous SIS studies

Prior studies have suggested that seeding SIS with autologous cells may be advantageous in regenerating functional and mechanically sound tissue replacements. Autologous skeletal muscle cells suspended in a collagen gel seeded onto SIS showed higher mechanical tensile strength than unseeded SIS when implanted into the abdominal muscles of Lewis rats [107]. In addition, using a de-cellularized bladder matrix seeded with canine autologous urothelial and bladder smooth muscle cells for bladder augmentation resulted in an increase bladder capacity [108] and a more complete retention of implanted diameter [109] compared to unseeded matrix. These studies provide evidence that a tissue engineering approach, utilizing autologous cells and a 3-D, biological scaffold, toward urologic tract repair and replacement may provide better long-term successes. Previously our laboratory demonstrated *in vitro*, muscle derived stem cells (MDSC) seeded on SIS formed a calcium-dependent contractile muscle-like tissue after 4 weeks in culture [167]. Additionally, we found that MDSC-seeded SIS after 10 and 20 days in culture is more compliant when compared to unseeded SIS as demonstrated through biaxial mechanical testing, but there was no change in mechanical compliance between 10 and 20 days of seeding [168]. To date, however, the mechanisms by which the MDSC remodel the SIS construct have yet to be elucidated.

One possible mechanism vital to the initial remodeling event is the release of matrix metalloproteinases (MMPs). MMPs are a family of zinc dependent proteolytic enzymes that function mainly in the ECM, where they contribute to the development, functioning, and pathology of a wide range of tissues [169]. Since collagen type-I is the main component of SIS,

it is possible that MMP-I plays a role in the interaction of MDSC with SIS during the initial remodeling process. Other studies have shown that MMP-2 and -9 may play a role in the break down of collagen type-I [170]. However, MMP-2 and -9 are active in degrading gelatin, which is the byproduct of collagen-I cleavage by MMP-I [169]. Since MMP-I acts on fibrillar collagen-I before MMP-2 and -9 are activated, we chose to examine MMP-I as our potential mechanism responsible for the initial remodeling event marked by an increase in mechanical compliance. We hypothesize that the release of MMPs and the resultant break-down of collagen fibers by MDSC seeded onto SIS is a potential mechanism responsible for the initial event in the remodeling process, signaled by an increase in mechanical compliance observed in our previous study [168]. In a previous study, we previously examined the role of MMP-I in the initial remodeling events, specifically studying the activity of MDSC seeded onto SIS as well as the impact of MMP-I on the mechanical properties of SIS.

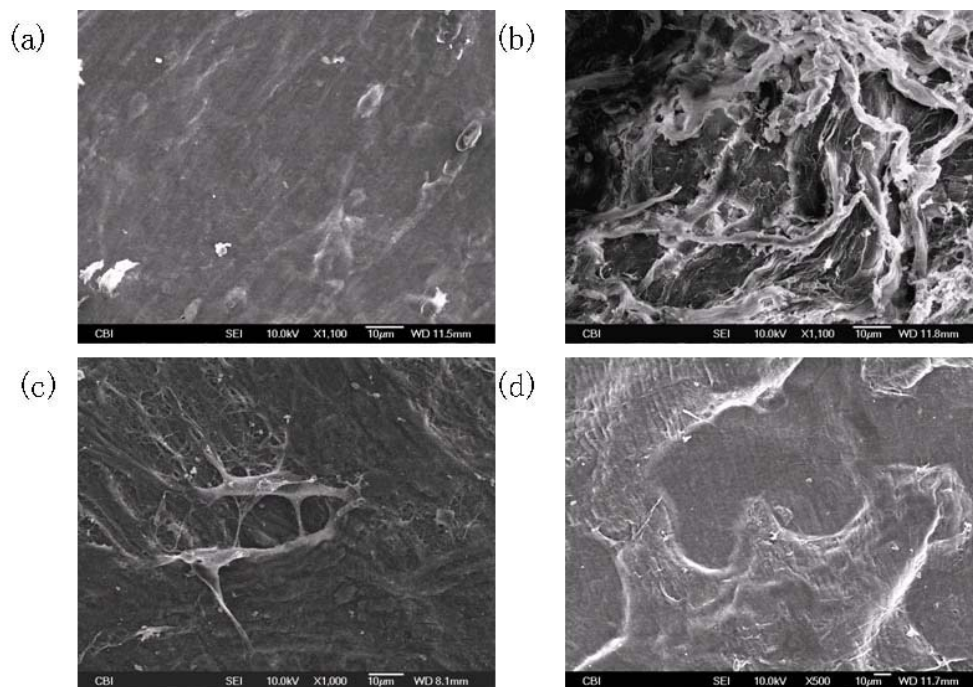
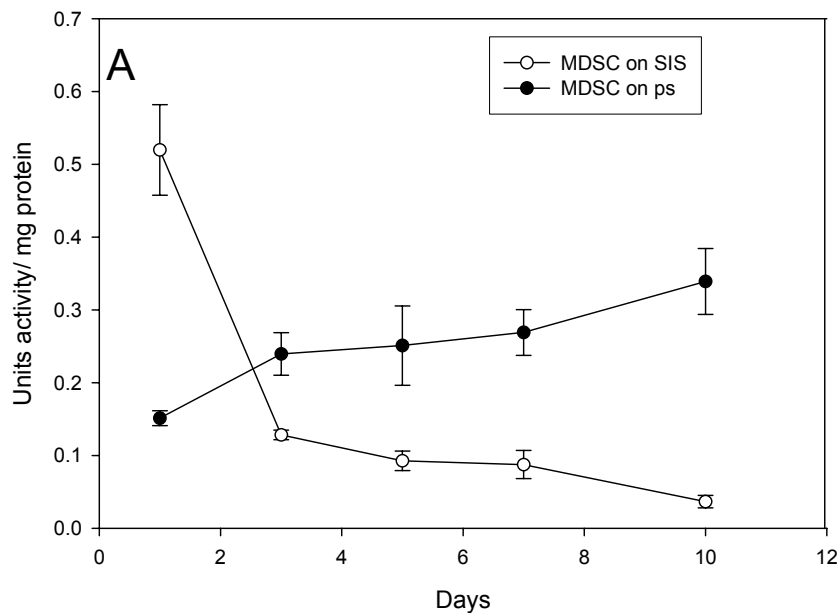


Figure 5-1. Scanning electron microscopy images of control SIS (a), SIS digested with collagenase-I for 5 hours (b), MDSC on SIS for 24 hours (c), and MDSC on SIS for 7 days in culture (d).[171]

The luminal surface of SIS appeared as a smooth surface with visible aligned collagen fibers (Fig. 5-1 A). When exposed to collagenase-I this surface became very rough with collagen fibers disrupted (Fig 5-1 B). MDSC seeded on SIS remained on the surface of the SIS and formed cell-cell protrusions (Fig 5-1 C) and eventually formed large groupings on the surface of the SIS (Fig 5-1 D). The MMP assay revealed that MMP-I activity (Fig. 5-2a) of the MDSC seeded SIS was significantly higher ($p < 0.0025$) after one day in culture compared to samples collected from subsequent time points and the unseeded control. Supernates from MDSC seeded on tissue culture polystyrene expressed a significantly higher amount of MMP-I activity ($p < 0.025$) after 3 and 5 days in culture and ($p < 0.0025$) after 7 and 10 days in culture compared to MDSC on SIS and SIS alone at corresponding time points. Additionally, there was a significant amount ($p < 0.05$) of MMP-I present in supernatant from soaked, unseeded SIS compared to media alone (Fig. 5-2b).



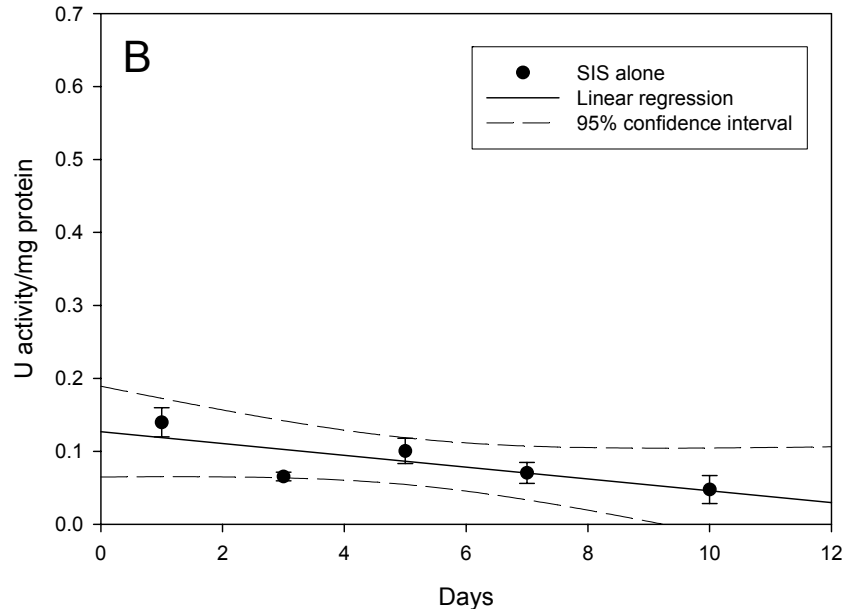


Figure 5-2. Normalized MMP-I activity of supernates of (a) MDSC on SIS and MDSC on tissue culture polystyrene and (b) SIS alone. In b, SIS releases residual MMP-I, which decreases linearly over time. Data are mean \pm SEM $n = 3$ per group in triplicate. [171]

When tested biaxially, SIS exhibited the classic non-linear stress-strain response common to soft tissues. All specimens tested were in a state of nearly pure biaxial strain with negligible shear. Mechanical anisotropy, different response to equi-biaxial stress between the longitudinal and circumferential directions, was found in each group. Samples that were incubated for 24 hours in media containing collagenase-I could not be tested due to the nearly complete break down in the collagen type-I fibers of the SIS. After 3 and 4.5 hours of digestion with collagenase I, the SIS had no significant change in compliance in either the circumferential or longitudinal directions compared to SIS soaked in media alone. After 5 hours of digestion with collagenase-I, mechanical compliance under 1 MPa peak stress was increased by 7% in the circumferential direction, compared to control SIS (Fig 5-3). Peak stretch in the longitudinal direction (Fig. 5-3) did not change with digestion. Areal strain was significantly greater ($p < 0.007$) after digestion

with collagenase-I for 4.5 and 5 hours when compared to the control. Additionally, there was no significant difference ($p=0.356$) in areal strain between SIS digested for 5 hours and SIS seeded with MDSC for 10 days. These results from this study supported our initial hypothesis, that the MDSC synthesize and release MMP-1 into the ECM to digest the SIS substrate early in the remodeling process, which may allow the cells to attach, penetrate and integrate into the substrate. The break down of collagen fibers may lead to the increase in compliance of the MDSC seeded SIS. However, the MDSC did not further utilize this mechanism to penetrate the SIS.

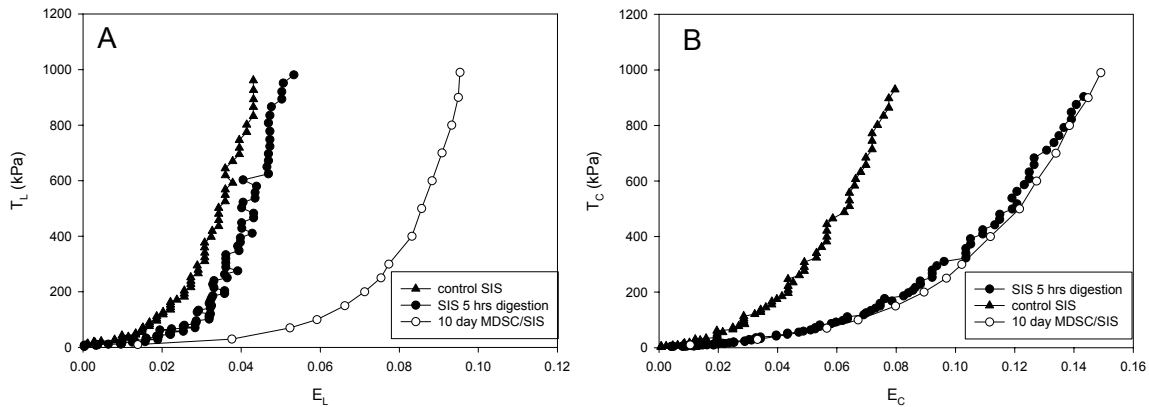


Figure 5-3. Representative plot of equi-biaxial testing experiments in the longitudinal direction (a) and circumferential direction (b) on SIS digested with 0.16 U/mL collagenase-I for 5 hours, MDSC seeded SIS for 10 days, and control.

While interesting from a biological perspective, the aforementioned study was not useful for tissue engineering or utilizing the system to examine the mechanobiology of cell-seeded SIS due to the lack of penetration of the MDSC into the SIS. Other studies utilizing bladder smooth muscle cells (BSMC) seeded on an ECM scaffold (SIS or bladder acellular matrix) proved that cellular penetration was difficult to achieve in vitro without the use of co-culture with urothelium

[94, 140]. Other studies have also shown that cell penetration into SIS takes on the order of weeks (REF). In order to obtain a construct that may be mechanically stimulated to promote ECM remodeling, cell penetration is necessary. Although the exact signaling mechanisms between the urothelium and BSMC in culture are unclear, it has been noted previously that soluble growth factors are likely involved [172]. Therefore in order to increase cellular penetration, growth factors that are released in culture by the urothelium may be utilized.

5.1.2 Growth factors VEGF and FGF-2

SIS itself contains a number of growth factors and cytokines. Among the most abundant are basic fibroblast growth factor (bFGF or FGF-2) and transforming growth factor beta (TGF- β) [173]. SIS also contains other factors such as vascular endothelial growth factor (VEGF), but VEGF is degraded in the processing of the matrix [174]. These growth factors and cytokines likely aid in the remodeling response that occurs following implantation of SIS; however, in vitro, the inherent growth factors in the SIS may not be adequate to promote penetration of cell types other than fibroblasts.

FGF-2 is expressed in cell types from the mesoderm and neuroectoderm [175]. FGF-2 has additionally been shown to play a role in angiogenesis, proliferation, and differentiation in nearly every organ system [175]. FGF-2 has been identified to play a crucial role for stimulating skeletal muscle regeneration [176]. It has also been demonstrated that FGF-2 retains its bioactivity in SIS following processing [174]. The growth factors FGF-2 and VEGF simulate urothelial cell presence [142], have been shown to increase proliferation in neurogenic BSMC

[177] and have an anti apoptotic effect in culture of human BSMC [72]. Additionally, VEGF plays a role in bladder development [172].

For these aforementioned reasons, we hypothesize that the growth factors VEGF and FGF-2 may be utilized to increase cellular penetration into the SIS. Furthermore, we hypothesize that BSMC seeded SIS exposed to mechanical stimulation will produce significant changes in the amount of ECM components collagen and elastin dependent on the frequency of stretch.

5.2 PROTOCOL

5.2.1 Cell culture

Bladder smooth muscle cells (BSMC) were isolated from female Sprague Dawley Rat bladders as described previously [165] and expanded in culture in RPMI 1640 media with 10% FBS and 1% Pen/Strep. All cells were used between passages 6-9 and seeded at 0.5×10^6 cells/cm² onto the luminal side of SIS inserts (Cook Biotech). A pilot study was performed wherein 2 concentrations of VEGF (low 10 ng/mL and high 20 ng/mL; Sigma) and 2 concentrations of FGF-2 (low 5 ng/mL and high 10 ng/mL; Sigma) were utilized based upon concentrations reported previously in the literature. A DNA quantification assay was performed at 7 days in culture and no significant differences in cellular proliferation were observed between the low and high concentrations. Therefore, VEGF (10 ng/mL) and FGF-2 (5 ng/mL) were added to each insert in the media every other day for up to 7 days in culture. Following culture in growth factor treated media, samples were switched to regular culture media (RPMI 1640 supplemented with

10% FBS and 1% PS) and then either grown in static culture or dynamic culture for an additional 7 days.

5.2.2 Mechanical stimulation

Following 7 days in static culture with the exogenous growth factors, BSMC seeded SIS was affixed with tissue grip springs to a tension bioreactor as described previously [150] and stretched at 15%, 0.1 Hz or 15%, 0.5 Hz under strip biaxial stretch with the primary direction of stretch in the longitudinal direction , for an additional 7 days.

5.2.3 DNA quantification

Following static and dynamic culture samples were snap frozen and stored at -80 C for biochemical assays. DNA quantification was performed as described previously [171]. Each sample was cut into fourths and weighed prior to extraction. Samples were placed in a microcentrifuge tube and extracted in 1 ml of 0.125 mg/ml papain solution for 10 hours in a 60 °C water bath. Digested samples were analyzed with a PicoGreen dsDNA quantitation kit (Molecular Probes, Eugene, OR) as per the manufacturer's instructions and using the blue channel of a TBS-380 Mini-Fluorometer (Turner Biosystems, Sunnyvale, CA). There was a small amount of DNA found in the unseeded SIS scaffold; this amount was subtracted from the DNA found in each sample. The total DNA quantitation was done in triplicate with n=3 per group.

5.2.4 Collagen and elastin assessment

Collagen and elastin concentrations were determined based on techniques adapted from Brown et al [128], which have previously been used to quantify ECM synthesis of ovine vascular smooth muscle cells under cyclic mechanical flexure [129]. Soluble collagen was extracted from tissue samples using a solution of 0.5 M acetic acid (Sigma) and 1 mg/mL Pepsin A (Sigma). Each sample was placed in a microcentrifuge tube and incubated in 1 ml of extraction solution overnight (~16 h) on a rocker table operating inside a refrigerator at 2–8°C. Elastin was extracted using a hot oxalic acid treatment. The supernates from the oxalic acid treatments were loaded onto Centricon RC/YM-3 centrifugal filter units (Millipore, Bedford, MA) and centrifuged at 3000g for an additional hour. The concentrate was then be re-suspended in cold (<5°C) Elastin Precipitating Reagent (UK Biocolor). Soluble collagen from the collected media samples at days 2, 4, 6, 8, 10, 12 and 14 was precipitated with 4 M NaCl. Fresh media was used as the control. Following the extraction steps, the collagen and elastin extracts were assayed according to the guidelines provided with the Sircol™ and Fastin™ assay kits, respectively (UK Biocolor).

5.2.5 Matrix metalloproteinase (MMP) activity

Since the pepsin soluble collagen found in the tissue may be either newly formed collagen or degraded collagen, the culture media was assayed for both collagen and bulk matrix

metalloproteinase activity. MMP activity was assayed from the conditioned media at days 2, 4, 6, 9, 11, 13 utilizing a similar method to Aitken et al 2006 [130]. Net activity was assayed using the EnzCheck collagenase/gelatinase assay kit (Invitrogen). DQ-gelatin fluorescein conjugate (0.1 mg/mL) was incubated in Tris buffer (50 mmol/L) with conditioned media for 2 hours. The MMPs then released the quenched activity of the FITC from the FITC-gelatin. The released FITC was measured on a fluorescent microplate reader at 495 nm absorption and 525 nm excitation. Collagenase produced in *Clostridium histolyticum* provided in the kit was used as a positive control. Negative controls were performed with 20 μ mol/L of 1,10-phenanthroline to inhibit the MMP activity. Background from SIS incubated in media was subtracted from all samples at corresponding time points. Data are reported as a summed total of activity from each day media was changed (2, 4, 6, 9, 11, and 13).

5.2.6 Cell migration assays

Migration of the BSMC was assessed in two ways. First, BSMC were seeded at 0.5×10^6 cells/cm² on SIS. 3 samples at 2, 4, and 6 days following culture were fixed in 10% NBF for sectioning and nuclei staining to visualize nuclei distribution in the SIS. Additionally in order to quantify the effects of VEGF and FGF-2 on cellular migration without confounding effects of the inherent growth factors in SIS, cells were seeded on Costar Transwell Inserts (6.5 mm, 8 μ m pore size, Fisher Scientific) coated overnight at 4 C with Type I collagen (PureCol). Following coating, the collagen was aspirated and inserts were dried under a laminar flow hood for 4 hours. Cells were seeded at 4×10^4 cells/mL in either 10ng/mL VEGF media or 5ng/mL FGF-2 in RPMI-1640 media supplemented with 10% FBS and 1% PS (Invitrogen). Following 24 hours,

cells were scraped off of the surface of the membrane and image analysis was performed with Sigmascan 4 to quantify the live cells that had migrated to the bottom of the membrane. These cells were also imaged with fluorescence microscopy.

5.2.7 Histological staining

Three samples from each experimental group were fixed in 10% NBF, coated in 4% agar, paraffin embedded and sectioned. Sections were stained with 4',6-diamidino-2-phenylindole (DAPI) to visualize cell nuclei or stained with Masson's trichrome or Voerhof's Van Gieson Staining to visualize ECM components. Sections were imaged with light microscopy and captured with a digital camera (Nikon).

5.2.8 Statistical analysis

All data are presented as mean +/- s.e.m. Analysis of data was performed using SigmaStat 3.0. One-way analysis of variance (ANOVA) was performed followed by Tukey tests for pair wise comparisons. Data were considered statistically significantly different if $p < 0.05$.

5.3 RESULTS

5.3.1 Cellular proliferation

In static culture, VEGF promotes significantly higher ($p < 0.05$) BSMC proliferation than standard media alone or FGF-2 treated groups (Fig 5-4). Under dynamic culture, there were no statistical differences amongst the stretch or static cycles in the FGF-2 or VEGF treated groups (Fig 5-5). The regular media treated group did not retain any attached cells when stretched during a preliminary experiment and therefore was not cycled as a control for the VEGF or FGF-2 treated groups. This result was likely due to the cells on the surface of the SIS detaching with the application of mechanical stretch. Therefore, the DNA quantification of the dynamic cultures was nearly completely that of cells that had penetrated the SIS.

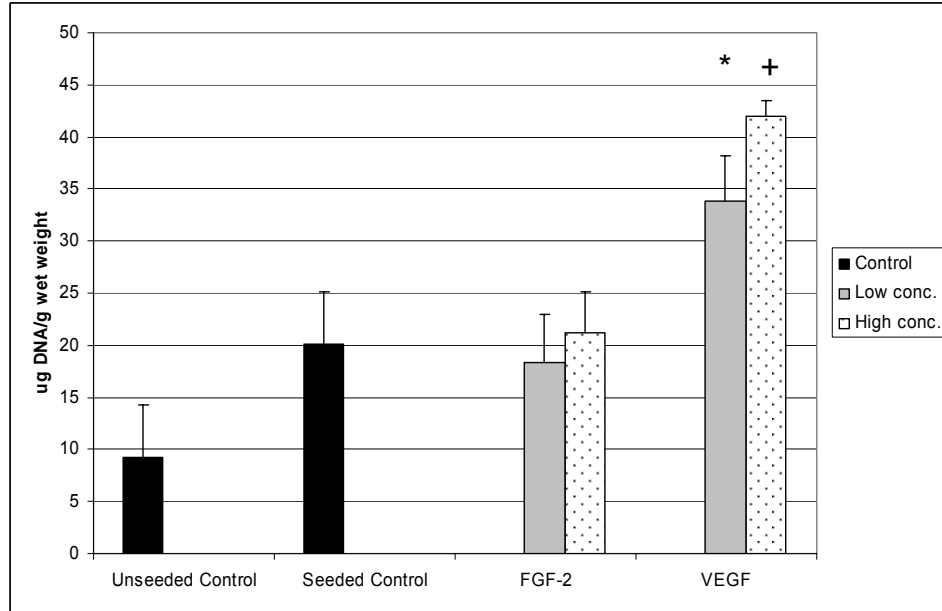


Figure 5-4. DNA quantification at 7 days growth factor treatment. $n=6$ per group. *,+ $p<0.05$ compared to all other groups except each other.

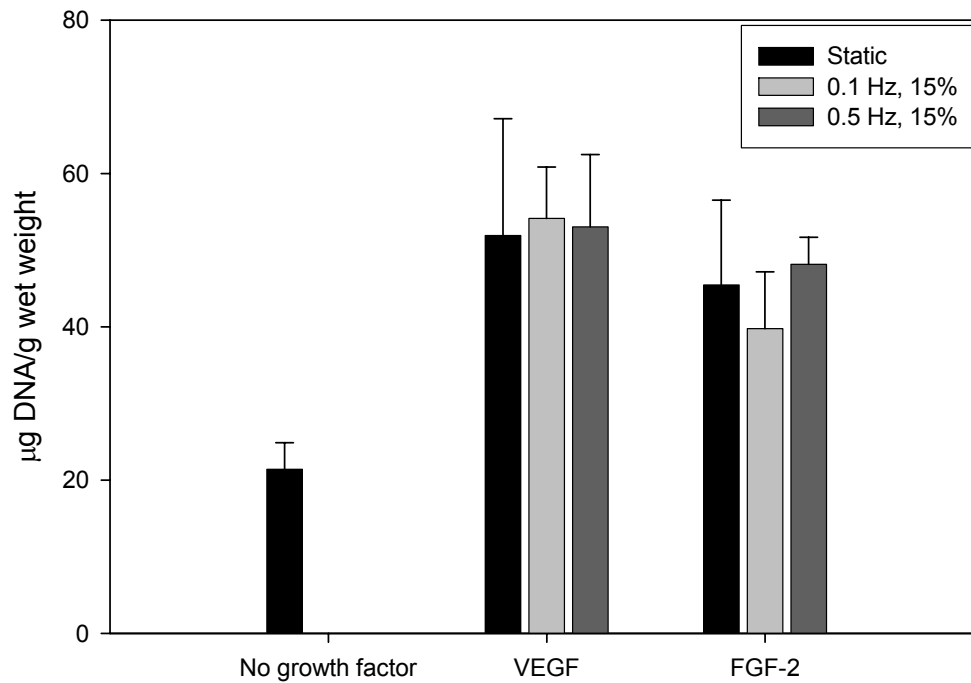


Figure 5-5. DNA quantification following 14 days culture with 7 days static growth factor treatment, 7 days no treatment static or stretched. Data are presented as mean \pm s.e.m, $n=6$ per group. All VEGF groups and FGF-2 groups are statistically significantly greater than the no growth factor treated group, $p<0.01$.

5.3.2 Cellular migration

Histological analysis showed that in standard culture media BSMC remained on the surface of the SIS while both FGF-2 and VEGF profoundly promoted in-growth of the BSMC into the SIS (Fig 5-6). In the FGF-2 treated group the BSMC appeared to grow into the SIS in a cluster while in the VEGF treated group the cells were more spread throughout the tissue. In the transwell migration experiments, BSMC migrated more rapidly from one side of the culture insert to the other with the addition of the exogenous growth factors. (Fig 5-7) Furthermore, the exogenous growth factors enhanced cellular migration into unoccupied space in the culture well with a significantly greater number of cells migrated in VEGF and FGF-2 than in standard media alone (Fig 5-7).

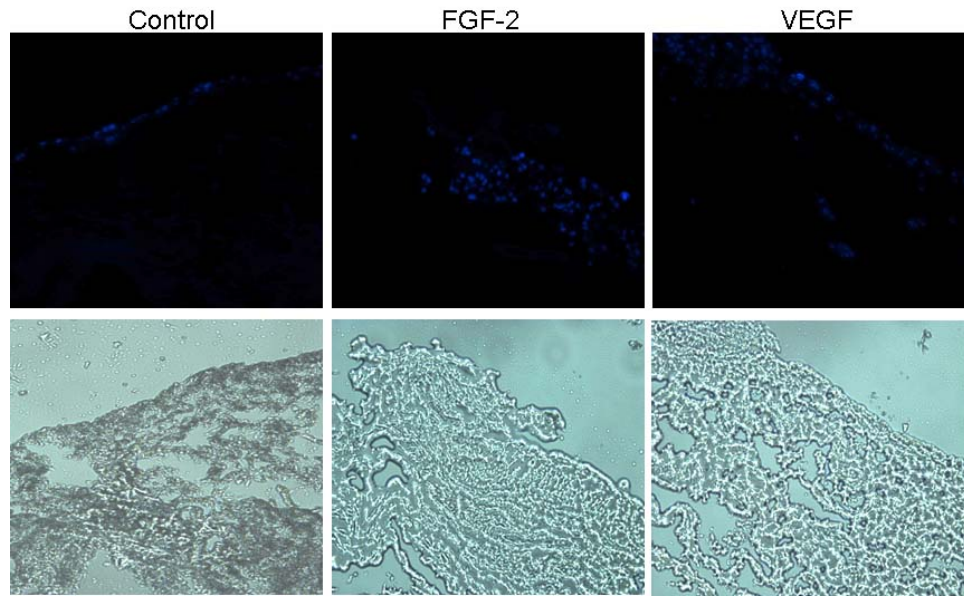


Figure 5-6. Top panel, DAPI stained nuclei (blue) following 7 days with growth factor treatment on SIS. Bottom panel, light microscopy image of SIS cross section.

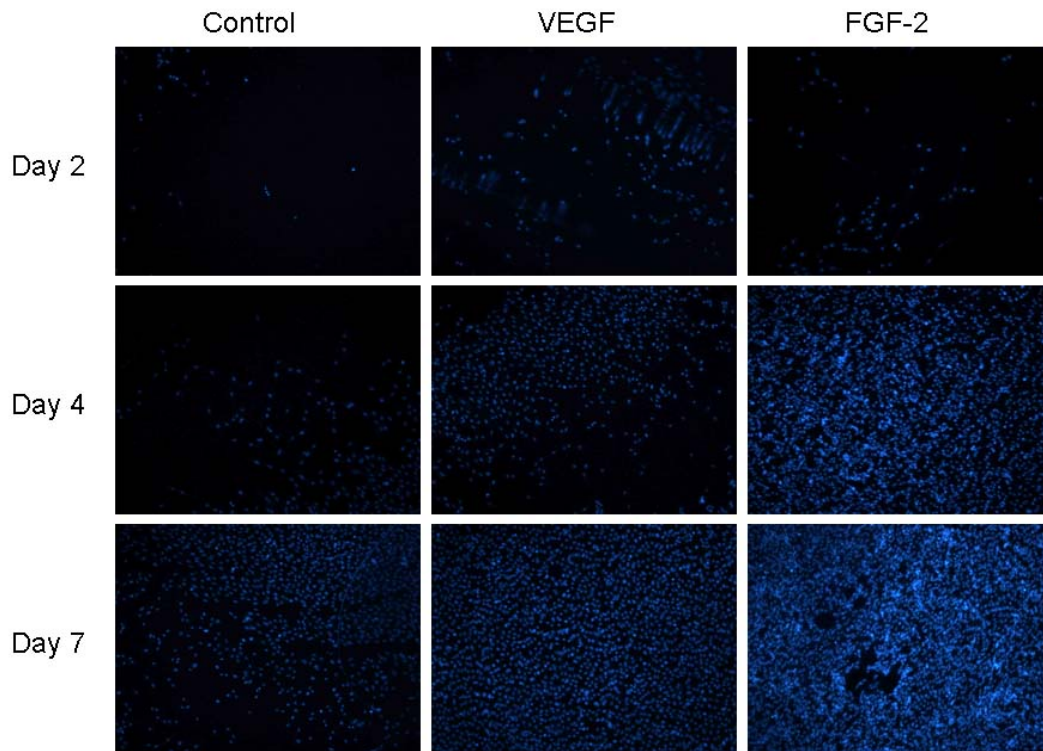


Figure 5-7. DAPI stained cell nuclei at days 2, 4, and 7. Images are reduced from 100x

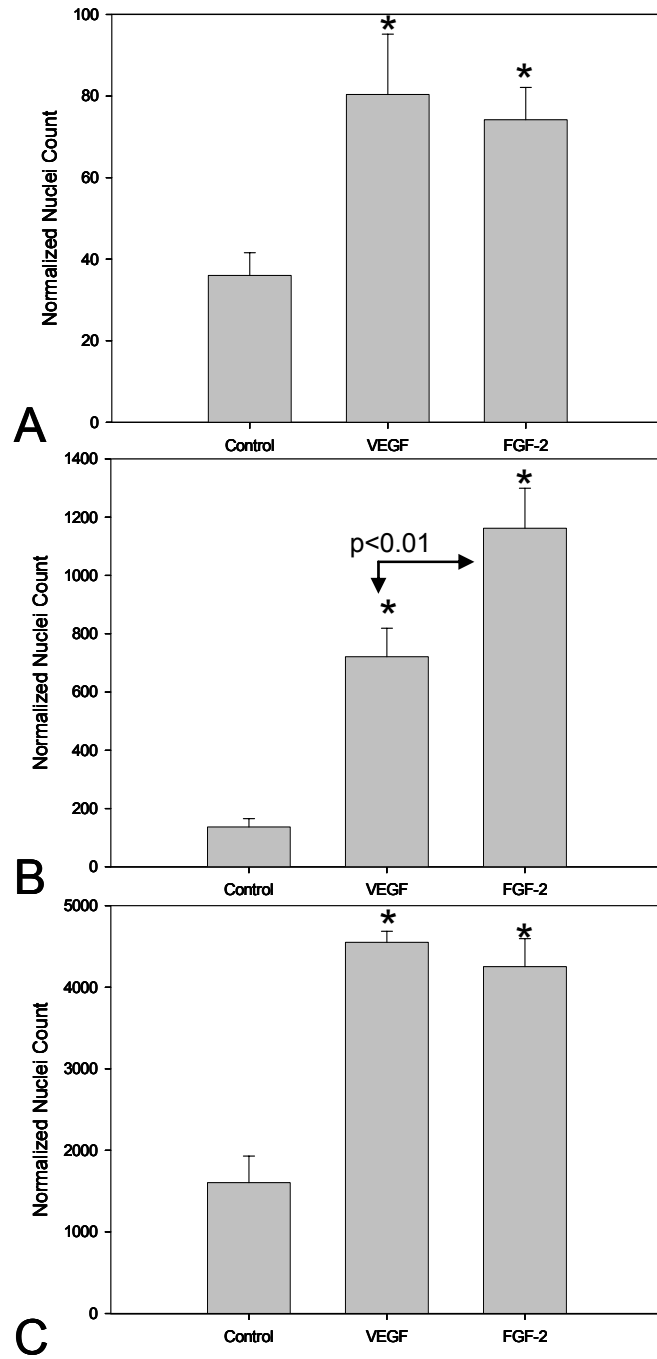


Figure 5-8. Normalized cell nuclei counts on the unseeded side of transwell inserts at A. 2 days, B. 4 days, C. 7 days. *N*=3 transwells per group with 5 images from each transwell analyzed. **p*<0.01 compared to regular media controls.

At 14 days total culture time, there still appeared to be more cellular penetration of the BSMC into the SIS in the VEGF and FGF-2 treated groups compared to the regular media group in static culture (Fig 5-9 A-C). When constructs were cyclically stretched, there appeared to be fewer cells within the construct. However, upon further histological examination the cells were spread throughout the construct in the stretched groups (Fig 5-9, E-H) than in the static groups where the cells remained in the central portion of the SIS where seeding occurred (Fig 5-9 B,C). Furthermore, DNA quantification revealed that an equivalent number of cells were present in the constructs following stretch as in the statically cultured constructs (Fig 5-9). In the FGF-2 treated group under 0.5 Hz stretch, groupings of BSMC were seen to congregate in clusters which resembled rudimentary smooth muscle fascicles (Fig 5-9 H). This observation has been shown previously with the treatment of TGF- β 1 in bladders of rabbits [148] as well as in our laboratory's previous work with the addition of TGF- β 1 to BSMC seeded on collagen gels (Chapter 4). Although there appear to be differences in the thickness of the samples in the histology, there were no measured differences in thickness of any of the samples with an average thickness of 120 μ m. What appears to be thickness variability in the histological sectioning was due to artifact of the SIS spreading when sectioned.

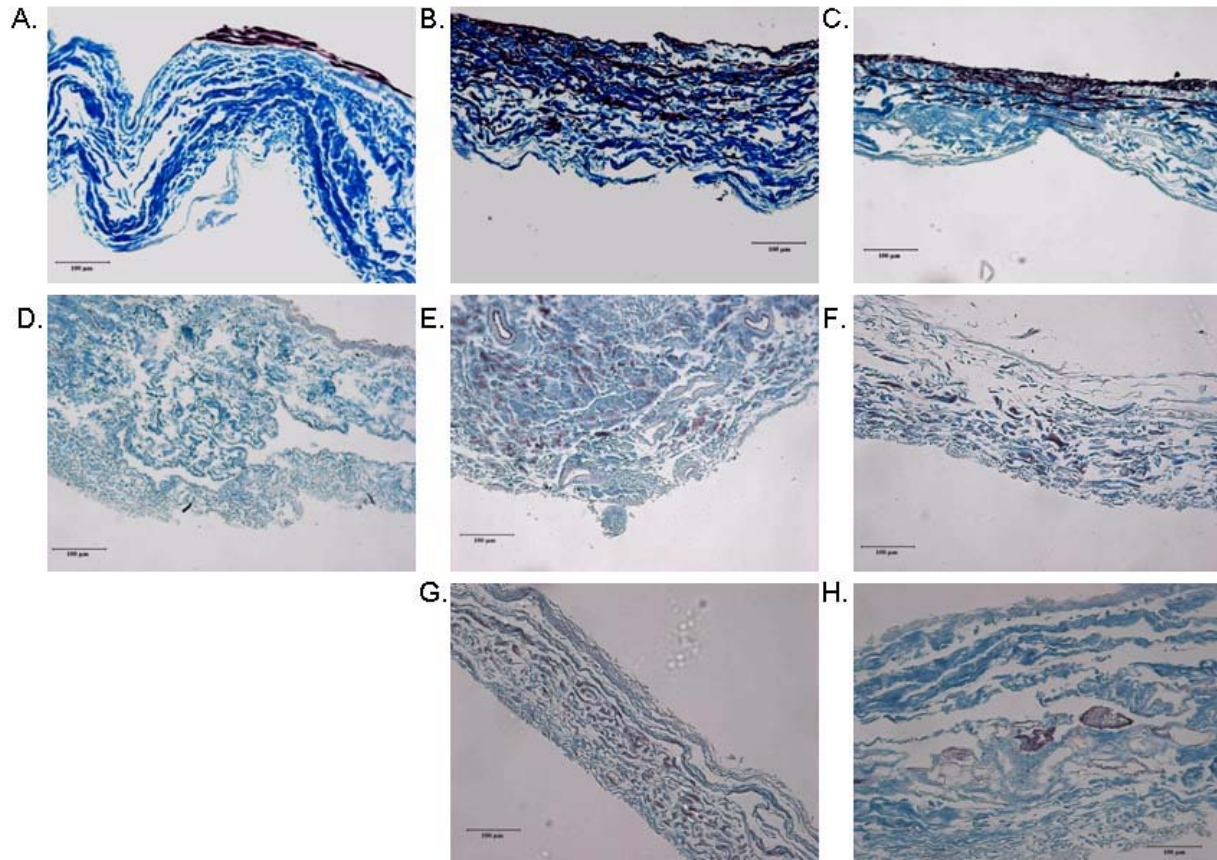


Figure 5-9. Elastic trichrome staining of A. NG 14 day static B. VEGF 7 day NG 7 day static C. FGF-2 7 day NG 7 day static D. Unseeded SIS E. VEGF 7 day Stretch 7 day 0.1 Hz F FGF-2 7 day Stretch 7 day 0.1 Hz G. VEGF 7 day 0.5 Hz 7 day, H. FGF-2 7 day 0.5 Hz 7 day. Images are reduced from 200x. Scale bar represents 100 µm.

5.3.3 Collagen and elastin

In static culture, there was no significant change in collagen content between treatment groups. Under dynamic culture, collagen content in the tissue was significantly higher in the 0.5 Hz stretch group in both the VEGF and the FGF-2 treated groups compared to all other groups (Fig. 5-10). In contrast, elastin content of the tissue was significantly higher in the 0.1 Hz stretch

group in both the VEGF and the FGF-2 treated groups compared to all other groups (Fig. 5-11). This elastin production was further confirmed with VVG staining (Fig 5-12) where black staining of elastin was apparent throughout the VEGF and FGF-2 treated tissues that were cyclically stretched at 0.1 Hz. The unseeded SIS is shown in figure 5-12 A. Very small amounts of elastin were visible in the unseeded SIS. Furthermore, with elastic trichrome staining elastin fibrils were only visible in the 0.1 Hz stretch groups.

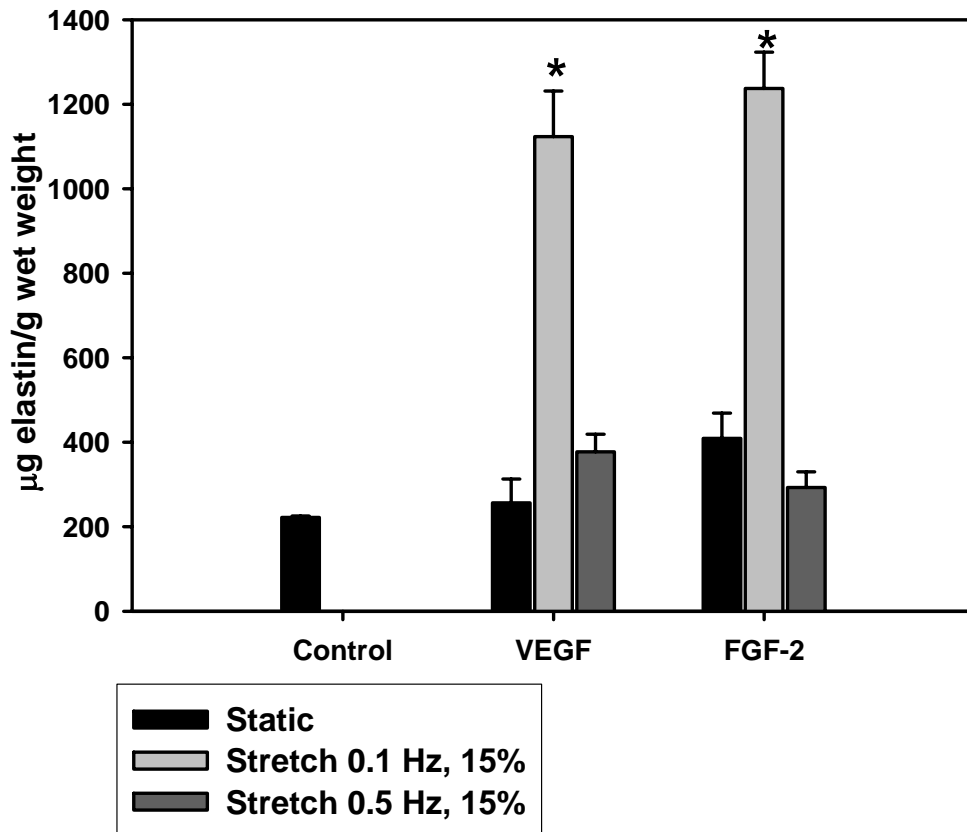


Figure 5-10. Elastin protein concentration per gram wet weight of BSMC seeded SIS. Data are presented as mean \pm s.e.m. with $n=6$ per group. *indicates statistical significance with $p<0.01$ compared to all other groups.

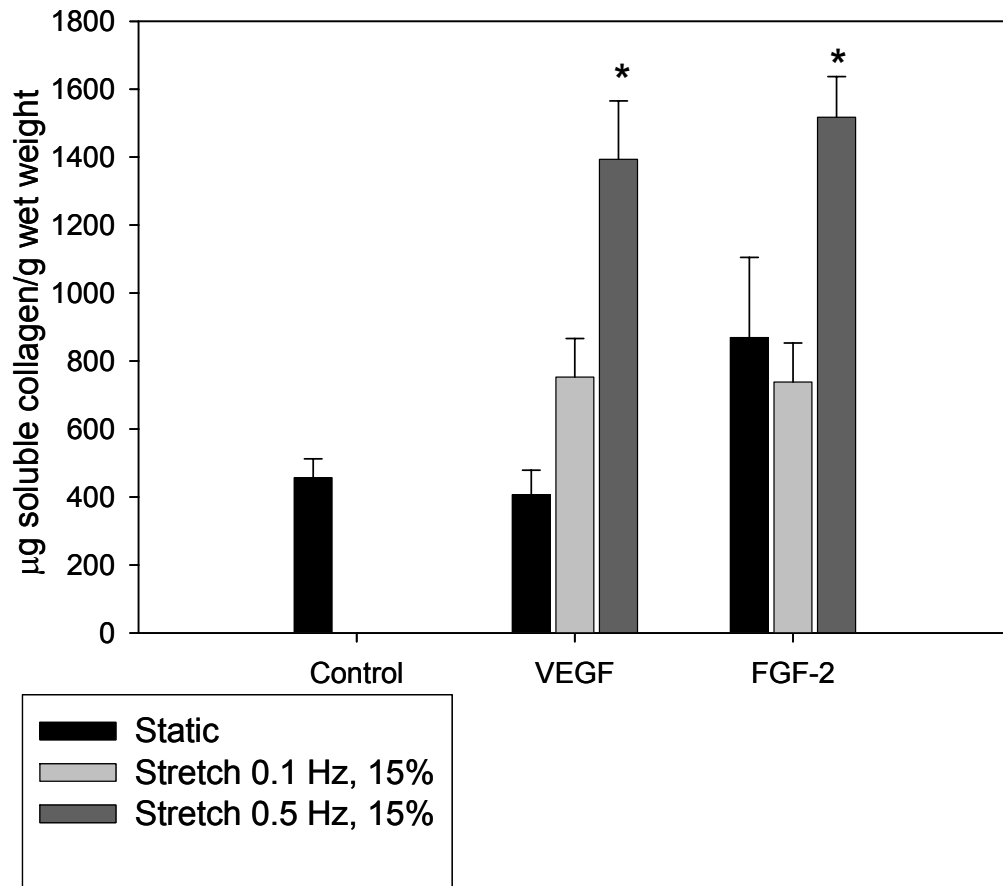


Figure 5-11. Soluble collagen concentration per gram wet weight of BSMC seeded SIS. Data are presented as mean \pm s.e.m. with $n=6$ per group. *indicates statistical significance with $p<0.05$ compared to all other groups.

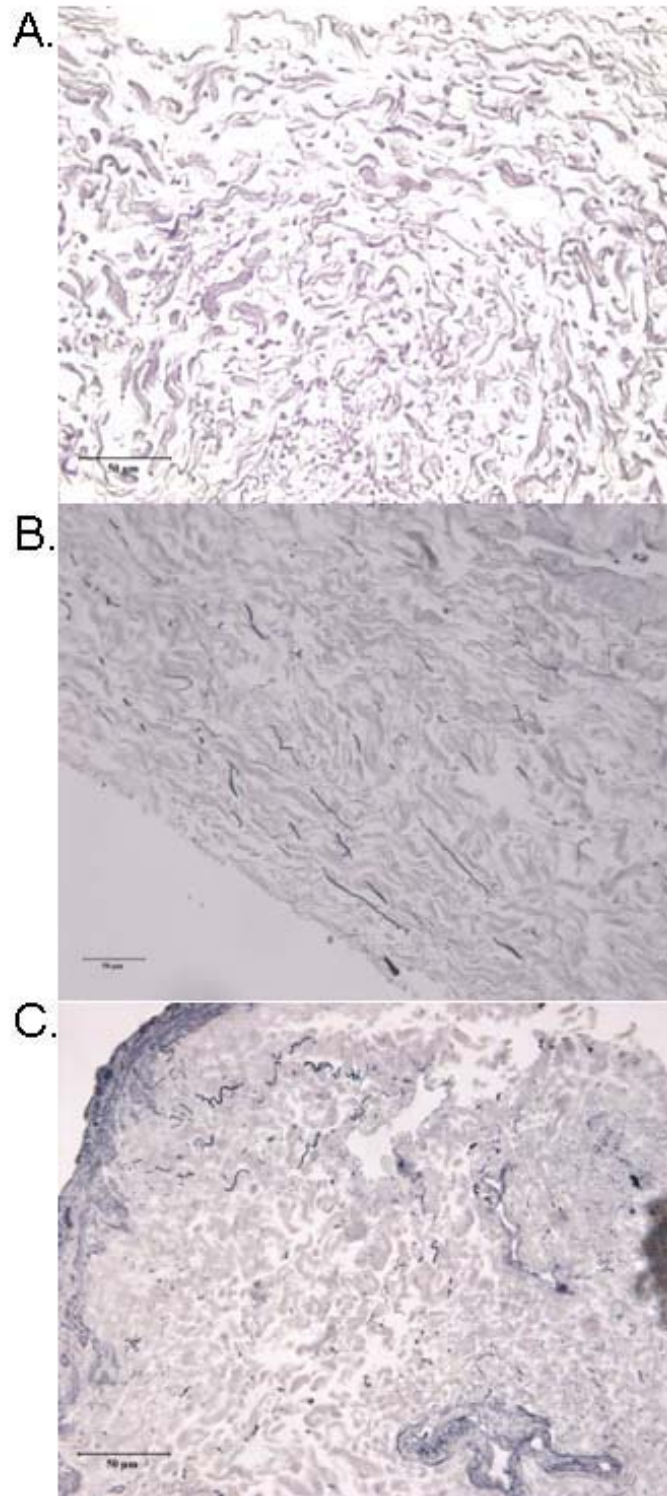


Figure 5-12. Verhoff's Van Gieson staining of elastin fibrils (black) within: A. SIS, B. Seeded SIS treated with VEGF for 7 days stretched at 0.1 Hz for 7 days, C. Seeded SIS treated with FGF-2 for 7 days then stretched at 0.1 Hz for 7 days. Black lines indicate presence of elastin. Images are representative from n=4 per group and are reduced from 400x. Scale bar represents 50 μm .

5.3.4 MMP activity and collagen in the media

Within the first 7 days of static culture in media alone, VEGF, or FGF-2, bulk MMP activity remained constant with no significant differences among groups (Fig 5-13). Additionally, within the first 7 days of static culture, VEGF treated groups released a significantly greater amount of collagen into the media than FGF-2 treated groups or control (Fig 5-13). FGF-2 treated BSMC/SIS released significantly greater amount of collagen after 2 days in culture compared to control; however the FGF-2 group released a significantly lower amount of collagen into the media than control at day 4 (Fig 5-13). There was a visible change in the behavior of the BSMC on the SIS with the switch to regular culture media at 7 days in both the MMP activity and the amount of soluble collagen (Fig 5-13).

During the second week of culture, MMP activity continued to increase in both the VEGF and FGF-2 groups (Fig 5-13). MMP activity became decreased with the addition of 0.5 Hz mechanical stimulation in the VEGF treated group (Fig 5-13). The FGF-2 treated group as well as the VEGF treated group at 0.1 Hz remained constant until day 13 where it became significantly greater than the 0.5 Hz groups ($p < 0.05$). The soluble collagen in the media became increased in the 0.1 Hz stretch groups compared to the values of the groups before stretch (Fig 5-13). In the static culture groups the switch to regular culture media caused an increase in collagen in the FGF-2 treated group and a decrease in collagen in the VEGF treated group. These groups essentially returned toward a baseline level of collagen secretion by the BSMC in static culture.

Summed totals of soluble collagen within the media showed that there was a significantly higher amount of collagen in the media in the 0.1 Hz group that was treated with VEGF for the first 7 days of culture (Figure 5-14). Summed totals of MMP activity at 14 days showed that

static culture with the addition of FGF-2 for 7 days followed by regular culture media for 7 days had significantly higher amounts of active MMPs released into the media than all other groups (Figure 5-14). Additionally, MMP activity was significantly lower at 14 days summed in the VEGF + 0.5 Hz group than all other groups except for the FGF-2 + 0.5 Hz stretch group (Figure 5-14).

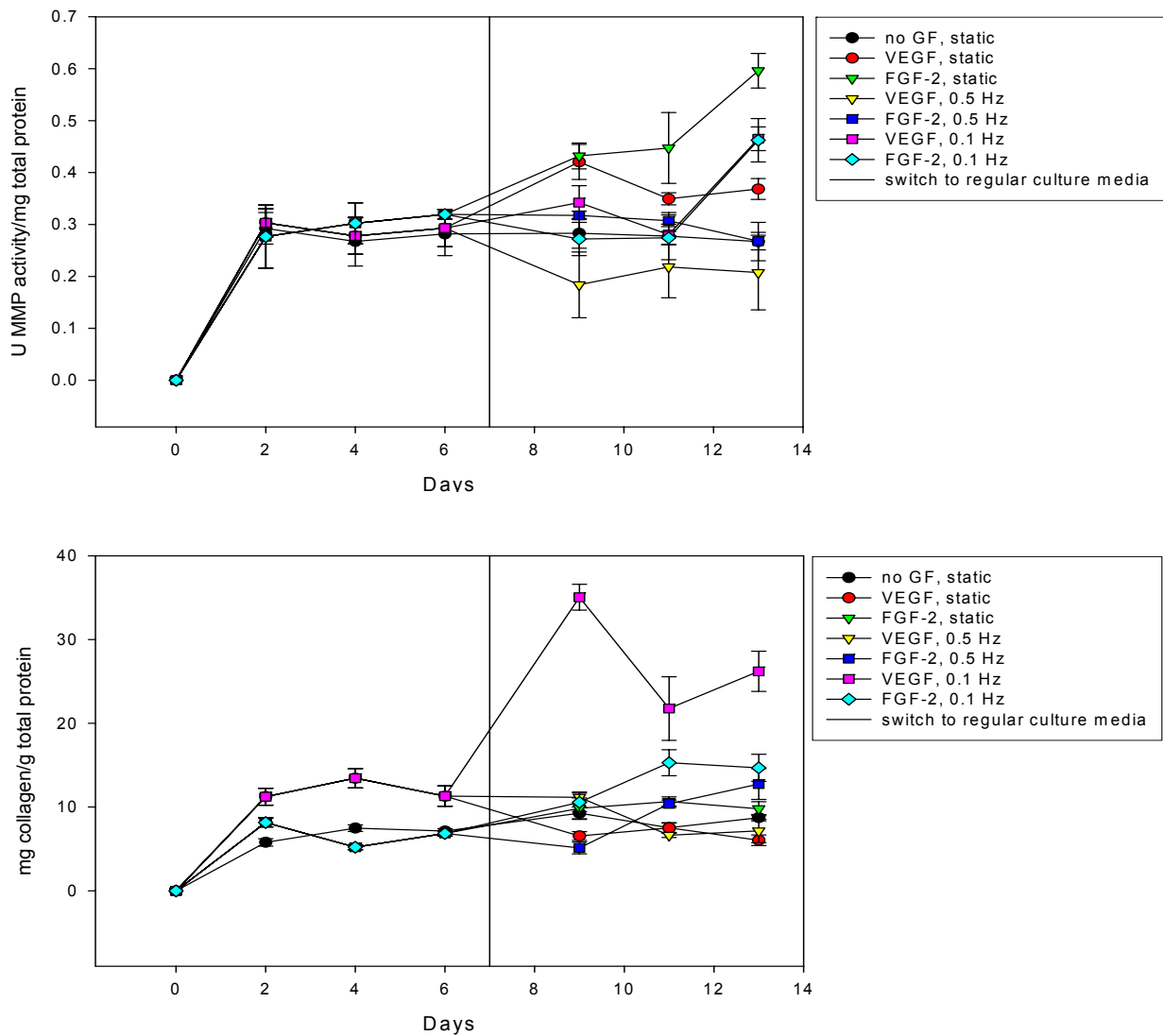


Figure 5-13. Top: MMP activity in collected media. Bottom: collagen in collected media.

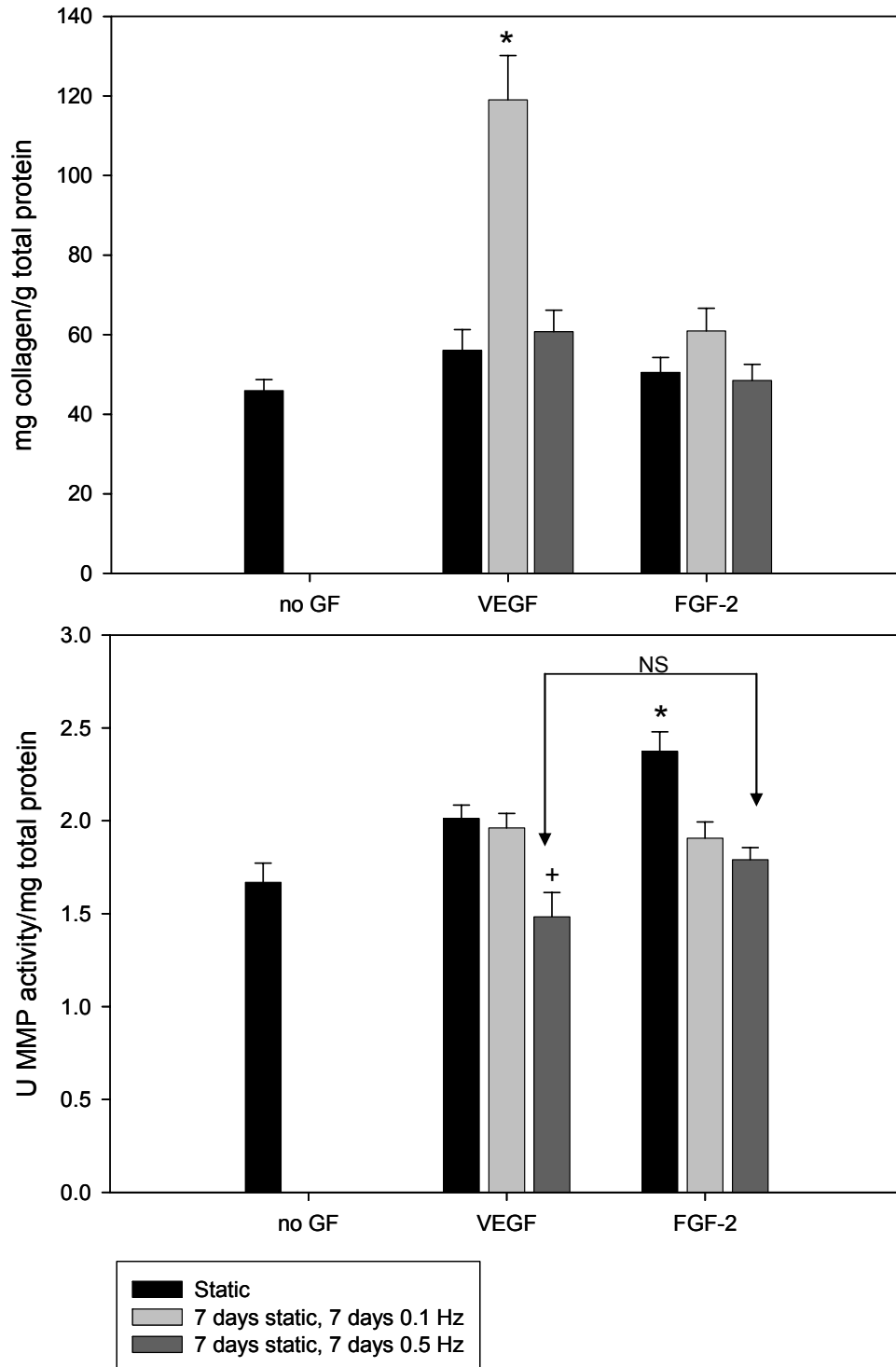


Figure 5-14. Summed totals of soluble collagen found in media (top) and MMP-2 and 9 activity found in media (bottom) of BSMC seeded SIS. Data are presented as mean \pm s.e.m. with $n=6$ per group. * indicates $p<0.05$ compared to all other groups. + indicates $p<0.05$ compared to all groups except FGF-2 at 0.5 Hz.

5.4 DISCUSSION

5.4.1 VEGF and FGF-2

The relative quantities of VEGF and FGF-2 added to the media were chosen based upon previous results in the literature wherein VEGF and FGF-2 were added to culture vascular smooth muscle cells to evoke a response [178]. These concentrations were also used in the ratio that they are released from the urothelium [142]. The response of the BSMC to the growth factor groups is similar to that found previously in co-culture of bladder urothelium with BSMC on SIS [94]. This finding further confirms a report that states that VEGF and FGF-2 are two key growth factors released by the urothelium [142]. Furthermore, VEGF is a known promoter of mitogenesis and has been shown to increase proliferation in many cell types previously while FGF-2 has been shown to up-regulate collagen type III production in BSMC [179]. FGF-2 has previously been shown to decrease elastin mRNA expression in aortic smooth muscle cells [180]. No differences were seen in the present study between groups treated with FGF-2 or VEGF in terms of elastogenesis.

Small differences were seen in MMP activity and collagen in the media. Additionally collagen production in the media during both the first 7 days and the last 7 days in culture varied dependent upon what growth factors were used. These differences demonstrate that the growth factor FGF-2 and VEGF impacted the cells during the first 7 days in culture and had persisting effects on the cells once the growth factors were removed from the system.

While it would be scientifically interesting to combine growth factors and mechanical stimulation, the amount of growth factor necessary to add to the bioreactors would significantly increase the cost of the experiment. In the present study our primary use for the growth factors

was to promote in-growth of the BSMC into the SIS. Growth factors were not added to the media during the last 7 days of culture so that the effects of mechanical stimulation alone could be examined.

5.4.2 Stretch protocols

The stretch frequencies of the SIS were chosen to be non-physiologic and to be within a range found to promote mRNA expression of various ECM genes [69]. Additionally, the 0.5 Hz frequency has been shown by our laboratory to produce significant quantities of elastin in ex vivo organ culture (Chapter 2). Interestingly, the large amounts of elastin production were seen in the 0.1 Hz stretched groups, but not in the 0.5 Hz stretched groups. This difference is likely due to the environment of the cells either being in an intact tissue or an actively remodeling piece of ECM scaffold. The amount of stretch “seen” by the BSMC in each of these cases may be different and will be the subject of future experimentation. Furthermore, it is possible that frequency and stretch ratios both play a role in the BSMC production of elastin and collagen. The SIS samples in the present study were stretched to 1.15 while the bladder strips in the previous study described in Chapter 2 were stretched to 1.20. The SIS samples were stretched to this lesser ratio due to the less compliant nature of the SIS compared with the urinary bladder wall.

A previous study wherein BSMC were seeded on collagen and laminin coated flexcell TM plates examined varying stretch frequencies [69]. The study by Adam et al showed that collagen type I and III expression is dependent upon frequency of stretch [69]. However, in this study the authors only examined one stretch level of 20% in the maximal direction. Isenberg and Tranquillo showed that vascular smooth muscle cells produce small quantities of elastin when

cycled at 0.5 Hz at 5% stretch within collagen gels [137]. It is clear from these previous studies that the ECM production of the smooth muscle cell may depend on several factors of mechanical stimulation including time of stretch, stretch rate, and extent of stretch. A future study should examine the range of stretch protocols that trigger either collagen or elastin production in the BSMC.

In static culture, increases in MMP -2 and -9 were not visible. This finding is in contrast to the increased MMP-1 activity found when MDSC are seeded on SIS [171]. This finding gives some insight into the kinetics of the MMPs. It is known that MMP-1 is a main collagenase that breaks down collagen type-I fibrils. It is likely that MMP-1 in the present study was increased early on in culture while MMP-2 and -9 (the gelatinases) had impact on breaking down the collagen further. The lower MMP activity in the summed total of 14 days culture in the VEGF + 0.5 Hz stretch group corresponds to the VEGF + 0.5 Hz stretch group having a significantly greater amount of soluble collagen within the tissue. Increased amounts of collagen were found in the VEGF + 0.1 Hz group. The groups stretched at 0.1 Hz had increased elastogenesis within the tissue; however, there may have been collagen production in the VEGF group that was released into the media.

5.4.3 Limitations

It is common in utilizing exogenous growth factors to do the experiments in serum free or low serum media to gain biological impact of growth factors themselves. However, in the present study, the growth factors were utilized as an aid in order to promote enhanced penetration of the BSMC. Proliferation and enhanced cell survival were warranted to engineer a cellular construct for bladder wall repair. Therefore, the addition of serum during growth was necessary to

maintain high cell numbers in the construct, especially during the cyclic mechanical strain. The specific mechanisms by which the BSMC are coaxed to penetrate will be the focus of future studies. An additional limitation to this study as well as many similar studies utilizing an ECM scaffold in vitro was the difficulty in histological sectioning. Somewhat reasonable images were obtained by coating the fixed SIS strips in a solution of 4% agar prior to paraffin embedding and sectioning. This coating aided in the sectioning of the SIS with limited shredding of the thin collagenous material.

5.4.4 Summary

Both VEGF and FGF-2 promote ingrowth of BSMC into SIS under static and dynamic culture conditions. Dynamically cultured BSMC in the SIS matrix produce varied ECM dependent upon frequency of stretch. These findings may lead to more functional tissue engineered bladder wall replacements.

6.0 SUMMARY, IMPLICATIONS, AND FUTURE DIRECTIONS

6.1 SUMMARY OF MAIN FINDINGS

The main findings of the present study are summarized according to specific aim. The overall impact of this work is described in the following section 6.2.

6.1.1 Specific Aim 1: Determine the effect of strain history on ECM remodeling of the ex vivo organ cultured bladder

In the first aim of the present study our hypothesis was that abnormal strain frequency would promote ECM synthesis. We found that the bladder wall smooth muscle is capable of profound elastogenesis in response to mechanical strain. This finding was somewhat surprising in that the elastogenesis occurred in response to very rapid cycling (0.5 Hz) even though two other strain histories were explored. The two other strain histories (1 hr cycling and 8 hr cycling) are more physiologic in terms of large deformations that the bladder undergoes in vivo. Additionally in this aim, we found that the elastogenesis occurring at the 0.5 Hz strain history was also accompanied by greater quantities of collagen and active gelatinases released into the media. The results from this aim supported our hypothesis, that bladder wall remodeling of ECM is dependent on strain history.

6.1.2 Specific Aim 2: Examine the role of TGF- β 1 with and without cyclic stretch on bladder smooth muscle remodeling

In the second aim of the present study hypothesized that TGF- β 1 will increase BSMC mediated ECM remodeling in the ex vivo organ culture by altering BSMC phenotype and that TGF- β 1 will increase BSMC mediated ECM remodeling of collagen gels. We found that the phenotype and remodeling response of BSMC both within cultured bladder strips and isolated and seeded on collagen gels was altered with the addition of TGF- β 1 to the culture media. We found that the phenotypic shift of the BSMC within the 0.5 Hz cycled bladder strips mimicked the SCI BSMC phenotype following 7 days of SCI. Furthermore, we found that the contractile phenotype of the BSMC was diminished with the addition of TGF- β 1 both within the cycled and static bladders as well as in the collagen gel experiments. This phenotypic shift was further confirmed by passive strip biomechanical testing whereby the bladder groups treated with TGF- β 1 were more compliant than all other groups. Elastogenesis was not impacted by the addition of TGF- β 1 to the culture media of cycled bladder strips; however, TGF- β 1 did increase soluble collagen production in the cultured bladders. Also, bladders cultured under mechanical stimulation of 0.5 Hz were more mechanically compliant once decellularized than all other treatment groups indicating that the elastin produced may play a structural role in the bladders. Additionally, TGF- β 1 increased collagen gel organization by promoting BSMC bundle formation and local physical remodeling.

6.1.3 Specific Aim 3: Engineer a cell-ECM construct to further examine the effect of strain on BSMC remodeling with future applicability in tissue engineering the bladder wall

In the third aim we hypothesized that cytokines VEGF and FGF-2 will promote cellular penetration into SIS and that non-physiologic strain histories will promote a similar response in the cell-ECM construct as demonstrated in organ culture. We found a method to improve migration of BSMC into SIS constructs by adding the exogenous growth factors VEGF and FGF-2 to culture. The migratory effect of the growth factors on the BSMC was confirmed using a Boyden chamber assay. Additionally, we were able to capture the elastogenic capability of the BSMC with cyclic mechanical stretching once the BSMC were integrated into the SIS constructs. Interestingly, large amounts of elastin were produced under cyclic at 0.1 Hz with 15% stretch and not under 0.5 Hz 15% stretch as seen in the intact bladder strips. Stretching at the slightly faster frequency of 0.5 Hz promoted greater collagen production within the BSMC/SIS constructs. Within this aim we confirmed that mechanical stimulation may be used to manipulate the BSMC in a tissue engineered construct.

6.2 IMPLICATIONS OF MAIN FINDINGS

6.2.1 Implication for treatment of pathological bladders

The findings in the first two aims of this study contribute to the body of knowledge of remodeling in the pathologic bladder, particularly in response to prescribed strain regimens and

the impact of one biochemical factor, TGF- β 1. These findings indicate that strain may be a key stimulus for remodeling seen in the bladder wall following SCI; however, it is important to note that strain history is particularly crucial to the type of remodeling that occurs by the BSMC within the bladder wall. Strain at a specific frequency induced large amounts of elastin production that were similar to that seen in the SCI bladder at 10 days. While these studies did not mimic a pathological condition explicitly, they give insight into the role of strain in elastin production within the bladder. Further experimentation would be necessary to explore the range of strain frequencies at which the BSMC produce elastin and how that range relates to the pathologic condition.

Further impact of strain was seen in the change in phenotype of the BSMC within our cycled bladder strips and the phenotype of the SCI bladders at 10 days. The phenotype was shifted toward being more contractile in these bladders; however, with the addition of TGF- β 1 to culture the phenotype was shifted toward being more synthetic. This finding may be of particular importance in future studies in examining pharmacologic inhibitors of the phenotypic shift in order to prevent long-term fibrosis.

6.2.2 Implication for mathematical modeling the remodeling of the urinary bladder wall

Previous studies have shown that viscoelastic properties of the urinary bladder wall are altered following SCI [7, 23]. These studies found that the SCI bladder exhibits significantly less stress relaxation than the normal bladder wall [23]. Furthermore, these studies showed that the mechanical properties of the bladder wall in the pathological state are highly interrelated to the structure of the bladder wall [112]. This structure function relationship is crucial in modeling the behavior of smooth muscle tissues like the bladder. Using in vivo data only, it is difficult to

assess the time-course changes in structure and biomechanical properties of the bladder tissue. The experimental models described in this study may be utilized to assess the affect of varied mechanical stimulation on the remodeling of the bladder wall ECM proteins. This data may be used in future studies in order to aid in the formulation of a mathematical model of remodeling in the pathological bladder and may additionally be of use to modeling other smooth muscle organs such as the esophagus and vasculature.

6.2.3 Impact on tissue engineering urinary bladder wall replacements

The greatest implication of the present study is in the field of tissue engineering. The third aim of the study showed the applicability of the information found utilizing *ex vivo* models of aspects of bladder pathologies. The ability of the BSMC to produce significant quantities of elastin may be utilized to engineer compliant smooth muscle tissues such as blood vessels, airway, or esophageal tissue. The specifics of how to control this elastogenesis and the organization of the elastin within the ECM still remain to be known. Also of importance to tissue engineering with biologic scaffolds is the ability to more rapidly engineer a tissue that may be mechanically stimulated with the addition of exogenous growth factors. To date, the lack of penetration of many cell types other than fibroblasts into biologic scaffolds such as SIS has been a time limiting factor. In order for engineered bladder wall replacements to be utilized in humans, the time it takes to grow the replacement needs to be minimized.

6.3 FUTURE STUDIES

6.3.1 Examining remodeling in augmented smooth muscle tissues

The present study provides a basis for many future studies involving tissue engineering and the remodeling process that occurs in augmented tissues. The cell/ECM interactions within bladders replaced partially or fully with an acellular or cell seeded biological scaffold, such as SIS that was used in the present study or urinary bladder matrix (UBM), are currently unknown. The dynamic organ culture experimental set up from aims 1 and 2.1 may be utilized to explore the augmented bladder in a controlled in vitro system. Seeded or unseeded portions of SIS or UBM may be sutured into strips of urinary bladder wall and set up in the strip biaxial bioreactor (Figure 6-1 and 6-2). These augmented bladder strips may then be mechanically stimulated at varied strain protocols that may mimic normal bladder filling and voiding. After set periods of culture time, the augmented strips may be assessed using methods described in the present study to examine cellular penetration, proliferation, collagen synthesis, and elastogenesis. Additionally cell phenotype may be explored as well as passive mechanical testing to examine BSMC tone. These studies will be valuable in understanding how engineered tissue constructs are maintained and remodeled by the surrounding native tissue. This information may then be utilized in vivo to improve upon animal models of bladder wall replacement.

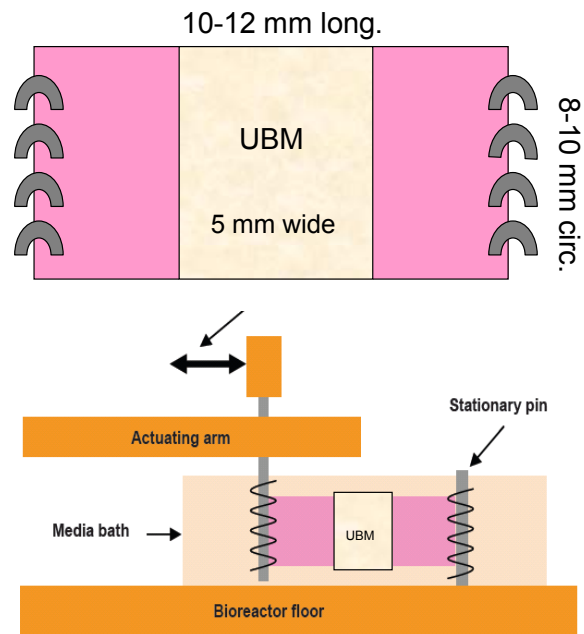


Figure 6-1. Organ culture preparation. A. Bladder wall divided with UBM sutured in between the two halves B. Schematic of uniaxial bioreactor set up with UBM augmented bladder strip.



Figure 6-2. UBM sutured in between 2 halves of a rat bladder strip. The bladder strip was prepared with stainless steel spring grips attached to the longitudinal ends (original length 10 mm), it was then cut in half and a piece of UBM (8 mm) was sutured to each edge. Arrows show interface between UBM and bladder wall.

6.3.2 Examining regulation of elastogenesis and phenotypic shift in the BSMC

Of additional importance in future work are basic studies on the cell and molecular level to understand the regulation of elastogenesis in response to mechanical stimulation as well as the role of phenotypic shift of the BSMC in the pathological bladder. Specific molecular regulation of elastogenesis is not currently understood outside of development. It is at present unclear what the role of mechanical forces is during development of elastin. There are many pathways that are mechanosensitive in smooth muscle cells. Several of these pathways have been examined primarily in vascular SMCs. However, the BSMC appear to have the unique ability to promote elastogenesis in response to mechanical stimulation that VSMC do not possess. Future studies could begin to address understanding of BSMC elastogenesis by doing comparative studies with VSMC or other SMC cell types to assess triggers of elastin production.

It remains unclear what the precise biophysical and biochemical stimuli are for phenotypic shift in the bladder following SCI. The present study examined one biological factor that is known to be up-regulated in the SCI bladder and found it to impact cells to switch to a synthetic phenotype. However, there are a wide range of molecules that may influence this shift. One potentially fruitful study would be examining the role of IGF-1 on BSMC phenotype and remodeling abilities. IGF-1 was another up-regulated molecule following SCI [35]. The time course of the molecular signaling events during the remodeling process may be the subject of future studies and would go a long way in regulating remodeling in the bladder following SCI for optimal bladder function.

6.3.3 BSMC response to contact guidance and cyclic mechanical stretch

In order for a smooth muscle tissue to produce functional contractile forces, it must possess proper architecture of the BSMC as well as the collagen and elastin components of the ECM. To date, many tissue engineering (TE) approaches for bladder wall reconstruction have had some success engineering smooth muscle tissue for bladder wall replacement, though few techniques have made it to human patients. Among the most successful are autologous cell-based and include seeding on either a biodegradable polymeric scaffold [138] or on a xenographic decellularized matrix such as small intestinal submucosa (SIS) [140] or bladder acellular matrix (BAM) [100]. Additionally, smooth muscle cell sheets grown on temperature sensitive polymers have been explored as scaffold free approaches with promising results in vivo [181]. These current cell sheet approaches are an improvement over single cell suspension or scaffold-based approaches due to their ability to retain cell-cell interactions; however, they do not allow for proper nutrient diffusion and lack the mechanical stability and organization of both SMC and ECM that is necessary for a functional bladder wall. These current TE based technologies for bladder wall repair result in incomplete, disorganized tissue regeneration. One possible reason for these shortcomings is that most TE approaches for the bladder wall give little regard to SMC and ECM alignment or interaction prior to implantation. In order to engineer functional bladder wall smooth muscle, one must understand the bladder SMC/ECM interactions and development. In the current study, we isolated BSMC from a bladder biopsy and utilized contact guidance, via a microgrooved substrate, and mechanical stimulation during SMC tissue culture to align our contiguous sheet of bladder smooth muscle.

Microgrooved PDMS was able to be fabricated with uniform grooves of varying dimensions (Fig 6-3). These grooves provided contact guidance for the bladder SMCs and

promoted alignment (Figure 6-3,4). Narrower grooves led to qualitatively higher alignment of bladder SMCs. Bladder SMCs exhibited collagen and elastin production on flat as well as microgrooved surfaces. Cyclic uniaxial stretch led to more proliferation than static culture exhibited by a statistical increase in DNA content from the cell lysates. Elastin was decreased at 0.5 Hz uniaxial stretch compared with biaxial stretch (Figure 6-5). Collagen was found to be 4 fold higher ($p=0.013$) in the mechanically stretched samples than in static culture after 5 days (Figure 6-6). The stained F-actin of uniaxial mechanically stimulated samples shows a preferential orientation of the BSMC perpendicular to the direction of strain (see Chapter 1).

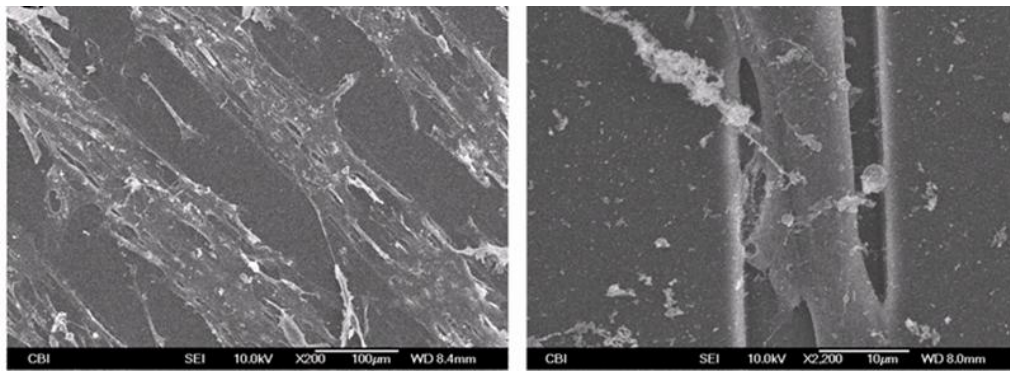


Figure 6-3. Scanning electron microscopy of BSMC on alternating 100 μm grooves (A) and 10 μm grooves with 100 μm raised in between (B), depth of all grooves was 5 μm .

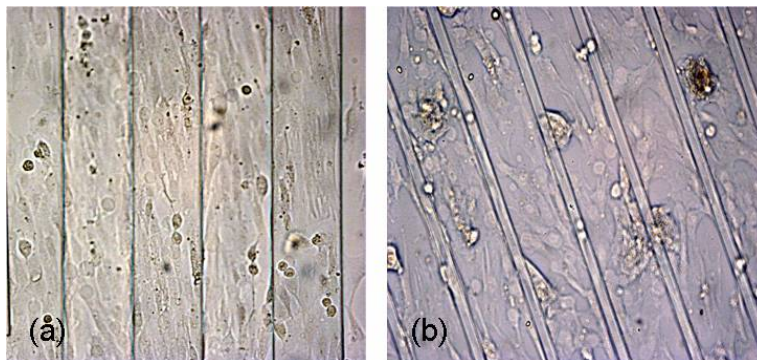


Figure 6-4. Bright field microscopy of overgrown BSMC on alternating 100 μm grooves (A) and 10 μm grooves with 100 μm raised in between (B), depth of all grooves was 5 μm .

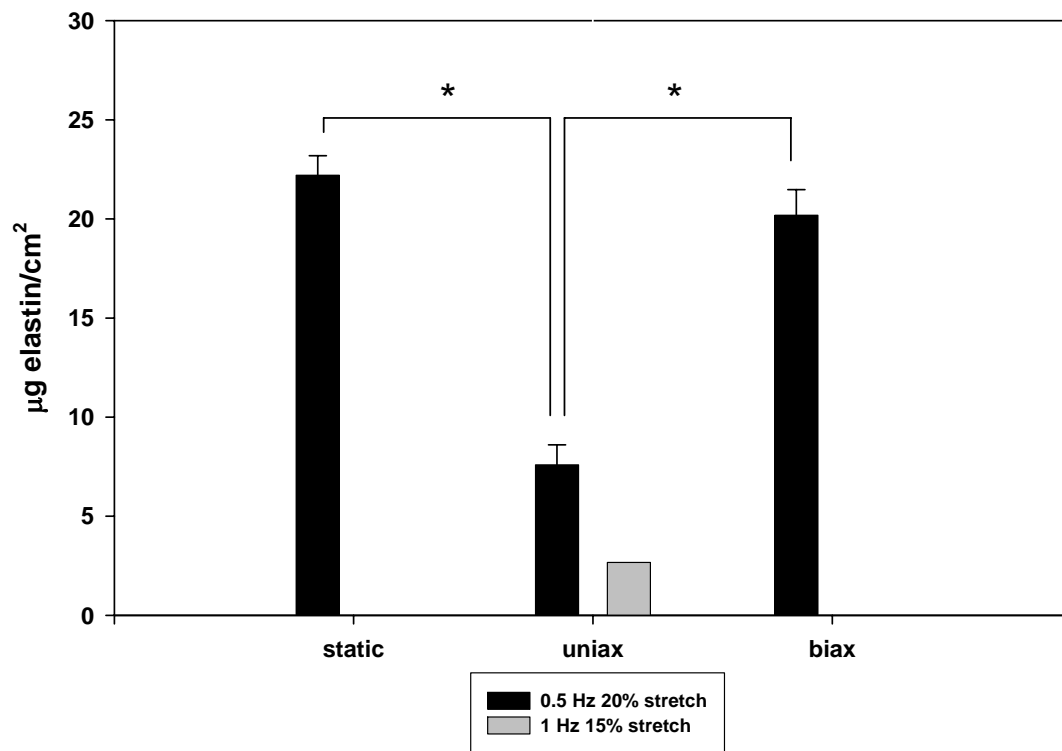


Figure 6-5. *Elastin deposition onto silicone under static, uniaxial, and biaxial stretch.* n=4 for static and uniax, n=3 for biax in 0.5Hz group n=1 for 1Hz group; * p<0.05

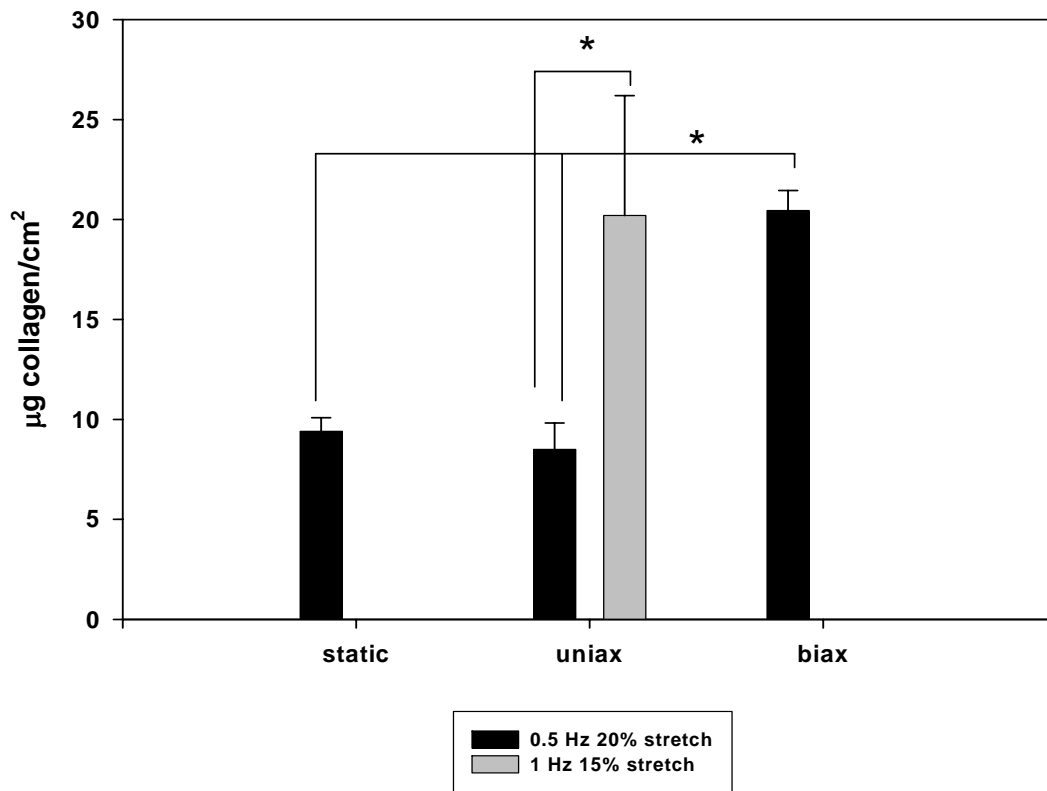


Figure 6-6. Collagen deposition onto silicone surface under static, uniaxial, and biaxial conditions. $n=3$ or 4 for each group, $*p<0.05$

This study examined methods to grow BSMC in a physically and mechanically controllable environment with the aim to promote BSMC alignment and ECM production. The use of PDMS microgrooves provided necessary contact guidance for the bladder SMC organization. In this study, we also have verified that uniaxial stretch of bladder smooth muscle cells results in alignment perpendicular to the direction of strain. We have also found that cyclic uniaxial stretch results in higher collagen production than static culture. It is known in the literature that cyclic mechanical stretch to bladder smooth muscle cells results in increased collagen synthesis; however, most of these studies use commercially available devices that produce anisotropic non-reproducible stretch. Through the use of our biaxial stretch bioreactor,

we were able to controllably mimic normal and increased micturation cycles over 48 hours. Future experiments need to be performed investigating a wider range of stretch frequency, longer time periods, and the effects of stretching the bladder SMC on the grooved PDMS surfaces both uni- and biaxially. This study showed that isolated cell experiments may also be valuable in examining the effects of strain on ECM production as well as engineering organized sheets of BSMC.

6.3.4 Summary of future directions

This section outlined studies that may be performed on both the tissue level, cell level, and molecular level. There are clearly a multitude of questions that may be asked on all of these levels of how the BSMC are prompted to penetrate scaffolds, remodel tissues, and change cellular phenotype and alignment. Understanding BSMC remodeling in response to strain is important both macroscopically in the behavior of the tissue as well as microscopically in the behavior of the cells and signaling pathways.

APPENDIX A

BSMC RESPONSES TO CONTACT GUIDANCE AND CYCLIC MECHANICAL STRETCH - METHODS

A.1 METHODS

A.1.1 Microgroove fabrication

Polydimethylsiloxane (PDMS) microgrooves were fabricated using soft photolithography. Briefly, a mask was fabricated with 4, 1.5 cm x 1.5 cm, groove patterns. These patterns were deposited onto a silicon wafer using negative photoresist and UV exposure. PDMS was mixed, degassed, and poured onto the patterned silicon wafer. The wafer coated in PDMS was baked at 60°C for 2 hours and incubated at room temperature overnight. The PDMS was then peeled off of the wafer using forceps. The microgrooves resulting from this processing were ranging from 100-1000 μm long, 10-200 μm wide, and 2-10 μm high. The patterned side of the PDMS was exposed to UV light for 12 hours, then it was rinsed 1x in DIH₂O, and 2x in HBSS.

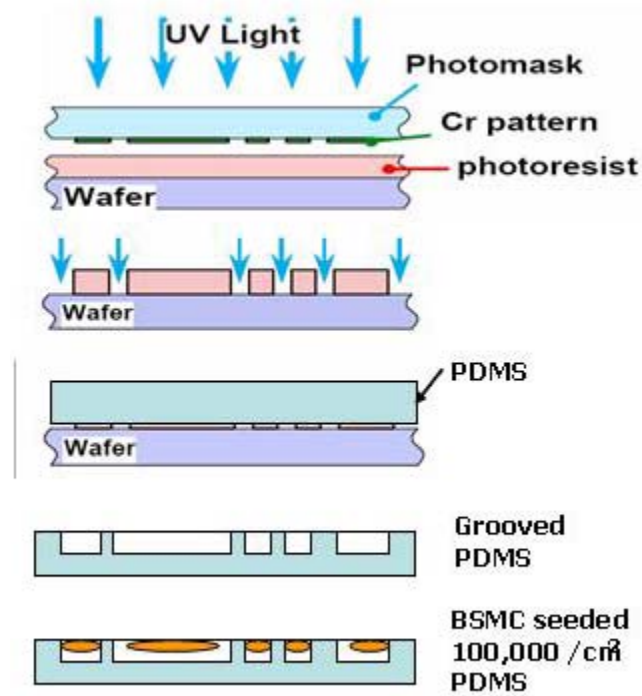


Figure A-1. *Photolithography process.*

A.1.2 Cell isolation and seeding

The smooth muscle cells were isolated from the bladders of normal Sprague-Dawley rats (170 – 250g) according to the methods adapted from the literature [165]. Briefly, under sterile conditions the bladder was cut open and pinned down on silicone-bottomed dissection Petri dish with the luminal side up. Under the dissection light microscope, the mucosal layer was mechanically removed from the rest of the bladder using fine forceps and scissors. The remaining smooth muscle layer was minced into small pieces and incubated in a 10mL beaker containing RPMI 1640 (Invitrogen, Carlsbad, CA) medium supplemented with collagenase (1 mg/mL; Sigma, St.Louis, MO), and trypsin (Invitrogen) (0.025%) with gentle spinning at 37 °C for 30 minutes. The cell suspension was passed through 100- μ m cell strainer and centrifuged at

1,000g for 5 minutes to remove collagenase/trypsin; the pellets were resuspended in RPMI 1640 medium supplemented with 10% fetal bovine serum (Hyclone, Logan, UT) and cultured in tissue-culture polystyrene dishes. All smooth muscle cells were cultured under standard cell culture conditions (sterile, 37 °C, humidified, 5% CO₂ / 95% air environment) and were used in experiments at low (up to 8) passages. SMC isolated from rat bladders were seeded 100,000 cells/cm² onto the patterned and non-patterned PDMS.

A.1.3 Cyclic stretch

Rat bladder SMCs were seeded on PDMS in static culture for 4 days. Then, samples were affixed to stretch bioreactor rods via tissue grip springs fabricated in our laboratory. Half of the samples were exposed to 10% uniaxial cyclic stretch at 1 Hz in a tension bioreactor for an additional 48 hours. The other half of the seeded samples were exposed to 10% biaxial cyclic stretch at 1 Hz in a custom-made biaxial stretch bioreactor (Fig. A-2) for an additional 48 hours. Following stretching protocols, samples were removed for imaging and biological assays.

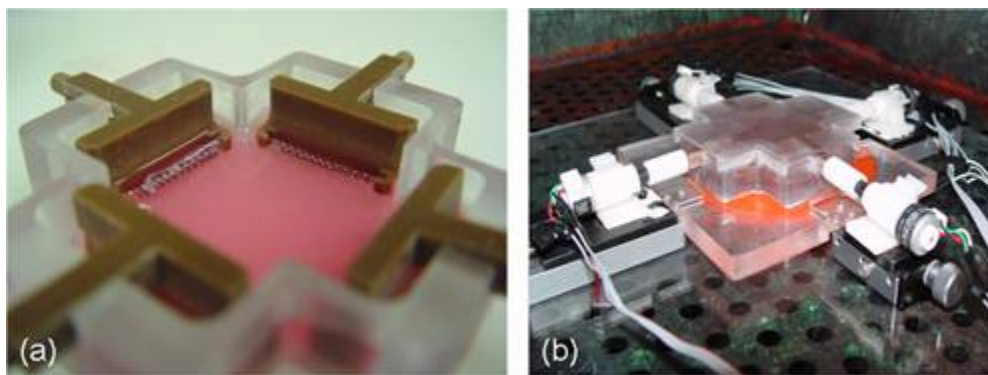


Figure A-2. *Biaxial stretch bioreactor. A. Bath with 4 grips and silicone sample, B. Running bioreactor with 4 linear actuator motors*

A.1.4 Scanning electron microscopy

Samples were fixed in 2.5% gluteraldehyde, rinsed in PBS, soaked in 1% OsO₄, and dehydrated in EtOH. Samples underwent critical point drying and sputter coating. Then, samples were viewed with a JSM6330F Scanning Electron Microscope in order to examine initial cell attachment and alignment with respect to microgrooves.

A.1.5 Biological assays

In order to examine cell proliferation, a PicoGreen dsDNA quantitation kit (Molecular Probes, Eugene, OR) was used on cell lysates according to the manufacturer's instructions. The primary components in the bladder ECM are Collagen I and III and elastin. Based on techniques adapted from Brown et al [128] total collagen was extracted from samples using a solution of 0.5 M acetic acid (Sigma) and pepsin (1 mg/ml Pepsin A (P-7000); Sigma). Each sample was placed in a microcentrifuge tube and incubated in 1 ml of extraction solution overnight (~16 h) on a rocker table (Orbitron Rotator I™; Boekel Scientific, Feasterville, PA) operating inside a refrigerator at 2–8°C. Elastin was extracted using a hot oxalic acid treatment. The concentrate was then resuspended in cold (<5°C) Elastin Precipitating Reagent (Fastin™ assay kit, Biocolor Ltd., Newtownabbey, N. Ireland). Following the extraction steps, the collagen and elastin extracts were assayed according to the guidelines provided with the Sircol™ and Fastin™ assay kits, respectively (Biocolor Ltd., Newtownabbey, N. Ireland) using a Genesys 20 spectrophotometer (Thermo Spectronic, Rochester, NY).

A.1.6 Statistical analysis

All assays were analyzed with a statistical software package (SigmaStat) using ANOVA with $p < 0.05$ considered significant.

BIBLIOGRAPHY

1. Campbell, M.F., A.J. Wein, and L.R. Kavoussi, *Campbell-Walsh urology*. 9th ed. 2007, Philadelphia: W.B. Saunders. 4 v. (xlii, 3945, cxv).
2. Ewalt, D.H., P.S. Howard, B. Blyth, H.M.d. Snyder, J.W. Duckett, R.M. Levin, and E.J. Macarak, *Is lamina propria matrix responsible for normal bladder compliance?* J Urol, 1992. **148**(2 Pt 2): p. 544-9.
3. Fry, C.H., G.P. Sui, A.J. Kanai, and C. Wu, *The function of suburothelial myofibroblasts in the bladder*. Neurourol Urodyn, 2007. **26**(6 Suppl): p. 914-9.
4. Andersson, K.E. and A. Arner, *Urinary bladder contraction and relaxation: physiology and pathophysiology*. Physiol Rev, 2004. **84**(3): p. 935-86.
5. Gray, H., P.L. Williams, and L.H. Bannister, *Gray's anatomy : the anatomical basis of medicine and surgery*. 38th ed. 1995, New York: Churchill Livingstone. xx, 2092.
6. Nagatomi, J., K. Evanui, D.C. Gloeckner, K. Torimoto, R.H. Getzenberg, M.B. Chancellor, and M.S. Sacks. *Spinal Cord Injury Induces Early Changes in Urinary Bladder Wall Composition*. in *Society for Basic Urologic Research Fall 2002 Meeting*. 2002. Tucson, AZ.
7. Nagatomi, J., D.C. Gloeckner, M.B. Chancellor, W.C. DeGroat, and M.S. Sacks, *Changes in the biaxial viscoelastic response of the urinary bladder following spinal cord injury*. Ann Biomed Eng, 2004. **32**(10): p. 1409-19.
8. Gabella, G., *The structural relations between nerve fibres and muscle cells in the urinary bladder of the rat*. J Neurocytol, 1995. **24**(3): p. 159-87.

9. Brading, A.F., J.E. Greenland, I.W. Mills, G. McMurray, and S. Symes, *Blood supply to the bladder during filling*. Scand J Urol Nephrol Suppl, 1999. **201**: p. 25-31.
10. Seki, S., K. Sasaki, M.O. Fraser, Y. Igawa, O. Nishizawa, M.B. Chancellor, W.C. de Groat, and N. Yoshimura, *Immunoneutralization of nerve growth factor in lumbosacral spinal cord reduces bladder hyperreflexia in spinal cord injured rats*. J Urol, 2002. **168**(5): p. 2269-74.
11. Sellers, J.R., *In vitro motility assay to study translocation of actin by myosin*. Curr Protoc Cell Biol, 2001. **Chapter 13**: p. Unit 13 2.
12. Arafat, H.A., G.S. Kim, M.E. DiSanto, A.J. Wein, and S. Chacko, *Heterogeneity of bladder myocytes in vitro: modulation of myosin isoform expression*. Tissue Cell, 2001. **33**(3): p. 219-32.
13. Morano, I., G.X. Chai, L.G. Baltas, V. Lamounier-Zepter, G. Lutsch, M. Kott, H. Haase, and M. Bader, *Smooth-muscle contraction without smooth-muscle myosin*. Nat Cell Biol, 2000. **2**(6): p. 371-5.
14. Deng, M., S. Mohanan, E. Polyak, and S. Chacko, *Caldesmon is necessary for maintaining the actin and intermediate filaments in cultured bladder smooth muscle cells*. Cell Motil Cytoskeleton, 2007. **64**(12): p. 951-65.
15. North, A.J., M. Gimona, Z. Lando, and J.V. Small, *Actin isoform compartments in chicken gizzard smooth muscle cells*. J Cell Sci, 1994. **107** (Pt 3): p. 445-55.
16. Sievert, K.D., T. Fandel, J. Wefer, C.A. Gleason, L. Nunes, R. Dahiya, and E.A. Tanagho, *Collagen I:III ratio in canine heterologous bladder acellular matrix grafts*. World J Urol, 2006. **24**(1): p. 101-9.
17. Macarak, E.J., D. Ewalt, L. Baskin, D. Coplen, H. Koo, R. Levin, J.W. Duckett, H. Snyder, J. Rosenbloom, and P.S. Howard, *The collagens and their urologic implications*. Adv Exp Med Biol, 1995. **385**: p. 173-7.
18. Koopman, W.J., Moreland, L.W., *Arthritis & allied conditions*. 2002, Philadelphia: Lippincott Williams & Wilkins.

19. Kajbafzadeh, A.M., S. Payabvash, A.H. Salmasi, Z. Sadeghi, A. Elmi, K. Vejdani, S.M. Tavangar, P. Tajik, and F. Mahjoub, *Time-dependent neovasculogenesis and regeneration of different bladder wall components in the bladder acellular matrix graft in rats*. J Surg Res, 2007. **139**(2): p. 189-202.
20. Landau, E.H., V.R. Jayanthi, B.M. Churchill, E. Shapiro, R.F. Gilmour, A.E. Khoury, E.J. Macarak, G.A. McLorie, R.E. Steckler, and B.A. Kogan, *Loss of elasticity in dysfunctional bladders: urodynamic and histochemical correlation*. J Urol, 1994. **152**(2 Pt 2): p. 702-5.
21. Macarak, E.J. and P.S. Howard, *The collagens and their urologic significance*. Scand J Urol Nephrol Suppl, 1997. **184**: p. 25-33.
22. Macarak, E.J., *Overview of muscle and extracellular matrix in the bladder*. Adv Exp Med Biol, 1999. **462**: p. 117-9.
23. Nagatomi, J., K.K. Toosi, M.B. Chancellor, and M.S. Sacks, *Contribution of the extracellular matrix to the viscoelastic behavior of the urinary bladder wall*. Biomech Model Mechanobiol, 2007.
24. Chang, S.L., J.S. Chung, M.K. Yeung, P.S. Howard, and E.J. Macarak, *Roles of the lamina propria and the detrusor in tension transfer during bladder filling*. Scand J Urol Nephrol Suppl, 1999. **201**: p. 38-45.
25. Chang, S.L., P.S. Howard, H.P. Koo, and E.J. Macarak, *Role of type III collagen in bladder filling*. Neurourol Urodyn, 1998. **17**(2): p. 135-45.
26. Gloeckner, D.C., *Tissue Biomechanics of the Urinary Bladder Wall*, in *Department of Bioengineering*. 2003, University of Pittsburgh: Pittsburgh. p. 258.
27. Shewry, P.R., A.S. Tatham, and A.J. Bailey, *Elastomeric proteins : structures, biomechanical properties, and biological roles*. 2002, Cambridge, UK ; New York: Cambridge University Press : Royal Society. xiv, 391.
28. Koo, H.P., E.J. Macarak, S.L. Chang, J. Rosenbloom, and P.S. Howard, *Temporal expression of elastic fiber components in bladder development*. Connect Tissue Res, 1998. **37**(1-2): p. 1-11.

29. Starcher, B. and S. Percival, *Elastin turnover in the rat uterus*. Connect Tissue Res, 1985. **13**(3): p. 207-15.
30. Guyot, C., C. Combe, and A. Desmouliere, *The common bile duct ligation in rat: A relevant in vivo model to study the role of mechanical stress on cell and matrix behaviour*. Histochem Cell Biol, 2006. **126**(4): p. 517-23.
31. Desmouliere, A., I. Darby, A.M. Costa, M. Raccurt, B. Tuchweber, P. Sommer, and G. Gabbiani, *Extracellular matrix deposition, lysyl oxidase expression, and myofibroblastic differentiation during the initial stages of cholestatic fibrosis in the rat*. Lab Invest, 1997. **76**(6): p. 765-78.
32. Parameswaran, K., A. Willems-Widyastuti, V.K. Alagappan, K. Radford, A.R. Kranenburg, and H.S. Sharma, *Role of extracellular matrix and its regulators in human airway smooth muscle biology*. Cell Biochem Biophys, 2006. **44**(1): p. 139-46.
33. Sutcliffe, M.C. and J.M. Davidson, *Effect of static stretching on elastin production by porcine aortic smooth muscle cells*. Matrix, 1990. **10**(3): p. 148-53.
34. Gray, M.A., C.C. Wang, M.S. Sacks, N. Yoshimura, M.B. Chancellor, and J. Nagatomi, *Time-Dependent Alterations of Select Genes in Streptozotocin-Induced Diabetic Rat Bladder*. Urology, 2008.
35. Nagatomi, J., F. DeMiguel, K. Torimoto, M.B. Chancellor, R.H. Getzenberg, and M.S. Sacks, *Early molecular-level changes in rat bladder wall tissue following spinal cord injury*. Biochem Biophys Res Commun, 2005. **334**(4): p. 1159-64.
36. Holm, N.R., T. Horn, F. Smedts, J. Nordling, and J. de la Rossette, *The detrusor muscle cell in bladder outlet obstruction--ultrastructural and morphometric findings*. Scand J Urol Nephrol, 2003. **37**(4): p. 309-15.
37. Kielty, C.M., *Elastic fibres in health and disease*. Expert Rev Mol Med, 2006. **8**(19): p. 1-23.
38. Kolpakov, V., M.D. Rekhter, D. Gordon, W.H. Wang, and T.J. Kulik, *Effect of mechanical forces on growth and matrix protein synthesis in the in vitro pulmonary artery. Analysis of the role of individual cell types*. Circ Res, 1995. **77**(4): p. 823-31.

39. Grunheid, T. and A. Zentner, *Extracellular matrix synthesis, proliferation and death in mechanically stimulated human gingival fibroblasts in vitro*. Clin Oral Investig, 2005. **9**(2): p. 124-30.
40. Gupta, V. and K.J. Grande-Allen, *Effects of static and cyclic loading in regulating extracellular matrix synthesis by cardiovascular cells*. Cardiovasc Res, 2006. **72**(3): p. 375-83.
41. Chun, S.Y., G.J. Lim, T.G. Kwon, E.K. Kwak, B.W. Kim, A. Atala, and J.J. Yoo, *Identification and characterization of bioactive factors in bladder submucosa matrix*. Biomaterials, 2007. **28**(29): p. 4251-6.
42. Eaton, D.C., J. Pooler, A.J. Vander, and A.J. Vander, *Vander's renal physiology*. 6th ed. 2004, New York: Lange Medical Books/McGraw Hill Medical Pub. Division. vii, 214.
43. Aminoff, M.J., Daroff, R.B., ed. *Encyclopedia of neurological sciences*. 2003, London Academic: San Diego.
44. de Groat, W.C., *A neurologic basis for the overactive bladder*. Urology, 1997. **50**(6A Suppl): p. 36-52; discussion 53-6.
45. Mimata, H., F. Satoh, T. Tanigawa, Y. Nomura, and J. Ogata, *Changes of rat urinary bladder during acute phase of spinal cord injury*. Urol Int, 1993. **51**(2): p. 89-93.
46. Ogawa, T., *Bladder deformities in patients with neurogenic bladder dysfunction*. Urol Int, 1991. **47 Suppl 1**: p. 59-62.
47. Deveaud, C.M., E.J. Macarak, U. Kucich, D.H. Ewalt, W.R. Abrams, and P.S. Howard, *Molecular analysis of collagens in bladder fibrosis*. J Urol, 1998. **160**(4): p. 1518-27.
48. Weld, K.J., M.J. Graney, and R.R. Dmochowski, *Differences in bladder compliance with time and associations of bladder management with compliance in spinal cord injured patients*. J Urol, 2000. **163**(4): p. 1228-33.
49. Shin, J.C., C.I. Park, H.J. Kim, and I.Y. Lee, *Significance of low compliance bladder in cauda equina injury*. Spinal Cord, 2002. **40**(12): p. 650-5.

50. Hackler, R.H., M.K. Hall, and T.A. Zampieri, *Bladder hypocompliance in the spinal cord injury population*. J Urol, 1989. **141**(6): p. 1390-3.
51. Kruse, M.N., L.A. Bray, and W.C. de Groat, *Influence of spinal cord injury on the morphology of bladder afferent and efferent neurons*. J Auton Nerv Syst, 1995. **54**(3): p. 215-24.
52. Watanabe, T., D.A. Rivas, and M.B. Chancellor, *Urodynamics of spinal cord injury*. Urol Clin North Am, 1996. **23**(3): p. 459-73.
53. Drake, M.J., P. Hedlund, I.W. Mills, R. McCoy, G. McMurray, B.P. Gardner, K.E. Andersson, and A.F. Brading, *Structural and functional denervation of human detrusor after spinal cord injury*. Lab Invest, 2000. **80**(10): p. 1491-9.
54. Nagatomi, J., K.K. Toosi, J.S. Grashow, M.B. Chancellor, and M.S. Sacks, *Quantification of bladder smooth muscle orientation in normal and spinal cord injured rats*. Ann Biomed Eng, 2005. **33**(8): p. 1078-89.
55. Gloeckner, D.C., M.S. Sacks, M.O. Fraser, G.T. Somogyi, W.C. de Groat, and M.B. Chancellor, *Passive biaxial mechanical properties of the rat bladder wall after spinal cord injury*. J Urol, 2002. **167**(5): p. 2247-52.
56. Gloeckner, D.C., M.B. Chancellor, and M.S. Sacks. *Material Classification of Biaxial Soft Tissue Response*. in *Fourth World Congress of Biomechanics*. 2002. Calgary, Canada.
57. Wang, C.C., J. Nagatomi, K.K. Toosi, N. Yoshimura, J.H. Hsieh, M.B. Chancellor, and M.S. Sacks, *Diabetes induced alterations in the biomechanical properties of the urinary bladder wall*. The Journal of Urology, 2005. **(Submitted)**.
58. Austin, J.C., S.K. Chacko, M. DiSanto, D.A. Canning, and S.A. Zderic, *A male murine model of partial bladder outlet obstruction reveals changes in detrusor morphology, contractility and Myosin isoform expression*. J Urol, 2004. **172**(4 Pt 1): p. 1524-8.
59. Elbadawi, A., *Functional anatomy of the organs of micturition*. Urol Clin North Am, 1996. **23**(2): p. 177-210.

60. Mirone, V., C. Imbimbo, G. Sessa, A. Palmieri, N. Longo, A.M. Granata, and F. Fusco, *Correlation between detrusor collagen content and urinary symptoms in patients with prostatic obstruction*. J Urol, 2004. **172**(4 Pt 1): p. 1386-9.
61. Association of Program Directors in Surgery (U.S.). *Current surgery*. [cited; Available from: Access via Elsevier ScienceDirect for authorized Pitt and UPMC affiliated users <http://www.sciencedirect.com/science/journal/01497944>
62. Fry, C.H., *Experimental models to study the physiology, pathophysiology, and pharmacology of the lower urinary tract* Journal of Pharmacological and Toxicological Methods, 2004. **49**(3): p. 201-210.
63. Wagg, A. and C.H. Fry, *Visco-elastic properties of isolated detrusor smooth muscle*. Scand J Urol Nephrol Suppl, 1999. **201**: p. 12-8.
64. Toosi, K., J. Nagatomi, M. Chancellor, and M. Sacks, *The effects of long-term spinal cord injury on urinary bladder biaxial mechanical properties*. Annals of Biomedical Engineering, In revision.
65. Estrada, C.R., R.M. Adam, S.H. Eaton, D.J. Bagli, and M.R. Freeman, *Inhibition of EGFR signaling abrogates smooth muscle proliferation resulting from sustained distension of the urinary bladder*. Lab Invest, 2006. **86**(12): p. 1293-302.
66. Hardin, C.D., B.D. Kleiber, and T.M. Roberts, *Mitochondrial oxidative substrate selection in porcine bladder smooth muscle*. J Urol, 2003. **170**(5): p. 2063-6.
67. Beauboeuf, A., S. Ordille, D.R. Erickson, and H.P. Ehrlich, *In vitro ligation of ureters and urethra modulates fetal mouse bladder explants development*. Tissue Cell, 1998. **30**(5): p. 531-6.
68. Capolicchio, G., K.J. Aitken, J.X. Gu, P. Reddy, and D.J. Bagli, *Extracellular matrix gene responses in a novel ex vivo model of bladder stretch injury*. J Urol, 2001. **165**(6 Pt 2): p. 2235-40.
69. Adam RM, E.S., Estrada C, Nimgaonkar A, Shih SC, Smith LE, Kohane IS, Bagli D, Freeman MR., *Mechanical stretch is a highly selective regulator of gene expression in human bladder smooth muscle cells*. Physiol Genomics, 2004. **20**(1): p. 36-44.

70. Fujiyama, C., A. Jones, S. Fuggle, R. Bicknell, D. Cranston, and A.L. Harris, *Human bladder cancer invasion model using rat bladder in vitro and its use to test mechanisms and therapeutic inhibitors of invasion*. Br J Cancer, 2001. **84**(4): p. 558-64.
71. Estrada, C.R., M. Salanga, D.R. Bielenberg, W.B. Harrell, D. Zurakowski, X. Zhu, M.R. Palmer, M.R. Freeman, and R.M. Adam, *Behavioral profiling of human transitional cell carcinoma ex vivo*. Cancer Res, 2006. **66**(6): p. 3078-86.
72. Galvin, D.J., R.W. Watson, J.I. Gillespie, H. Brady, and J.M. Fitzpatrick, *Mechanical stretch regulates cell survival in human bladder smooth muscle cells in vitro*. Am J Physiol Renal Physiol, 2002. **283**(6): p. F1192-9.
73. Persson, K., T. Dean-Mckinney, W.D. Steers, and J.B. Tuttle, *Activation of the transcription factors nuclear factor-kappaB and activator protein-1 in bladder smooth muscle exposed to outlet obstruction and mechanical stretching*. J Urol, 2001. **165**(2): p. 633-9.
74. Chaqour B, H.J., Tamura I, Macarak E, *Mechanical regulation of IGF-I and IGF-binding protein gene transcription in bladder smooth muscle cells*. J Cell Biochem, 2002. **84**(2): p. 264-77.
75. Maksym, G.N., L. Deng, N.J. Fairbank, C.A. Lall, and S.C. Connolly, *Beneficial and harmful effects of oscillatory mechanical strain on airway smooth muscle*. Can J Physiol Pharmacol, 2005. **83**(10): p. 913-22.
76. Duel BP, G.R., and Barthold JS, *Alternative techniques for augmentation cystoplasty*. J Urol, 1998. **159**: p. 998-1005.
77. Ghei, M., B.H. Maraj, R. Miller, S. Nathan, C. O'Sullivan, C.J. Fowler, P.J. Shah, and J. Malone-Lee, *Effects of botulinum toxin B on refractory detrusor overactivity: a randomized, double-blind, placebo controlled, crossover trial*. J Urol, 2005. **174**(5): p. 1873-7; discussion 1877.
78. Blyth, B., D.H. Ewalt, J.W. Duckett, and H.M. Snyder, 3rd, *Lithogenic properties of enterocystoplasty*. J Urol, 1992. **148**(2 Pt 2): p. 575-7; discussion 578-9.
79. Rosen, M.A. and J.K. Light, *Spontaneous bladder rupture following augmentation enterocystoplasty*. J Urol, 1991. **146**(5): p. 1232-4.

80. Baskin LS, H.S., Sutherland RA, DiSandro MS, Thomson AA, and Cunha GR, *Cellular Signaling in the Bladder*. *Frontiers in Bioscience*, 1997. **2**: p. 592-595.
81. Baskin LS, H.S., Sutherland RA, DiSandro MS, Thomson AA, Goodman J, Cunha GR, *Mesenchymal-epithelial interactions in the bladder*. *World Journal of Urology*, 1996. **14**(5): p. 301-309.
82. Reddy, P.P., D.J. Barriera, G. Wilson, D.J. Bagli, G.A. McLorie, A.E. Khoury, and P.A. Merguerian, *Regeneration of functional bladder substitutes using large segment acellular matrix allografts in a porcine model*. *J Urol*, 2000. **164**(3 Pt 2): p. 936-41.
83. Baskin LS, H.S.e., *Advances in Bladder Research*. *Advances in Experimental Medicine and Biology*, 1999. **462**.
84. Baskin LS, H.S., Young P, Cunha GR., *Role of mesenchymal-epithelial interactions in normal bladder development*. *Journal of Urology*, 1996. **156**: p. 1820-1827.
85. Disandro MJ, L.Y., Baskin LS, Hayward S, Cunha G, *Mesenchymal-epithelial interactions in bladder smooth muscle development: epithelial specificity*. *Journal of Urology*, 1998. **160**: p. 3-11.
86. Park J, F.M., Peters C, Arend L, Yang T and Schermann J, *Stretch-induced cyclooxygenase-2 expression in bladder smooth muscle cells*. *International Bladder Research Congress*, 1998. **Abstract**.
87. Bassuk JA, G.R., Mitchell M., *Review article: The molecular era of bladder research. Transgenic mice as experimental tools in the study of outlet obstruction*. *Journal of Urology*, 2000. **164**: p. 170-179.
88. Szucsik JC, L.A., Marmer DJ, Lessard JL., *Urogenital tract expression of enhanced green fluorescent protein in transgenic mice driven by a smooth muscle gamma-actin promoter*. *Journal of Urology*, 2004. **171**: p. 944-949.
89. Hainau B, a.D.P., *Histology and cell proliferation in human bladder tumors. An autoradiographic study*. *Cancer*, 1974. **33**: p. 115.
90. Saeyer RH, F.J., *Epithelial-Mesenchymal Interactions in Development*. 1983.

91. Pritchett TR, W.J., Jones PA, *Mesenchymal-epithelial interactions between normal and transformed human bladder cells*. Cancer Research, 1989. **49**(10): p. 2750-2754.
92. Mai KT, Y.H., Farmer J., *Changes of phenotypic expression of prostatic antigen in secondary transitional cell carcinoma of the prostate: evidence for induction phenomenon as a mechanism for acquisition of prostatic antigens in prostatic transitional cell carcinoma*. Prostate, 2001. **47**(3): p. 172-82.
93. Li Y, L.W., Hayward SW, Cunha GR, Baskin LS, *Plasticity of the urothelial phenotype: Effects of gastro-intestinal mesenchyme/stroma and implications for urinary tract reconstruction*. Differentiation, 2000. **66**: p. 126-135.
94. Brown, A.L., T.T. Brook-Allred, J.E. Waddell, J. White, J.A. Werkmeister, J.A. Ramshaw, D.J. Bagli, and K.A. Woodhouse, *Bladder acellular matrix as a substrate for studying in vitro bladder smooth muscle-urothelial cell interactions*. Biomaterials, 2005. **26**(5): p. 529-43.
95. Lai, J.Y., P.Y. Chang, and J.N. Lin, *Bladder autoaugmentation using various biodegradable scaffolds seeded with autologous smooth muscle cells in a rabbit model*. J Pediatr Surg, 2005. **40**(12): p. 1869-73.
96. Kropp, B.P., B.D. Sawyer, H.E. Shannon, M.K. Rippey, S.F. Badylak, M.C. Adams, M.A. Keating, R.C. Rink, and K.B. Thor, *Characterization of small intestinal submucosa regenerated canine detrusor: assessment of reinnervation, in vitro compliance and contractility*. Journal of Urology, 1996. **156**: p. 599-607.
97. Hodde, J.P., R.D. Record, R.S. Tullius, and S.F. Badylak, *Retention of endothelial cell adherence to porcine-derived extracellular matrix after disinfection and sterilization*. Tissue Eng, 2002. **8**(2): p. 225-34.
98. Bidmead, J. and L. Cardozo, *Genuine stress incontinence: colpocystourethropexy versus sling procedures*. Curr Opin Obstet Gynecol, 2000. **12**(5): p. 421-6.
99. Atala, A., S.B. Bauer, S. Soker, J.J. Yoo, and A.B. Retik, *Tissue-engineered autologous bladders for patients needing cystoplasty*. Lancet, 2006. **367**(9518): p. 1241-6.
100. Santucci RA, B.T., *Resorbable extracellular matrix grafts in urologic reconstruction*. Int Braz J Urol, 2005. **31**(3): p. 192-203.

101. Atala, A., *Tissue engineering and regenerative medicine: concepts for clinical application*. Rejuvenation Res, 2004. **7**(1): p. 15-31.
102. Badylak, S.F., B. Kropp, T. McPherson, H. Liang, and P.W. Snyder, *Small intestinal submucosa: a rapidly resorbed bioscaffold for augmentation cystoplasty in a dog model*. Tissue Eng, 1998. **4**(4): p. 379-87.
103. Hiles, M.C., S.F. Badylak, G.C. Lantz, K. Kokani, L.A. Geddes, and R.J. Morff, *Mechanical properties of xenogeneic small-intestinal submucosa when used as an aortic graft in the dog*. Journal of Biomedical Materials Research, 1995. **29**: p. 883-891.
104. Cheng, E.Y. and B.P. Kropp, *Urologic tissue engineering with small-intestinal submucosa: potential clinical applications*. World J Urol, 2000. **18**(1): p. 26-30.
105. Zhang, Y., D. Frimberger, E.Y. Cheng, H.K. Lin, and B.P. Kropp, *Challenges in a larger bladder replacement with cell-seeded and unseeded small intestinal submucosa grafts in a subtotal cystectomy model*. BJU Int, 2006. **98**(5): p. 1100-5.
106. Atala, A., *Tissue engineering in urologic surgery*. Urol Clin North Am, 1998. **25**(1): p. 39-50.
107. Lai, J.Y., P.Y. Chang, and J.N. Lin, *Body wall repair using small intestinal submucosa seeded with cells*. J Pediatr Surg, 2003. **38**(12): p. 1752-5.
108. Yoo, J.J., J. Meng, F. Oberpenning, and A. Atala, *Bladder augmentation using allogenic bladder submucosa seeded with cells*. Urology, 1998. **51**(2): p. 221-5.
109. Atala, A., *Tissue engineering for the replacement of organ function in the genitourinary system*. Am J Transplant, 2004. **4 Suppl 6**: p. 58-73.
110. Oberpenning, F., J. Meng, J.J. Yoo, and A. Atala, *De novo reconstitution of a functional mammalian urinary bladder by tissue engineering [see comments]*. Nat Biotechnol, 1999. **17**(2): p. 149-55.
111. Atala, A., *Tissue engineering for bladder substitution*. World J Urol, 2000. **18**(5): p. 364-70.

112. Nagatomi J, T.K., Grashow JS, Chancellor MB, Sacks MS, *Quantification of bladder smooth muscle orientation in normal and spinal cord injured rats*. Ann Biomed Eng, 2005. **33**(8): p. 1078-89.
113. Nagatomi, J., M.B. Chancellor, and M.S. Sacks. *Active biaxial mechanical properties of the bladder wall*. in *IMECE 2003*. 2003. Washington DC: ASME.
114. Chichester, P., J. Lieb, S.S. Levin, R. Buttyan, P. Horan, and R.M. Levin, *Vascular response of the rabbit bladder to short term partial outlet obstruction*. Mol Cell Biochem, 2000. **208**(1-2): p. 19-26.
115. Gosling, J.A., L.S. Kung, J.S. Dixon, P. Horan, C. Whitbeck, and R.M. Levin, *Correlation between the structure and function of the rabbit urinary bladder following partial outlet obstruction*. J Urol, 2000. **163**(4): p. 1349-56.
116. LaBelle, E., S. Zderic, D. Delaney, J. Hypolite, A. Wein, and S. Chacko, *Lipid signaling changes in smooth muscle remodeling associated with partial urinary bladder outlet obstruction*. Neurourol Urodyn, 2006. **25**(2): p. 179-84.
117. Pitre, D.A., T. Ma, L.J. Wallace, and J.A. Bauer, *Time-dependent urinary bladder remodeling in the streptozotocin-induced diabetic rat model*. Acta Diabetol, 2002. **39**(1): p. 23-7.
118. Murakumo, M., T. Ushiki, K. Abe, K. Matsumura, Y. Shinno, and T. Koyanagi, *Three-dimensional arrangement of collagen and elastin fibers in the human urinary bladder: a scanning electron microscopic study*. J Urol, 1995. **154**(1): p. 251-6.
119. Gabella, G. and B. Uvelius, *Urinary bladder of rat: fine structure of normal and hypertrophic musculature*. Cell Tissue Res, 1990. **262**(1): p. 67-79.
120. Rosenbloom, J., H. Koo, P.S. Howard, R. Mecham, and E.J. Macarak, *Elastic fibers and their role in bladder extracellular matrix*. Adv Exp Med Biol, 1995. **385**: p. 161-72.
121. Korossis, S., F. Bolland, E. Ingham, J. Fisher, J. Kearney, and J. Southgate, *Review: tissue engineering of the urinary bladder: considering structure-function relationships and the role of mechanotransduction*. Tissue Eng, 2006. **12**(4): p. 635-44.

122. Shapiro, S.D., S.K. Endicott, M.A. Province, J.A. Pierce, and E.J. Campbell, *Marked longevity of human lung parenchymal elastic fibers deduced from prevalence of D-aspartate and nuclear weapons-related radiocarbon*. J Clin Invest, 1991. **87**(5): p. 1828-34.
123. Duby, J.J., R.K. Campbell, S.M. Setter, J.R. White, and K.A. Rasmussen, *Diabetic neuropathy: an intensive review*. Am J Health Syst Pharm, 2004. **61**(2): p. 160-73; quiz 175-6.
124. Rohrmann, D., S.A. Zderic, J.W. Duckett, Jr., R.M. Levin, and M.S. Damaser, *Compliance of the obstructed fetal rabbit bladder*. Neurourol Urodyn, 1997. **16**(3): p. 179-89.
125. Crook, T.J., I.S. Hall, L.Z. Solomon, B.R. Birch, and A.J. Cooper, *A model of superficial bladder cancer using fluorescent tumour cells in an organ-culture system*. BJU Int, 2000. **86**(7): p. 886-93.
126. Coplen, D.E., E.J. Macarak, and P.S. Howard, *Matrix Synthesis by Bladder Smooth Muscle Cells Is Modulated by Stretch Frequency*. In Vitro Cell Dev Biol Anim, 2003. **39**(3): p. 157-162.
127. Stella, J.A. and M.S. Sacks, *On the biaxial mechanical properties of the layers of the aortic valve leaflet*. J Biomech Eng, 2007. **129**(5): p. 757.
128. Brown, A.N., B.S. Kim, E. Alsberg, and D.J. Mooney, *Combining chondrocytes and smooth muscle cells to engineer hybrid soft tissue constructs*. Tissue Eng, 2000. **6**(4): p. 297-305.
129. Engelmayr, G.C., Jr., E. Rabkin, F.W. Sutherland, F.J. Schoen, J.E. Mayer, Jr., and M.S. Sacks, *The independent role of cyclic flexure in the early in vitro development of an engineered heart valve tissue*. Biomaterials, 2005. **26**(2): p. 175-87.
130. Aitken, K.J., G. Block, A. Lorenzo, D. Herz, N. Sabha, O. Dessouki, F. Fung, M. Szybowska, L. Craig, and D.J. Bagli, *Mechanotransduction of extracellular signal-regulated kinases 1 and 2 mitogen-activated protein kinase activity in smooth muscle is dependent on the extracellular matrix and regulated by matrix metalloproteinases*. Am J Pathol, 2006. **169**(2): p. 459-70.
131. Kim, K.M., B.A. Kogan, C.A. Massad, and Y.C. Huang, *Collagen and elastin in the obstructed fetal bladder*. J Urol, 1991. **146**(2 (Pt 2)): p. 528-31.

132. Wood DN, B.R., Fry CH, *Characterization of the control of intracellular [Ca²⁺] and the contractile phenotype of cultured human detrusor smooth muscle cells.* J Urol, 2004. **172**(2): p. 753-7.
133. Jesudason, R., L. Black, A. Majumdar, P. Stone, and B. Suki, *Differential effects of static and cyclic stretching during elastase digestion on the mechanical properties of extracellular matrices.* J Appl Physiol, 2007. **103**(3): p. 803-11.
134. Streng, T., P. Hedlund, A. Talo, K.E. Andersson, and J.I. Gillespie, *Phasic non-micturition contractions in the bladder of the anaesthetized and awake rat.* BJU Int, 2006. **97**(5): p. 1094-101.
135. Baskin, L.S., P.S. Howard, J.W. Duckett, H.M. Snyder, and E.J. Macarak, *Bladder smooth muscle cells in culture: I. Identification and characterization.* J Urol, 1993. **149**(1): p. 190-7.
136. Pattison MA, W.S., Webster TJ, Haberstroh KM., *Three-dimensional, nano-structured PLGA scaffolds for bladder tissue replacement applications.* Biomaterials, 2005. **26**(15): p. 2491-500.
137. Isenberg, B.C. and R.T. Tranquillo, *Long-term cyclic distention enhances the mechanical properties of collagen-based media-equivalents.* Ann Biomed Eng, 2003. **31**(8): p. 937-49.
138. Lai JY, Y.C., Yoo JJ, Wulf T, Atala A., *Phenotypic and functional characterization of in vivo tissue engineered smooth muscle from normal and pathological bladders.* J Urol, 2002. **168**(4 Pt 2): p. 1853-7.
139. Rohman, G., J.J. Pettit, F. Isaure, N.R. Cameron, and J. Southgate, *Influence of the physical properties of two-dimensional polyester substrates on the growth of normal human urothelial and urinary smooth muscle cells in vitro.* Biomaterials, 2007. **28**(14): p. 2264-74.
140. Zhang Y, L.H., Frimberger D, Epstein RB, Kropp BP, *Growth of bone marrow stromal cells on small intestinal submucosa: an alternative cell source for tissue engineered bladder.* BJU Int, 2005. **96**(7): p. 1120-5.

141. Schultheiss D, G.A., Cebotari S, Tudorache I, Walles T, Schlote N, Wefer J, Kaufmann PM, Haverich A, Jonas U, Stief CG, Mertsching H., *Biological vascularized matrix for bladder tissue engineering: matrix preparation, reseeding technique and short-term implantation in a porcine model*. J Urol, 2005. **173**(1): p. 276-80.
142. Kanematsu, A., S. Yamamoto, E. Iwai-Kanai, I. Kanatani, M. Imamura, R.M. Adam, Y. Tabata, and O. Ogawa, *Induction of smooth muscle cell-like phenotype in marrow-derived cells among regenerating urinary bladder smooth muscle cells*. Am J Pathol, 2005. **166**(2): p. 565-73.
143. Brown, A.L., W. Farhat, P.A. Merguerian, G.J. Wilson, A.E. Khoury, and K.A. Woodhouse, *22 week assessment of bladder acellular matrix as a bladder augmentation material in a porcine model*. Biomaterials, 2002. **23**(10): p. 2179-90.
144. Barendrecht, M.M., A.C. Mulders, H. van der Poel, M.J. van den Hoff, M. Schmidt, and M.C. Michel, *Role of transforming growth factor beta in rat bladder smooth muscle cell proliferation*. J Pharmacol Exp Ther, 2007. **322**(1): p. 117-22.
145. Leask, A. and D.J. Abraham, *TGF-beta signaling and the fibrotic response*. Faseb J, 2004. **18**(7): p. 816-27.
146. Bagli, D.J., B.D. Joyner, S.R. Mahoney, and L. McCulloch, *The hyaluronic acid receptor RHAMM is induced by stretch injury of rat bladder in vivo and influences smooth muscle cell contraction in vitro [corrected]*. J Urol, 1999. **162**(3 Pt 1): p. 832-40.
147. Neuhaus, J., M. Heinrich, T. Schwalenberg, and J.U. Stolzenburg, *TGF-beta1 Inhibits Cx43 Expression and Formation of Functional Syncytia in Cultured Smooth Muscle Cells from Human Detrusor*. Eur Urol, 2008.
148. Roelofs, M., L. Faggian, F. Pampinella, T. Paulon, R. Franch, A. Chiavegato, and S. Sartore, *Transforming growth factor beta1 involvement in the conversion of fibroblasts to smooth muscle cells in the rabbit bladder serosa*. Histochem J, 1998. **30**(6): p. 393-404.
149. Bai, J., X.S. Liu, Y.J. Xu, Z.X. Zhang, M. Xie, and W. Ni, *Extracellular signal-regulated kinase activation in airway smooth muscle cell proliferation in chronic asthmatic rats*. Sheng Li Xue Bao, 2007. **59**(3): p. 311-8.
150. Merryman, W.D., H.D. Lukoff, R.A. Long, G.C. Engelmayr, Jr., R.A. Hopkins, and M.S. Sacks, *Synergistic effects of cyclic tension and transforming growth factor-beta1 on the aortic valve myofibroblast*. Cardiovasc Pathol, 2007. **16**(5): p. 268-76.

151. Merryman, W.D., J. Liao, A. Parekh, J.E. Candiello, H. Lin, and M.S. Sacks, *Differences in tissue-remodeling potential of aortic and pulmonary heart valve interstitial cells*. Tissue Eng, 2007. **13**(9): p. 2281-9.
152. Schultz, K., V. Murthy, J.B. Tatro, and D. Beasley, *Endogenous interleukin-1 alpha promotes a proliferative and proinflammatory phenotype in human vascular smooth muscle cells*. Am J Physiol Heart Circ Physiol, 2007. **292**(6): p. H2927-34.
153. Fujigaki, Y., D.F. Sun, T. Fujimoto, T. Suzuki, T. Goto, K. Yonemura, T. Morioka, E. Yaoita, and A. Hishida, *Mechanisms and kinetics of Bowman's epithelial-myofibroblast transdifferentiation in the formation of glomerular crescents*. Nephron, 2002. **92**(1): p. 203-12.
154. Butler, G.B., K.B. Adler, J.N. Evans, D.W. Morgan, and J.L. Szarek, *Modulation of rabbit airway smooth muscle responsiveness by respiratory epithelium. Involvement of an inhibitory metabolite of arachidonic acid*. Am Rev Respir Dis, 1987. **135**(5): p. 1099-104.
155. Yu, J., Y.F. Wang, and J.W. Zhang, *Structure of slowly adapting pulmonary stretch receptors in the lung periphery*. J Appl Physiol, 2003. **95**(1): p. 385-93.
156. Howard, P.S., U. Kucich, D.E. Coplen, and Y. He, *Transforming growth factor-beta1-induced hypertrophy and matrix expression in human bladder smooth muscle cells*. Urology, 2005. **66**(6): p. 1349-53.
157. Kaplan, E.P., J.C. Richier, P.S. Howard, D.H. Ewalt, and V.K. Lin, *Type III collagen messenger RNA is modulated in non-compliant human bladder tissue*. J Urol, 1997. **157**(6): p. 2366-9.
158. Gawaziuk, J.P., F. Sheikh, Z.Q. Cheng, P.A. Cattini, and N.L. Stephens, *Transforming growth factor-beta as a differentiating factor for cultured smooth muscle cells*. Eur Respir J, 2007. **30**(4): p. 643-52.
159. Yang, L., D.L. He, S. Wang, H.P. Cheng, and X.Y. Wang, *Effect of long-term partial bladder outlet obstruction on caldesmon isoforms and their correlation with contractile function*. Acta Pharmacol Sin, 2008. **29**(5): p. 600-5.
160. Burkhard, F.C., G.E. Lemack, P.E. Zimmern, V.K. Lin, and J.D. McConnell, *Contractile protein expression in bladder smooth muscle is a marker of phenotypic modulation after outlet obstruction in the rabbit model*. J Urol, 2001. **165**(3): p. 963-7.

161. Chacko, S., S. Chang, J. Hypolite, M. Disanto, and A. Wein, *Alteration of contractile and regulatory proteins following partial bladder outlet obstruction*. Scand J Urol Nephrol Suppl, 2004(215): p. 26-36.
162. Matsumoto, S., T. Hanai, N. Ohnishi, K. Yamamoto, and T. Kurita, *Bladder smooth muscle cell phenotypic changes and implication of expression of contractile proteins (especially caldesmon) in rats after partial outlet obstruction*. Int J Urol, 2003. **10**(6): p. 339-45.
163. Mannikarottu, A.S., M.E. Disanto, S.A. Zderic, A.J. Wein, and S. Chacko, *Altered expression of thin filament-associated proteins in hypertrophied urinary bladder smooth muscle*. Neurourol Urodyn, 2006. **25**(1): p. 78-88.
164. Lin HK, C.R., Moore P, Zhang Y, Yang Q, Peterson JA Jr, Tomasek JJ, Kropp BP, Cheng EY., *Characterization of neuropathic bladder smooth muscle cells in culture*. J Urol, 2004. **171**(3): p. 1348-52.
165. Kropp, B.P., Y. Zhang, J.J. Tomasek, R. Cowan, P.D. Furness, 3rd, M.B. Vaughan, M. Parizi, and E.Y. Cheng, *Characterization of cultured bladder smooth muscle cells: assessment of in vitro contractility*. J Urol, 1999. **162**(5): p. 1779-84.
166. Sacks, M.S. and C.J. Chuong, *Characterization of Collagen Fiber Architecture in the Canine Central Tendon*. Journal of Biomechanical Engineering, 1992. **114**: p. 183-190.
167. Lu, S.H., T.W. Cannon, C. Chermanski, R. Pruchnic, G. Somogyi, M. Sacks, W.C. de Groat, J. Huard, and M.B. Chancellor, *Muscle-derived stem cells seeded into acellular scaffolds develop calcium-dependent contractile activity that is modulated by nicotinic receptors*. Urology, 2003. **61**(6): p. 1285-91.
168. Lu, S.H., M.S. Sacks, S.Y. Chung, D.C. Gloeckner, R. Pruchnic, J. Huard, W.C. de Groat, and M.B. Chancellor, *Biaxial mechanical properties of muscle-derived cell seeded small intestinal submucosa for bladder wall reconstitution*. Biomaterials, 2005. **26**(4): p. 443-9.
169. Lauer-Fields, J.L., T. Sritharan, M.S. Stack, H. Nagase, and G.B. Fields, *Selective hydrolysis of triple-helical substrates by matrix metalloproteinase-2 and -9*. J Biol Chem, 2003. **278**(20): p. 18140-5.

170. Daniels, J.T., G.S. Schultz, T.D. Blalock, Q. Garrett, G.R. Grotendorst, N.M. Dean, and P.T. Khaw, *Mediation of transforming growth factor-beta(1)-stimulated matrix contraction by fibroblasts: a role for connective tissue growth factor in contractile scarring*. Am J Pathol, 2003. **163**(5): p. 2043-52.
171. Long RA, N.J., Chancellor MB, Sacks MS., *The role of MMP-1 up-regulation in the increased compliance in muscle-derived stem cell-seeded small intestinal submucosa*. Biomaterials, 2006. **27**(11): p. 2398-404.
172. Burgu, B., L.S. McCarthy, V. Shah, D.A. Long, D.T. Wilcox, and A.S. Woolf, *Vascular endothelial growth factor stimulates embryonic urinary bladder development in organ culture*. BJU Int, 2006. **98**(1): p. 217-25.
173. Voytik-Harbin, S., A. Brightman, B. Waisner, J. Robinson, and C. Lamar, *Small intestinal submucosa: a tissue-derived extracellular matrix that promotes tissue-specific growth and differentiation of cell in-vitro*. Tissue Engineering, 1998. **4**(2): p. 157-174.
174. Hodde, J., A. Janis, and M. Hiles, *Effects of sterilization on an extracellular matrix scaffold: part II. Bioactivity and matrix interaction*. J Mater Sci Mater Med, 2007. **18**(4): p. 545-50.
175. Chen, C.H., S.M. Poucher, J. Lu, and P.D. Henry, *Fibroblast growth factor 2: from laboratory evidence to clinical application*. Curr Vasc Pharmacol, 2004. **2**(1): p. 33-43.
176. Liu, H.Z., Q. Li, X.Y. Yang, L. Liu, L. Liu, X.R. An, and Y.F. Chen, *Expression of basic fibroblast growth factor results in the decrease of myostatin mRNA in murine C2C12 myoblasts*. Acta Biochim Biophys Sin (Shanghai), 2006. **38**(10): p. 697-703.
177. Beqaj SH, D.J., Liu DB, Harrington DA, Alpert SA, Cheng EY, *Role of basic fibroblast growth factor in the neuropathic bladder phenotype*. J Urol, 2005. **174**(4 Pt 2): p. 1699-703.
178. Sung HJ, J.C., Lessner SM, Magid R, Drury DN, Galis ZS., *Matrix metalloproteinase 9 facilitates collagen remodeling and angiogenesis for vascular constructs*. Tissue Eng, 2005. **11**(1-2): p. 267-76.
179. Imamura, M., A. Kanematsu, S. Yamamoto, Y. Kimura, I. Kanatani, N. Ito, Y. Tabata, and O. Ogawa, *Basic fibroblast growth factor modulates proliferation and collagen expression in urinary bladder smooth muscle cells*. Am J Physiol Renal Physiol, 2007. **293**(4): p. F1007-17.

180. Carreras, I., C.B. Rich, M.P. Panchenko, and J.A. Foster, *Basic fibroblast growth factor decreases elastin gene transcription in aortic smooth muscle cells*. J Cell Biochem, 2002. **85**(3): p. 592-600.
181. Shiroyanagi Y, Y.M., Yamazaki Y, Toma H, Okano T., *Urothelium regeneration using viable cultured urothelial cell sheets grafted on demucosalized gastric flaps*. BJU Int, 2004. **93**(7): p. 1069-75.